Identification of possible diagnostic and prognostic markers in human astrocytoma and targeting JNK, NF-κB signaling in glioma

Thesis submitted to the University of Hyderabad for the award of Ph.D. degree in Department of Biotechnology and Bioinformatics

By

Khamushavalli G

Department of Biotechnology and Bioinformatics

School of Life Sciences

University of Hyderabad

(P.O.) Central University, Gachibowli

Hyderabad-500 046

Telangana (India)

Enrolment no. 09LTPH13 **April 2015**

University of Hyderabad

(A central university established in 1974 by act of parliament)

Hyderabad-500046, INDIA

DECLARATION

I, **Khamushavalli G** hereby declare that this thesis entitled **"Identification of possible diagnostic and prognostic markers in human astrocytoma and targeting JNK, NF-κB signaling in glioma"** is an original and independent research work. I declare that it has not been submitted previously in part or in full to this University or any other University for the award of any degree or diploma.

Date: **Name:** Khamushavalli G

Signature of the Student

Regd. No. 09LTPH13

University of Hyderabad

(A central university established in 1974 by act of parliament)

Hyderabad-500046, INDIA

CERTIFICATE

This is to certify that this thesis entitled **"Identification of possible diagnostic and prognostic markers in human astrocytoma and targeting JNK, NF-κB signaling in glioma"** is a record of bonafide work done by **Khamushavalli G** research scholar for Ph.D. programme in Department of Biotechnology and Bioinformatics, School of Life Sciences, University of Hyderabad under my guidance and supervision.

The thesis has not been submitted previously in part or in full to this or any other University or Institution for the award of any degree or diploma.

Prof. P. Prakash Babu
Supervisor

Head
Department of Biotechnology
and Bioinformatics

Dean
School of Life sciences

Acknowledgements

It's a great privilege to express my deep sense of gratitude to my beloved supervisor **Prof. P. Prakash Babu** for his guidance, caring, freedom in designing experiments and unwavering support throughout the course of my work.

I thank the Dean **Prof. P. Reddanna**, School of Life Sciences and former deans, **Prof. M. Ramanadham, Prof. R.P. Sharma and Prof. A.S. Raghavendra** for allowing me to use the school facilities.

Many thanks to the Head, Department of Biotechnology and Bioinformatics, **Dr. Niyaz Ahmed** and former heads, **Prof. P. Prakash Babu, Prof. K. Anand Kumar** for allowing me to use the Department facilities.

I would like to thank my Doctoral Committee members **Dr. Niyaz Ahmed** and **Dr. M. Venakataramana** for their support during my work.

My thanks to the Head, Department of Animal Sciences, **Prof. B. Senthil Kumaran** and former Head **Prof. Aparna Dutta Gupta** for allowing me to use the Department facilities.

I express my whole hearted thanks to **Dr. Manas Panigrahi** (Dept. of Neurosurgery, Krishna Institute of Medical Sciences (KIMS)), **Dr. Sita Jyalakshmi** (Dept. of Neurosurgery, Krishna Institute of Medical Sciences (KIMS)), **Dr. Sundaram** (Dept. of pathology, Nizam Institute of Medical Sciences (NIMS)) for providing tumor samples and their constant support throughout the course of my work. I thank all the residents of neurosurgery and pathology for their co-operation.

I specially thank **all the students of Dr. K. Arun Kumar, Dr. Y. Suresh, Dr. M. Brahmanandam, Dr. Naresh Sepuri** and **Dr. Niyaz Ahmed** for allowing me to use their lab facilities.

My special thanks to **Dr. Shankar** and **Dr. Anita Mahadevan** (Dept. of Pathology), NIMHANS, Bangalore, for their valuable suggestions on rat model.

I thank **Dr. E. Prabhakar** for helping me in FACS analysis. I am thankful to **Dr. Ahmed** and **Ms. Nalini** (CIL) for their help in confocal microscopic images.

I thank all the **animal house staff** for their help during my animal experiments. I thank all the Department of Biotechnology and Bioinformatics office staff who helped me in different endeavours during my work.

I thank **CSIR** for giving me financial assistance throughout my Doctoral studies. I am thankful to **DST, CSIR, ICMR** and **DBT** for funding our laboratory.

I thank my current lab mates **Prabhakar, Ramu, Suraj, Noble, Apoorv, Deepak, Sirish, Naidu Babu, Praveen, Suresh, Dr. Anwita, Dr. Vimal Pandey, Dr. Parimala, Dr. Raghu Gogada, Dr. Venkat** and my senior lab mates **Dr. Gangadhar, Dr. Anand** for providing me a peaceful atmosphere during my work. Thanks to **Mr. Muthyam** (Lab Attendant) for his assistance in administrative work.

I specially thank my well-wishers **Gangadhar, Anand, Maruthi, Sirish, Anju** and **Niraj** for their moral support, encouragement and helping hand when ever needed. I specially thank **all my friends** in School of Life Sciences for helping me whenever required.

Finally no words are adequate to express thanks to my **parents and family members**.

Khamushavalli G

INDEX

ABBREVIATIONS

AA: Anaplastic astrocytoma

ALP: Alkaline phosphatase

BCIP: 5-Bromo-4-chloro-3'-indoylphosphate p- toluidine salt

Bcl-2: B-cell lymphoma protein-2

CNS: Central nervous system

Cox-2: Cyclo-oxygenase-2

CRB: Crumb

CSCs: Cancer stem cells

DA: Diffuse astrocytoma

DAB: Diamino benzidine

DCFH-DA: Dichloro-dihydro-fluorescein diacetate

ECM: Extracellular matrix

EDTA: Ethylene diamine tetra acetate

EGF: Epidermal growth factor

EGFR: Epidermal growth factor receptor

EGFR: Epidermal growth factor receptor

ENPs: Early neoplastic proliferations

ENU: n-Ethyl n-nitrosourea

Fzd: Frizzled

GBM: Glioblastoma multiforme

GFAP: Glial fibrillary acidic protein

GPX: Glutathione peroxidase

GSK3β: Glycogen synthase kinase 3β

GST: Glutathione-S-transferase

HRP: Horseradish peroxidase

IκB: Inhibitor of κB

JNK: c-Jun NH2 -terminal kinase

LOH: Loss of heterozygosity

LRP: Low density lipoprotein receptor related protein

MAPK: Mitogen activated protein kinase

MKK: MAP kinase kinases

MNU: n-Methyl n-nitrosourea

MRI: Magnetic resonance imaging

MTT: 3-(4,5-dimethylthiazol-2-yl)-2,5 diphenyltetrazolium bromide

NBT: Nitro-blue tetrazolium chloride

NF-κB: Nuclear factor κB

NPC: Neuronal precursor cells

NSCs: Neural stem cells

P135: Postnatal day-135

P180: Postnatal day-180

P90: Postnatal day-90

Par: Partitioning defective

PARP: Poly (ADP-ribosyl) polymerase

PBS: Phosphate buffered saline

PDGFR: Platelet derived growth factor receptor

PI: Propidium iodide

PMSF: Phenyl methyl sulphonyl fluoride

PNS: Peripheral nervous system

PPIs: Proton pump inhibitors

R123: Rhodamine 123

RIPA: Radioimmunoprecipitation assay

RTK: Receptor tyrosine kinase

SAPK: Stress activated protein kinase

SAPKs: Stress activated protein kinases

SCRIB: Scribble

SVZ: Sub-ventricular zone

TBS: Tris-buffered saline

TBST: Tris-buffered saline Tween 20

TMZ: Temozolamide

TNFα: Tumor necrosis factor α

TUNEL: TdT-mediated dUTP biotin nick end labelling

V-H^+-ATPases: Vacuolar type H^+-ATPases

WHO: World health organization

Chapter - 1

General Introduction

1.1. Introduction

Glioma is the term used to represent a group of lethal brain tumors originating from glial cells. They are regarded as most feared type of cancer due to their poor prognosis and dreadful effect on quality of life and cognitive functions of patients. Even though they occur in children they are most common in adults aging between 60 and 80 years, and the incidence increases with the aging of patients. They are more common in men than in women. Gliomas account for 30% of Central Nervous System (CNS) tumors and 80% of primary brain tumor. It has an annual incidence of 5.26 per 100,000 population. Every year most patients die within 16 months of diagnosis. In spite of significant amount of advances made in understanding the molecular mechanisms of glioma, notable improvement in imaging, surgery and radiotherapy, discovery of new promising drugs and targeted therapy, the overall prognosis and survival of glioma patients remains poor.

1.2. Classification of glioma and its characteristics

The term "glioma" was coined by Rudolf Virchow in the year 1860. Gliomas were first classified by Bailey and Cushing in 1926 based on histogenetic properties (Bailey and Cushing, 1926). Presently, the gliomas are classified based on WHO (World Health Organisation) guidelines. WHO has grouped gliomas into astrocytomas, oligodendrogliomas, ependymomas and oligo-astrocytomas based on the cell type they resemble (Louis et al, 2007). For convenience, each group is divided into different grades based on the malignant features like size of tumor and extent of penetration into adjacent tissue. Based on the grade of malignancy oligodendrogliomas and oligoastrocytomas are divided into grade II and grade III tumors. On the basis of degree of un-differentiation, anaplasia and aggressiveness, WHO has divided astrocytomas into four histological grades: Pilocytic astrocytoma (grade I), Diffuse astrocytoma (grade II), Anaplastic astrocytoma (grade III) and Glioblastoma multiforme or GBM (grade IV) (Louis et al, 2001; Okada et al, 2009). Grade I and II tumors are regarded as low grade tumors due to their complete curability and longer survival period of 10-15 years whereas grade III and grade IV tumors are high grade tumors since they recur even after treatment and have shorter survival of 1-3 years (Kleihues and Cavenee, 1997; Kleihues and Cavenee, 2000).

Pilocytic astrocytomas (grade I) are most common in children and they account for 5-6% of all glial tumors and constitute 20% of all childhood brain tumors (Rosemberg and Fujiwara, 2005; Rickert and Paulus, 2001). These tumors are benign, slow growing, having

well demarcated boundary with excellent prognosis. 90-97% of patients show 10 year survival period (Giannini and Scheithauer, 1997; Burkhard et al, 2003; CBTRUS, 2005). They mostly develop in cerebellum and often in optic pathway and brain stem having bad consequence (Fernandez et al, 2003). The recurrence and malignant transformation of these tumors in children is very rare where as in adults 30% of patients show tumor recurrence and progression into anaplastic astrocytoma is obvious (Ellis et al, 2009). These tumors show histological features like compact biphasic pattern, oligodendroglial morphology, glomeruloid vasculature, heterogeneity in cellular density, cellular pleomorphism and microglial distribution (Tibbetts et al, 2009). These tumors can be cured by complete surgery.

Diffuse astrocytomas (grade II) are slow growing tumors but show tendency to progress into high grade malignant tumor. They account for 5-10% of all glial tumors and are most common between 30-40 years age group. Patients with these tumors show median survival of 6-8 years (Ohgaki and Kleihues, 2005). These tumors are characterized by high degree of cellular differentiation, diffuse infiltration into neighbouring parenchyma, absence of microvasculature, whereas necrosis and single mitosis may or may not be present. 50-80% of grade II diffuse astrocytoma are associated with molecular changes like mutations in *TP53* and *IDH1/2* (Felix et al, 1995; Ichimura et al, 2009). In some of the grade II tumors copy number changes in chromosomes like 7q, 8q, 9 and 19 have been identified (Hirose et al, 2003).

Anaplastic astrocytomas (grade III) comprise 10-15% of all glial tumors. These tumors may arise from grade II tumors and are common in children and are termed as secondary. In adults grade III tumors arise *de novo* and are termed as primary. In general, anaplastic astrocytoma shows high cellularity, distinct nuclear atypia and increased mitotic activity with no obvious micro vascular proliferation and necrosis. These tumors comprise of cells with elongated or irregular, hyperchromatic nuclei and eosinophilic, glial fibrillary acidic protein (GFAP)-positive cytoplasm. They have high rate of *TP53* mutation, RB alteration and chromosomal aberrations like p16, p19 deletion and LOH on 19q (Nupponen et al, 2006; Von Deimling et al, 1993). These tumors display high tendency towards development into GBM.

Glioblastoma multiforme (GBM) is regarded as the most malignant type of glioma and it accounts for 60-70% of all glial tumors. Multiforme word describes the heterogeneity of tumor in clinical features, pathology, genetic alterations and response to treatment (Iacob and Dinca, 2009). GBM is characterized histologically by extensive cellularity and mitotic activity,

vascular proliferation and necrosis. Further, tumor area is composed of various types of cells in various differentiation stages, proliferative endothelial cells, macrophages and cells of healthy parenchyma. Tumor cells are polymorphic having nuclei of various shape and size. GBM exhibits a typical kind of necrosis called "pseudo palisading" necrosis in which necrotic area is compactly encircled by tumor cell nuclei. These tumors are highly invasive and invade into surrounding parenchyma thereby accumulating around blood vessels and neurons. GBM is classified into primary and secondary GBM. Primary GBM arise *de novo* from neural precursor cells whereas secondary GBM develops from low grade II and III tumors with step wise accumulation of genetic alterations. 90% of GBMs are primary and the patients with primary GBM are older (~55 years) than that of secondary GBM (~39 years) (Ohgaki and Kleihues, 2013). Patients with primary GBM have worst outcome and lesser survival period compared to secondary GBM patients. Histopathologically both the GBM are indistinguishable, but they differ in genetic alterations (Ohgaki and Kleihues, 1999). EGFR (Epidermal Growth Factor Receptor) amplification, PTEN (Phosphotase and tensin homolog) and loss of chromosome 10 are more frequent in primary GBM whereas in secondary GBM most common genetic alteration include isocitrate dehydrogenase-1 (IDH1) mutations, TP53 mutations, and 19q chromosome loss (Watanabe et al, 1996; Verhaak et al, 2010; Yan et al, 2009; Furnari et al, 2007).

1.3. Initiation of glioma

The origin of glioma is not well understood and various hypothesis have been proposed to describe this problem. As we know specific cell types are responsible for initiation of tumor formation. Multiple approaches have been employed to understand the origin of glioma. For example, clinical observations like expression of specific markers by tumor cells, location and onset timing of tumors provide vital clues towards the origin of glioma. Another example is molecular phenotyping at a genome-wide level. This approach has greatly advanced the categorization of gliomas by dividing morphologically indistinguishable tumors into four subtypes based on gene expression signatures and unique genomic aberrations. It also sheds light on potential cell types that are responsible for the origin of particular subtypes of glioma (Verhaak et al, 2010). One more approach is by using genetically modified mouse or rat models in which genetic mutations are directly introduced into progenitor cell types (Holland et al, 1998; Reilly et al, 2000; Xiao et al, 2002). Recent data hints at neural stem cells (NSCs) as cells of origin of gliomas. They mainly reside in sub ventricular and sub granular zone of human brain. This hypothesis is supported by presence of cancer stem cells (CSCs) in the tumor

which are thought to be multi-potent, capable of self-renewal and share markers like CD133 which are also present in NSCs (Beier et al, 2007). These human CSCs were able to re-initiate tumors in mouse brain than their non-stem counterparts in the tumor (Iacopino et al, 2014). This explains the possible reason behind the resistance of tumor to standard treatment and recurrence, as these CSCs may continue to seed the tumor formation despite treatment.

1.4. Genetic alterations in glioma

Classical cytogenetics and array-based comparative genomic hybridisation of gliomas have recognized different chromosomal aberrations like deletion or loss of heterozygosity of genes involved in tumor suppression and gain or amplification of genes involved in tumor progression. One example is the loss of tumor suppressors RB and P53. Both of them being cell cycle regulators, RB and P53 can either be directly deactivated by mutations in their genes or by amplification of their negative regulators CDK4 and MDM2 respectively (Shete et al, 2009; Wrensch et al, 2009). Similarly, glioma development is accompanied by activation of signaling pathways like Phosphatidylinositol 3-kinase (P13K) and mitogen activated protein kinases (MAPK) involved in the promotion of cell growth and survival (Knobbe and Reifenberger, 2003; Ohgaki et al, 2004). These signaling pathways are activated with amplification and overexpression of growth factor ligands such as epidermal growth factor (EGF), platelet derived growth factor (PDGF) and their respective receptors like epidermal growth factor receptor (EGFR) and platelet derived growth factor receptor (PDGFR) (Frederick et al, 2000). Even the genes involved in the metabolic processes are shown to be involved in glioma development. One such example is mutations in *isocitrate dehydrogenase1* (IDH1). 80% of human glioma patients possess IDH1 mutation that lead to gain in the enzymatic activity of IDH1 (Dang et al, 2009).

87% of human gliomas exhibit TP53 signaling alterations. TP53 signaling is important for apoptosis, cell senescence and cell cycle arrest during DNA damage. In 35-40% of GBM samples there is either heterozygous dominant negative point mutation or homozygous deletion in *TP53* gene. TP53 inhibitors *MDM2* and *MDM4* have been found to be amplified in 14% and 7% of glioblastoma. Activators of TP53 pathway like *CDKN2A* and *P14ARF* are found to be deleted in 40-59% of GBM. 11-12% of GBM show either homozygous deletion or mutation in *pRB* gene. This retinoblastoma protein (pRB) is involved in cell cycle progression from G1-S phase. Inhibitors of pRB protein *CDK4*, *CDK6* and *CCND2* are amplified in 14–18%, 1% and 2% of glioblastomas, respectively. Whereas these CDK inhibitors like *CDKN2A*/p16INK4A,

CDKN2B and *CDKN2C* are frequently found to be inactivated in GBM patients (Parsons et al, 2008).

PI3K and MAPK signaling pathways are receptor tyrosine kinase (RTK) pathways and are regularly activated in glioma patients. *EGFR* is the most frequently altered RTK gene in glioblastomas (around 45%). The other RTK's altered in GBM include *PDGFRA* (amplified in 13%), *ERBB2* (mutated in 8%) and *cMET* (amplified in 4%). Among PI3 kinases, *PIK3CA* and its adaptor protein *PIK3R1* are most commonly mutated in GBM (15-27%). Downstream effector of RTK pathway *PTEN* is homozygously deleted in 36% of GBMs. The other downstream effectors of RTK pathway *Ras* mutations (*N-Ras, H-Ras, KRas*) occur rarely in GBM (2% activating *Ras* mutations), whereas the Ras inhibitor NF1 is down regulated in 15-18% of glioblastomas (CGAR, 2008). Genetic abnormalities that occur in glioma are illustrated in fig. 1.1.

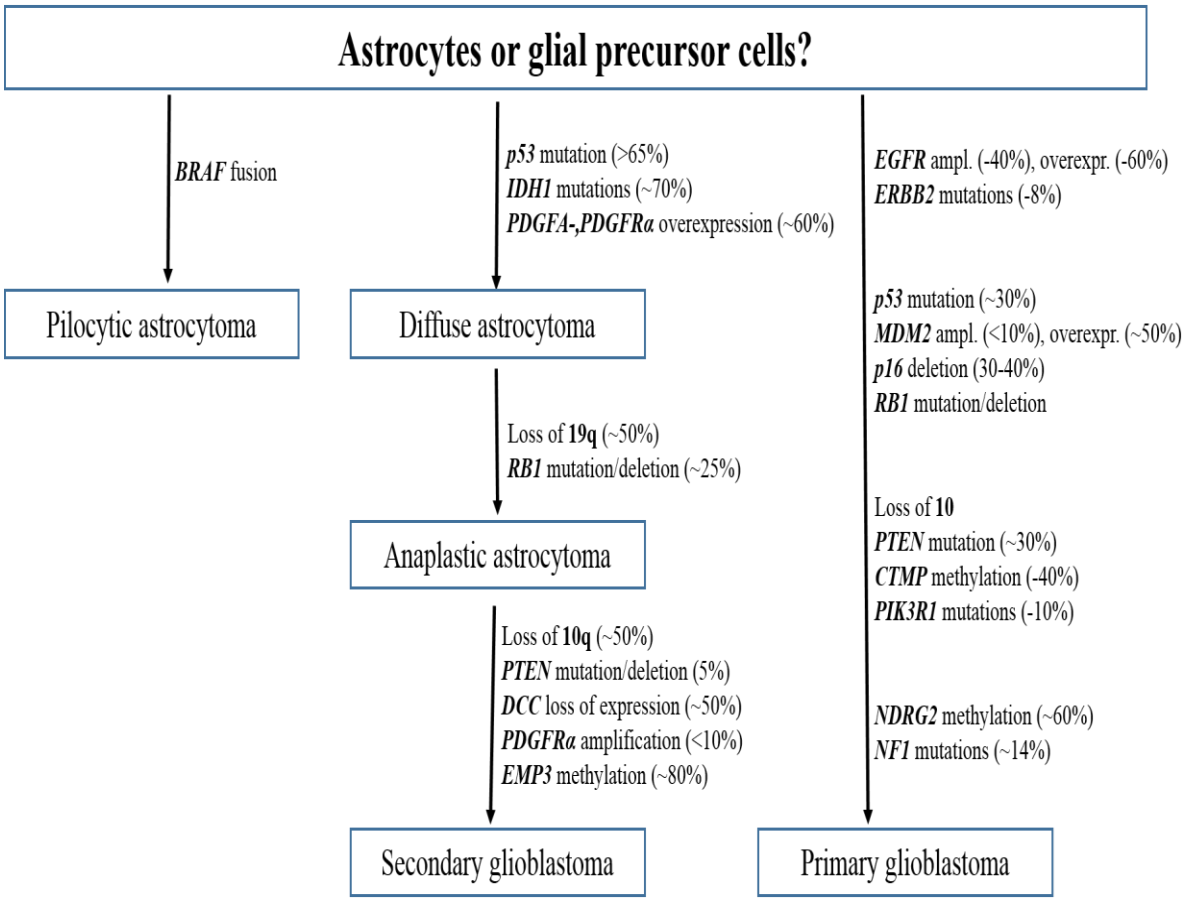

Fig.1.1. Genetic alterations associated with glioma (Kleihues and Ohgaki, 1999)

1.5. Epidemiology of glioma

In general, incidence of brain tumor is rare compared to other cancers. Only, 1 in 165 men or women will be diagnosed with brain tumors in their whole life time (Altekruse et al, 2010). Within glioma the occurrence of primary GBM (95%) is common compared to secondary GBM (5%) (Ohgaki et al, 2005). Frequency of diffuse and anaplastic astrocytoma is more than secondary GBM (Dropcho et al, 1996). The average time required for low grade glioma to progress to high grade GBM is around 2-5 years (Ohgaki et al, 2005). Incidence rates (IR) of glioma differ by histology, race and sex. Histology: for example, the age-adjusted rate per 100,000 persons per year for glioblastoma is 3.19 (95% CI=3.16-3.23) compared with less than 0.2 for anaplastic oligodendroglioma (IR=0.12, 95%CI=0.11-0.13) and protoplasmic/fibrillary astrocytoma (IR=0.11, 95%CI=0.10-0.11). Race: White people have higher incidence rate of glioma compared to blacks by histology groups (e.g., IR=3.55, 95%CI=3.52-3.59 vs. 1.64, 95%CI=1.57-1.72 for glioblastoma; IR=0.47, 95%CI=0.45-0.48 vs. 0.19, 95%CI=0.17-0.22 for anaplastic astrocytoma). Sex: males are more prone to brain tumors compared to females by histology of different markers (e.g., IR=3.99, 95%CI=3.94-4.04 vs. IR=2.53, 95%CI=2.49-2.57 for glioblastoma; IR=0.48, 95%CI=0.46-0.50 vs. 0.35, 95%CI=0.33-0.36 for anaplastic astrocytoma) (CBTRUS, 2001). Occurrence of primary GBM is more common in females (246.8 out of 100,000 per year) than in males (158.7 out of 100,000 per year). Mostly, less developed countries (e.g., Africa, Pacific Islands) report lower incidence rates (3 for males and 2.1 for females out of 100,000 persons per year) compared to more developed countries (e.g., New Zealand, Australia, North America) having incidence rate of 5.8 for males and 4.1 for females out of 100,000 persons per year (CBTRUS, 2001). Survival rate of patients diagnosed with brain tumor depends on the age of patient, grade of tumor and its location in the brain. For example, patients diagnosed between age 0-14 years with pilocytic astrocytoma (relative survival percentage-RSP =97.3%), will live beyond 5 years, compared with anaplastic astrocytoma (RSP=32.0%) and glioblastoma (RSP=20.9%) (CBTRUS 2001). On the other hand, 5-year RSP of glioma patients between age 45-54 is lower (e.g., RSP=82.4% for pilocytic astrocytoma; RSP=28.6% for anaplastic astrocytoma; and RSP=5.6% for glioblastoma). Only 0.8% of patients diagnosed between ages 55-64 years survive beyond 10 years. Examination of brain tumor incidence from past 10 years by CBTRUS has revealed slight but significant annual percentage increase (0.9%) in the incidence. Survival table 1.1.

Histologic Category	Survival upon 2 years (95%CI)	Survival upon 5 years (95%CI)
Pilocytic astrocytoma	95.9 (92.6-97.8)	99.2 (91.6-99.9)
Diffuse astrocytoma	53.6 (42.9-63.2)	73.7 (59.6-83.6)
Anaplastic astrocytoma	45.4 (38.2-52.3)	73.6 (62.7-81.8)
Glioblastoma multiforme	26.2 (20.6-32.1)	70.4 (55.6-81.2)

Table 1.1. Relative probability of a patient living 10 years beyond their diagnosis date if they have already survived 2 and 5 years (Jimmy T. Efird, 2011)

1.6. Risk factors for glioma

The specific factors responsible for glioma development are unknown and categorizing various risk factors have proven difficult. But epidemiologic data has suggested that factors like advancing age, environmental or life style exposure (e.g., smoking, alcohol consumption, coffee drinking), infectious agents (e.g., polyomaviruses, cytomegaloviruses, influenza, Toxoplasma gondii), diet/vitamins (e.g., nitrosamine compounds, vitamin C, vitamin D3), beauty products (e.g., hair dyes and lighteners, hair waving and straightening chemicals), industrial exposures (e.g., rubber manufacturing, petroleum products) might influence the occurrence of brain tumors (Bondy and Wrensch, 1996; Ostrom and Barnholtz-Sloan, 2011; Fisher et al, 2007; Schwartzbaum et al, 2006). The other factors like exposure to ionizing radiations during radiation therapy or radio surgery has proven to increase the risk of GBM, because these radiations have the ability to excite the electrons and damage DNA leading to mutations responsible for tumor formation. The overall risk of development of GBM by radiation therapy increases by 2.5% (Salvati et al, 2003). Head trauma is another factor responsible for occurrence of GBM. During trauma the glial cells divide rapidly leading to gliosis thereby damaging blood brain barrier. This causes glial cells to expose to carcinogens there by leading to tumor formation (Preston-Martin et al, 1998).

Besides these factors, development of glioma is greatly influenced by genetic syndromes, immunological risk factors and DNA repair gene polymorphisms. The inherited syndromes like neurofibromatosis 1 and 2, tuberous sclerosis, retinoblastoma, Li–Fraumeni syndrome, and Turcot's syndrome and multiple hamartoma have been connected with increased threats for development of gliomas and other types of primary brain tumor (Ichimura K et al, 2004). To some extent familial aggregation influences the occurrence of brain tumors. Familial glioma risk is two times higher than glioma risk in patients without family history of the disease. The relation between the immunological factor and glioma is inconclusive. But researchers have mentioned that there is inverse relation between adult glioma and histories of allergies or chicken pox and high serum levels of IgG and IgE during viral infections (Brenner et al, 2002). Due to complexity in DNA repair mechanism with 130 genes involved, genes associated with sensitivity to DNA damaging agents are also involved in DNA repair. Very few studies have shown association between DNA repair enzymes like ERCC1, ERCC2, GLTSCR1 and MGMT and glioma growth (Wrensch M, et al, 2005; Yang P, et al, 2005).

1.7. Symptoms

Symptoms of glioma are variable and depends on the size and location of the tumor. If tumor is present in temporal lobe, it could cause hearing and vision problems whereas tumors in frontal lobe affect personality behaviour. Most patients experience innumerable symptoms including headaches, nausea, vomiting, and seizures. GBM often presents with a multitude of varying symptoms like difficulty in walking, hearing loss, visual field defects, giddiness, acquired inability to smell, tremor, urinary urgency or incontinence, difficulty in speaking or understanding what others are saying, excessive thirst or appetite, inappropriate denial of illness, injury or bodily defects, visual hallucinations etc. (American Brain Tumor Association).

1.8. Diagnosis

Since glioma patients present various symptoms, diagnosis is more commonly made after surgical resection. Before surgery, brain imaging studies are performed in order to confirm presence, size and location of the tumor. Frequently used brain imaging technique is gadolinium-enhanced magnetic resonance imaging (MRI). GBM is most visible in T1-weighted MRIs and differences between white and gray matters are visible because of changes in contrast (Adamson, 2009). Other less commonly used techniques include magnetic resonance spectroscopy (MRS), positron emission tomography (PET), and CAT scans. If

doctor finds that tumor is located in highly dangerous or inoperable area, a stereotactic biopsy is operated. CT, MRI, PET scan of GBM is depicted in fig. 1.2.

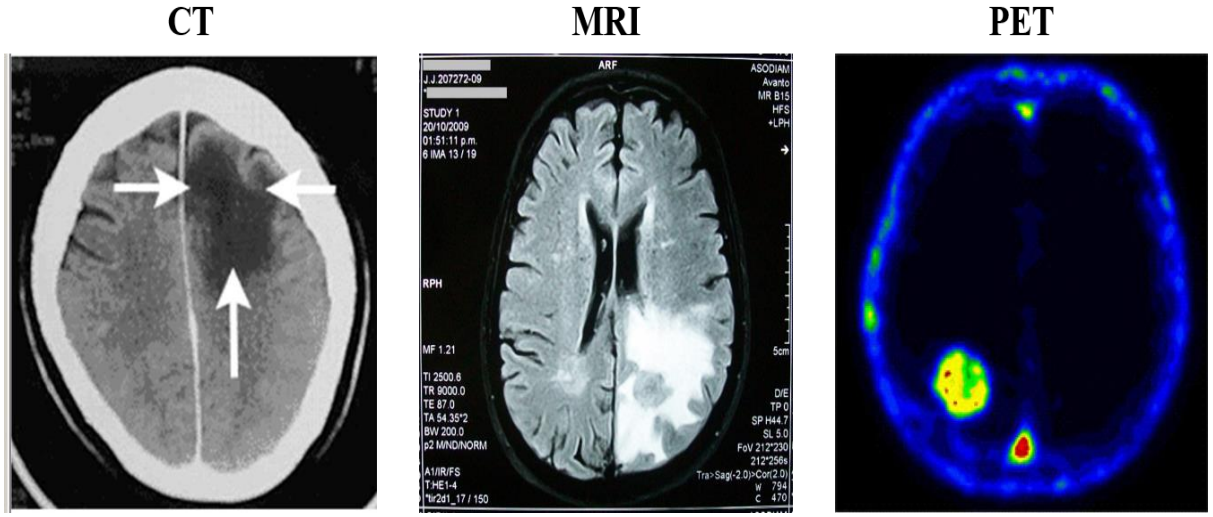

Fig.1.2. CT, MRI and PET scans of GBM

1.9. Treatment

Current conventional treatment strategy includes standard surgical removal of the tumor followed by radiation therapy. In certain cases, where the tumor cannot be cured completely by surgery and radiation therapy, chemotherapy is recommended. In general, whole brain radiation therapy coupled with surgery has the best outcome and few studies have shown that radiation therapy can be coupled with adjuvant chemotherapy (Tallet et al, 2012).

Surgical resection is considered to be the important component of multimodal management of malignant gliomas. For GBM patients, maximal resection of tumor improves the survival period of the patient. The advantages of surgical resection includes rapid cytoreduction, relief of symptoms related to mass effect, allows for institution of fractionated radiation therapy and chemotherapy with reduced target volumes, and provides tissue for diagnosis (Sanai 2012). Radiation therapy is often regarded as second component of cancer treatment. For newly diagnosed GBM patients, radiation therapy combined with chemotherapy has been proven to prolong overall survival period. Temozolamide is a proven antitumor chemotherapeutic alkylating agent. This drug acts by reducing the levels of O-methylguanine-DNA methyltransferase (*MGMT*), a DNA repair enzyme. Stupp et al, have shown that two-year survival rate was 26.5% with radiotherapy plus temozolamide and 10.4% with radiotherapy alone (Stupp et al, 2005). Glioma patients with *MGMT* promoter methylation showed better

response to temozolamide (overall survival – 49%) than patients without *MGMT* promoter methylation (overall survival – 27%) (Wick et al, 2009).

Since development of malignant tumor involves activation and interplay between different molecular pathways, extensive research in understanding these molecules has led to manufacturing of drugs targeting these molecules. For example, GBM is one of the most highly vascularised cancer and requires aggressive angiogenesis for its development and progression. Angiogenesis involves the interplay between different growth factors and their receptors. Therefore targeting these factors has proven to be better option for treatment. Table 1.2. illustrates targeting of angiogenic factors (Tanase et al, 2013).

Table 1.2. Targeting angiogenic factors in glioma treatment

Angiogenic factor	Compound Name	Mode of action
VEGF - directed monoclonal antibodies	Bevacizumab	specifically binds to VEGF-A and prevents ligand-receptor interaction
	Aflibercept	binds to all isoforms of VEGF-A with high affinity
VEGFR – directed monoclonal antibodies	Icrucumab	human IgG1 monoclonal antibody directed against human vascular endothelial growth factor receptor 1
	Ramucirumab	humanized monoclonal anti VEGFR-2
VEGFR small molecules kinase inhibitors	Sorafenib	inhibits the proangiogenic VEGFR-1, VEGFR-2, VEGFR-3, and PDGFR-βtyrosine kinases in biochemical assays in vitro
	Sunitinib	VEGF receptors-1, -2, and -3, PDGFR-α and -β, c-KIT, the receptor tyrosine kinase receptor encoded by the ret proto-oncogene (RET), and fms-like tyrosine kinase 3 (Flt3)
PDGFR – small molecules kinase inhibitors	Imatinib mesylate	inibitor of PDGFR, ABL, and c-KIT
	Tandutinib	inhibitor of PDGFR, FLT3, and c-KIT tyrosine kinase activity
EGFR - directed monoclonal antibodies	Cetuximab	binds to the second (L2) domain of EGFR thereby blocking its downstream signaling by prompting receptor internalization and encumbering ligand-receptor interaction
	Panitumumab	blocks the binding of both EGF and TGF-alpha to various EGFR
EGFR small molecule kinase inhibitors	Gefitinib	orally active low-molecular-weight EGFR inhibitor with selective tyrosine kinase activity but not serine threonine kinase inhibitory activity
	Erlotinib	anti-proliferative effects, cell-cycle arrest and apoptosis
	Lapatinib	reversible and specific RTK inhibitor of both EGFR and HER2 as well as against AkT
	Canertinib	orally active low-molecular-weight irreversible pan-EGFR family TKI

Besides this, targeting pathways like PI3K/AKT/mTOR involved in cell proliferation and differentiation, cell survival and metabolism, cell migration, and cell-cycle control has been shown to prolong the survival period of patients. Inhibitors of PI3K/AKT/mTOR are illustrated in table 1.3 (Tanase et al, 2013).

Table 1.3. Targeting signaling pathways involved in glioma development

Signaling pathway	Compound Name	Mode of action
PI-3K inhibitors	SF1126	Pan-class I PI-3K, mTOR, DNA-PK
	PX-866	Pan-class I PI-3K
	GDC-0941	Pan-class I PI-3K
	NVP-BEZ235	Pan-class I PI-3K,mTOR
	XL147	Pan-class I PI-3K
	XL765	Pan-class I PI-3K, mTOR
	D-87503	Pan-class I PI-3K, ERK2
	GSK615	Pan class I PI-3K
	CAL101	PI-3Kδ
Akt inhibitors	GSK690693	inhibits all three isoforms of Akt and some related AGC family kinases
	Akt VIII	selectivity towards Akt1 and Akt2
	MK-2206	targets all three Akt isoforms
mTOR inhibitors	Rapamycin	mTORC1 inhibitor
	Rapamycin analogs	mTORC1 inhibitor
	Torin	mTORC1,2 inhibitor
	Ku-0063794	mTORC1,2 inhibitor
	pp242	mTORC1,2 inhibitor
dual PI-3K/mTOR	PI-103	inhibits both PI-3K and mTOR kinase activity (in mTORC1 and mTORC2)
	GDC-0941	more selective towards PI-3K then mTOR and is currently in Phase I clinical trials

Recently, few researchers have demonstrated microRNAs (miRNAs) as promising therapeutic targets in cancers. miR-21, miR-196, miR-10b, miR-128-1, and miR128-2 are frequently found to be deregulated in glioblastoma. Besides their role as biological markers in assessing the disease, scientific literature suggests two possible treatment options for glioblastomas with regard to miRNA: substitution of miRNA with tumor suppression function (mimics) and inhibition of miRNAs with oncogenic properties (Mizoguchi M et al, 2013). *In vivo* and *in vitro* studies have shown to decrease tumor growth when oncogenic miRNAs were targeted and

down regulation of these miRNAs sensitized the GBM cells to 5-fluorouracil and temozolamide (Ujifuku et al, 2010; Ren et al, 2010).

During past ten years great amount of research has focused on cancer stem cells (CSCs) and targeting these cells for malignant glioma therapy. These CSCs have proven to be resistant to conventional mode of therapy, but scientists have proposed that resistance can be overcome either by blocking CSC functions through EGFR/PI-3K/Akt inhibition and inducing differentiation or targeting perivascular niche, hypoxic niche and immune evasion (Binello and Germano, 2011). For better outcome of a patient individual personalized medicine is adopted. In this tumors are classified based on molecular expression of biomarkers and individual proteome profile. This has helped in effective treatment and improved outcome of patient compared with current standard therapies.

1.10. Scope of the present study

Gliomas characterize most common primary tumors of the brain. In spite of great advancements in various treatment techniques, these tumors, GBMs in particular still carry a poor prognosis. Recent focus of current glioma research also lies in distinct characterization of tumors in low grade astrocytomas. That is differentiating pilocytic astrocytomas from diffuse astrocytomas showing the features of increased cellular and nuclear pleomorphism due to lack of potential immunohistochemical markers to differentiate between them. Thus current differential diagnosis between them is arbitrary. To date, very little information is available to distinguish pilocytic astrocytomas from grade II astrocytomas. So, understanding the molecular basis that leads to the development and progression of these tumors is important in their distinction and designing suitable treatment strategies. Many studies in different cancers including glioma have shown aberrant expression of Wnt signaling pathway. But the status of Wnt pathway in pilocytic astrocytomas is not well understood. Therefore, we have investigated the Wnt signaling pathway components β-catenin, Lef1, Tcf4 and c-Myc in a panel of pilocytic astrocytoma samples and compared with diffuse astrocytomas of all grades.

Highly aggressive treatment approaches, such as postoperative radiation therapy and chemotherapy, have been used clinically to treat glioma patients. However, these approaches do not benefit all patients equally. Adverse effects of these approaches even dramatically deteriorate the quality-of-life for some patients. Therefore, individualized therapy should be considered as a valuable approach for patients with high-grade gliomas. Recently, molecular diagnostics has emerged as a powerful tool to discover new biomarkers, network and

therapeutic targets, realizing the proof of principle that personalized medicine can increase survival and cure cancer patients. There have been several prognostic factors for glioma patients, such as age, preoperative duration of symptoms, Karnofsky performance status (KPS) score, histologic grade, tumor necrosis, surgical resection extent, use of postoperative radiation therapy and, probably, adjuvant chemotherapy. But these clinical parameters do not fully account for the observed variation in survival rates because of the heterogeneous nature of gliomas. Therefore, it is necessary to properly understand the molecular mechanism of glioma development in order to develop novel targeted approaches for management of this disease. According to previous literature loss of cell polarity was regarded as post effect of cancer, but recent research work led to discovery that cell polarity is lost and responsible for tumorigenesis and its progression. Cell polarity proteins regulate cancer cell properties like proliferation, apoptosis, and epithelial- mesenchymal transition. However, little is known about the role of cell polarity proteins in glioma or expression level of a cell polarity protein hSCRIB and its prognostic significance in human gliomas. Therefore, we investigated the expression pattern of hSCRIB in human glioma specimens and analyse the relationship between hSCRIB expression and the glioma stage as well as the survival of the patients.

Mitogen activated protein (MAP) kinases play essential role in the cellular response to extracellular stimuli. c-Jun N-terminal kinases (JNK) signaling is activated by various stress stimuli such as UV and ionizing radiation, heat shock, inflammatory cytokines, metabolic inhibitors, and osmotic or redox shock. The oncogenic role of JNK signaling pathway is well established in several cancers but little is known in glioma development. To unravel the role of JNK signaling in glioma development we used a rat model of neuro carcinogenesis in which gliomas invariably develop several months after a single prenatal exposure to ENU (N-ethyl-N-nitrosourea). Further, we wanted to investigate whether *in vitro* targeting of rat C6 glioma cell proliferation using small molecule inhibitor SP600125 (anthra [1.9-cd] pyrazole-6(2H)-one), which has been reported to be a potent and selective inhibitor of JNK1,-2 and -3 can inhibit the survival of glioma.

Despite aggressive therapy glioma remain to be an enormous therapeutic challenge. Temozolamide (TMZ) is currently the most promising chemotherapeutic drug to treat gliomas. Unfortunately, TMZ is not always effective in patients with GBM. The unsatisfactory outcome of chemotherapy with TMZ is mainly defined by the intrinsic or acquired chemoresistance in the tumor. Recent studies have shown that tumor microenvironment promotes the maturation

of tumor into malignant form. The extracellular pH of tumor being low compared to cell cytoplasm, impedes the uptake of weakly basic chemotherapeutic drug thereby reducing their cytotoxic effects on cancer cells. Vacuolar-type (V-type) H+-ATPases, are regarded as foremost players in regulating cellular pH. Drugs which inhibit the function of V-H+ -ATPases are regarded as proton pump inhibitors (PPI's). Many observations in cancer studies have pointed out anti-proliferative activity of PPI's, but there is no report on the efficacy of PPI's against glioblastoma cell lines, and the underlying mechanism involved in the growth inhibition of glioblastoma cell lines has not been elucidated. So, the present study was undertaken to examine the growth inhibitory effect of proton pump inhibitor pantoprazole on glioma cell line and reveal the molecular mechanism behind its cytotoxic activity.

Based on the existing lacunae in the glioma research the following objectives were designed.

Objectives of the study

1. **To identify novel diagnostic marker to distinguish pilocytic astrocytoma from diffuse astrocytoma based on differential expression of Wnt pathway components.**

2. **Study of cell polarity protein hSCRIB as a potential prognostic marker in human astrocytoma patients.**

3. **Role of JNK in ENU induced rat glioma progression.**

4. ***In vitro* inhibition of glioma cell survival by pantoprazole via targeting NF-κB**

References

1. Adamson C, Kanu OO, Mehta AI, Di C, Lin N, Mattox AK, Bigner DD (2009) Glioblastoma multiforme: A review of where we have been and where we are going. Expert Opinion on Investigational *Drugs* 18:1061-1083.
2. Altekruse S, Kosary C, Krapcho M, Neyman N (2010)SEER Cancer Statistics Review, 1975-2007, National Cancer Institute. Bethesda, MD, http://seer.cancer.gov/csr/1975_2007/, based on November 2009 SEER data submission, posted to the SEER web site.
3. American Brain Tumor Association. Retreived from www.abta.org.
4. Bailey P, Cushing H (1926) A Classification of the Tumors of the Glioma Group on a Histogenetic Basis with a Correlated Study of Prognosis. JB Lippincott & Co., Philadelphia, PA.
5. Beier D, Hau P, Proescholdt M, Lohmeier A, Wischhusen J, Oefner PJ, Aigner L, Brawanski A, Bogdahn U, Beier CP (2007) CD133(+) and CD133(-) glioblastoma-derived cancer stem cells show differential growth characteristics and molecular profiles. *Cancer Res* 67:4010-4015.
6. Binello E, Germano IM (2011) Targeting glioma stem cells: a novel framework for brain tumors. *Cancer Sci* 102:1958-1966
7. Bondy M, Wrensch M (1996) Epidemiology of primary malignant brain tumors. *Baillieres Clin Neurol* 5:251-270.
8. Brenner AV, Linet MS, Fine HA, Shapiro WR, Selker RG, Black PM, Inskip PD (2002) History of allergies and autoimmune diseases and risk of brain tumors in adults. *Int J Cancer* 99:252–259.
9. Burkhard C, Di Patre PL, Schuler D (2003) A population-based study of the incidence and survival rates in patients with pilocytic astrocytoma. *J Neurosurg* 98:1170–1174.
10. Cancer Genome Atlas Research Network (2008) Comprehensive genomic characterization defines human glioblastoma genes and core pathways. *Nature* 455:1061-1068.
11. CBTRUS (2001) CBTRUS Statistical Report: Primary Brain and Central Nervous System Tumors Diagnosed in the United States in 2004-2007. Source: Central Brain Tumor Registry of the United States, Hinsdale, IL. Website: www.cbtrus.org.
12. CBTRUS (2005) central brain tumor registry of the United States. http://www.cbtrus.org.

13. Dang L, White DW, Gross S, Bennett BD, Bittinger MA, Driggers EM, Fantin VR, Jang HG, Jin S, Keenan MC, Marks KM, Prins RM, Ward PS, Yen KE, Liau LM,Rabinowitz JD, Cantley LC, Thompson CB, Vander Heiden MG, Su SM (2009) Cancer-associated IDH1 mutations produce 2-hydroxyglutarate. *Nature* 462, 739–44.
14. Dropcho EJ, Soong SJ (1996) The prognostic impact of prior low grade histology in patients with anaplastic gliomas: a case-control study. *Neurology* 47:684–690.
15. Ellis JA, Waziri A, Balmaceda C, Canoll P, Bruce JN, Sisti MB (2009) Rapid recurrence and malignant transformation of pilocytic astrocytoma in adult patients. *J Neurooncol* 95:377–382.
16. Felix CA, Slavc I, Dunn M, Strauss EA, Phillips PC, Rorke LB, Sutton L, Bunin GR, Biegel JA (1995) p53 gene mutations in pediatric brain tumors. *Med Pediatr Oncol* 25:431–436.
17. Fernandez C, Figarella-Branger D, Girard N, Bouvier-Labit C, Gouvernet J, Paz Paredes A, Lena G (2003) Pilocytic astrocytomas in children: prognostic factors-a retrospective study of 80 cases. *Neurosurgery* 53:544–555.
18. Fisher J, Schwartzbaum J, Wrensch M, Wiemels J (2007) Epidemiology of Brain tumors. *Neurol Clin* 25:867-890.
19. Frederick L, Wang XY, Eley G, James CD (2000) Diversity and frequency of epidermal growth factor receptor mutations in human glioblastomas. *Cancer Res* 60:1383-7
20. Furnari FB, Fenton T, Bachoo RM, Mukasa A, Stommel JM, Stegh A, Hahn WC, Ligon KL, Louis DN, Brennan C, Chin L, DePinho RA, Cavenee WK (2007) Malignant astrocytic glioma: Genetics, biology, and paths to treatment. *Genes Dev* 21:2683–710.
21. Giannini C, Scheithauer BW (1997) Classification and grading of low-grade astrocytic tumors in children. Brain Pathol 7:785–798.
22. Hirose Y, Aldape KD, Chang S, Lamborn K, Berger MS, Feuerstein BG (2003) Grade II astrocytomas are subgrouped by chromosome aberrations. *Cancer Genet Cytogenet* 142:1–7.
23. Holland EC, Hively WP, Depinho RA, Varmus HE (1998) A constitutively active epidermal growth factor receptor cooperates with disruption of G1 cell-cycle arrest pathways to induce glioma-like lesions in mice. *Genes Dev* 12:3675–3685.
24. Iacob G, Dinca EB (2009) Current data and strategy in glioblastoma multiforme. *J Med Life* 2: 386-393.

25. Iacopino F, Angelucci C, Piacentini R, Biamonte F, Mangiola A, Maira G, Grassi C, Sica G (2014) Isolation of cancer stem cells from three human glioblastoma cell lines: characterization of two selected clones. *PLoS One* 14:9.
26. Ichimura K, Ohgaki H, Kleihues P, Collins VP (2004) Molecular pathogenesis of astrocytic tumors. *J Neurooncol* 70:137–160.
27. Ichimura K, Pearson DM, Kocialkowski S, Bäcklund LM, Chan R, Jones DT, Collins VP (2009) IDH1 mutations are present in the majority of common adult gliomas but rare in primary glioblastomas. *Neuro Oncol* 11:341–347.
28. Jimmy T. Efird (2011) Epidemiology of Glioma. ISBN: 978-953-307-379-8, *InTech*, DOI: 10.5772/21698.
29. Kleihues P, Cavenee WK (1997) Tumors of the central nervous system: pathology and genetics. Lyon, France: International Agency for Research on Cancer.
30. Kleihues P, Cavenee WK (2000) Pathology and Genetics of Tumors of the Central Nervous System (World Health Organization Classification of Tumors), 2nd edn. IARC: Lyon.
31. Kleihues P, Ohgaki H (1999) Primary and secondary glioblastomas: from concept to clinical diagnosis. *Neuro Oncol* 1:44-51.
32. Knobbe CB, Reifenberger G (2003) Genetic alterations and aberrant expression of genes related to the phosphatidyl-inositol-3'-kinase/protein kinase B (Akt) signal transduction pathway in glioblastomas. *Brain Pathol* 13, 507–18.
33. Louis DN, Holland EC, Cairncross JG (2001) Glioma classification: a molecular reappraisal. *Am J Pathol* 159:779-786.
34. Louis DN, Ohgaki H, Wiestler OD, Cavenee WK, Burger PC, Jouvet A, Scheithauer BW, Kleihues P (2007) The 2007 WHO classification of tumors of the central nervous system. *Acta Neuropathol* 114: 97-109.
35. Mizoguchi M, Guan Y, Yoshimoto K, Hata N, Amano T, Nakamizo A, Sasaki T (2013) Clinical implications of microRNAs in human glioblastoma. *Front Oncol* 3:1-6.
36. Nupponen NN, Joensuu H (2006) Molecular pathology of gliomas. *Curr Diagn Pathol* 12:394-402.
37. Ohgaki H, Dessen P, Jourde B, Horstmann S, Nishikawa T, Di Patre PL, Burkhard C, Schüler D, Probst-Hensch NM, Maiorka PC, Baeza N, Pisani P,Yonekawa Y, Yasargil MG, Lütolf UM, Kleihues P (2004) Genetic pathways to glioblastoma: A population based study. Cancer Res 64, 6892–99.

38. Ohgaki H, Kleihues P (1999) Primary and secondary glioblastomas: from concept to clinical diagnosis. *Neuro-oncology* 44-51.
39. Ohgaki H, Kleihues P (2005) Epidemiology and etiology of gliomas. *Acta Neuropathol* 109:93–108.
40. Ohgaki H, Kleihues P (2005) Population-based studies on incidence, survival rates, and genetic alterations in astrocytic and oligodendroglial gliomas. *J Neuropathol Exp Neurol* 64:479–489.
41. Ohgaki H, Kleihues P (2013) The definition of primary and secondary glioblastoma. *Clin Cancer Res* 19:764–72.
42. Okada H, Kohanbash G, Zhu X, Kastenhuber ER, Hoji A, Ueda R, Fujita M (2009) Immunotherapeutic approaches for glioma. *Crit Rev Immunol* 29:1-42.
43. Ostrom Q, Barnholtz-Sloan J (2011) Current state of our knowledge on brain tumor epidemiology. *Curr Neurol Neurosci Rep* 11:329-335.
44. Parsons DW, Jones S, Zhang X, Lin JC, Leary RJ, Angenendt P, Mankoo P, Carter H, Siu IM, Gallia GL, Olivi A, McLendon R, Rasheed BA, Keir S, Nikolskaya T, Nikolsky Y, Busam DA, Tekleab H, Diaz LA Jr, Hartigan J, Smith DR, Strausberg RL, Marie SK, Shinjo SM, Yan H, Riggins GJ, Bigner DD, Karchin R,Papadopoulos N, Parmigiani G, Vogelstein B, Velculescu VE, Kinzler KW (2008) An integrated genomic analysis of human glioblastoma multiforme. *Science* 321:1807-1812.
45. Preston-Martin S, Pogoda JM, Schlehofer B, Blettner M, Howe GR, Ryan P, Menegoz F, Giles GG, Rodvall Y, Choi NW, Little J, Arslan A (1998) An international case-control study of adult glioma and meningioma: The role of head trauma. *International Journal of Epidemiology* 27:579-586.
46. Reilly KM, Loisel DA, Bronson RT, Mclaughlin ME, Jacks T (2000) Nf1; Trp53 mutant mice develop glioblastoma with evidence of strain-specific effects. *Nat Genet* 26:109–113.
47. Ren Y, Kang CS, Yuan XB, Zhou X, Xu P, Han L, Wang GX, Jia Z, Zhong Y, Yu S, Sheng J, Pu PY (2010) Co-delivery of as-miR-21 and 5-FU by poly(amidoamine) dendrimer attenuates human glioma cell growth *in vitro*. *J Biomater Sci Polym Ed* 21:303-314.
48. Rickert CH, Paulus W (2001) Epidemiology of central nervous system tumors in childhood and adolescence based on the new WHO classification. *Childs Nerv Syst* 17:503–511.

49. Rosemberg CA, Fujiwara D (2005) Epidemiology of pediatric tumors of the central nervous system according to the WHO 2000 classification: a report of 1, 195 cases from a single institution. *Childs Nerv Syst* 21:940–944.
50. Salvati M, Frati A, Russo N, Caroli E, Polli FM, Minniti G, Delfini R (2003) Radiation-induced gliomas: Report of 10 cases and review of the literature. *Surgical Neurology* 60:60-7.
51. Sanai N (2012) Emerging operative strategies in neurosurgical oncology. *Curr Opin Neurol* 25:756–766.
52. Schwartzbaum J, Fisher J, Aldape K, Wrensch M (2006) Epidemiology and molecular pathology of glioma. *Nat Clin Pract Neurol* 2:494-503.
53. Shete S, Hosking FJ, Robertson LB, Dobbins SE, Sanson M, Malmer B, Simon M, Marie Y, Boisselier B, Delattre JY, Hoang-Xuan K, El Hallani S, Idbaih A,Zelenika D, Andersson U, Henriksson R, Bergenheim AT, Feychting M, Lönn S, Ahlbom A, Schramm J, Linnebank M, Hemminki K, Kumar R, Hepworth SJ, Price A, Armstrong G, Liu Y, Gu X, Yu R, Lau C, Schoemaker M, Muir K, Swerdlow A, Lathrop M, Bondy M, Houlston RS (2009) Genome-wide association study identifies five susceptibility loci for glioma. *Nat Genet* 41, 899–904.
54. Stupp R, Mason WP, van den Bent MJ, Weller M, Fisher B, Taphoorn MJ, Belanger K, Brandes AA, Marosi C, Bogdahn U, Curschmann J, Janzer RC, Ludwin SK, Gorlia T, Allgeier A, Lacombe D, Cairncross JG, Eisenhauer E, Mirimanoff RO; European Organisation for Research and Treatment of Cancer Brain Tumor and Radiotherapy Groups; National Cancer Institute of Canada Clinical Trials Group (2005) Radiotherapy plus concomitant and adjuvant temozolomide for glioblastoma. *N Engl J Med* 352:987-996.
55. Tallet AV, Azria D, Barlesi F, Spano JP, Carpentier AF, Goncalves A, Metellus P (2012) Neurocognitive function impairment after whole brain radiotherapy for brain metastases: actual assessment. *Radiat. Oncol* 7:1-8.
56. Tanase CP, Enciu AM, Mihai S, Neagu AI, Calenic B, Cruceru ML (2013) Anti cancer therapy in higi grade gliomas. *Curr Proteomics* 10:246-260.
57. Tibbetts KM, Emnett RJ, Gao F, Perry A, Gutmann DH, Leonard JR (2009) Histopathological predictors of pilocytic astrocytoma event-free survival. *Acta Neuropathol* 117:657–665.

58. Ujifuku K, Mitsutake N, Takakura S, Matsuse M, Saenko V, Suzuki K, Hayashi K, Matsuo T, Kamada K, Nagata I, Yamashita S (2010) miR-195, miR-455-3p and miR-10a(*) are implicated in acquired temozolomide resistance in glioblastoma multiforme cells. *Cancer Lett* 296:241-248.
59. Verhaak RG, Hoadley KA, Purdom E, Wang V, Qi Y, Wilkerson MD, Miller CR, Ding L, Golub T, Mesirov JP, Alexe G, Lawrence M, O'Kelly M, Tamayo P, Weir BA, Gabriel S, Winckler W, Gupta S, Jakkula L, Feiler HS, Hodgson JG, James CD, Sarkaria JN, Brennan C, Kahn A, Spellman PT, Wilson RK, Speed TP, Gray JW, Meyerson M, Getz G, Perou CM, Hayes DN; Cancer Genome Atlas Research Network (2010) Integrated genomic analysis identifies clinically relevant subtypes of glioblastoma characterized by abnormalities in PDGFRA, IDH1, EGFR, and NF1. *Cancer Cell* 17:98–110.
60. Verhaak RG, Hoadley KA, Purdom E, Wang V, Qi Y, Wilkerson MD, Miller CR, Ding L, Golub T, Mesirov JP, Alexe G, Lawrence M, O'Kelly M, Tamayo P, Weir BA, Gabriel S, Winckler W, Gupta S, Jakkula L, Feiler HS, Hodgson JG, James CD, Sarkaria JN, Brennan C, Kahn A, Spellman PT, Wilson RK, Speed TP, Gray JW, Meyerson M, Getz G, Perou CM, Hayes DN; Cancer Genome Atlas Research Network (2010) Integrated genomic analysis identifies clinically relevant subtypes of glioblastoma characterized by abnormalities in PDGFRA, IDH1, EGFR, and NF1. *Cancer Cell* 17:98–110.
61. Von Deimling A, von Ammon K, Schoenfeld DA, Wiestler OD, Seizinger BR, Louis DN (1993) Subsets of glioblastoma multiforme defined by molecular genetic analyses. *Brain Pathol* 3:19-26.
62. Watanabe K, Tachibana O, Sata K, Yonekawa Y, Kleihues P, Ohgaki H (1996) Overexpression of the EGF receptor and p53 mutations are mutually exclusive in the evolution of primary and secondary glioblastomas. *Brain Pathol* 6:217–23.
63. Wick W, Hartmann C, Engel C, Stoffels M, Felsberg J, Stockhammer F, Sabel MC, Koeppen S, Ketter R, Meyermann R, Rapp M, Meisner C, Kortmann RD,Pietsch T, Wiestler OD, Ernemann U, Bamberg M, Reifenberger G, von Deimling A, Weller M (2009) NOA-04 randomized phase III trial of sequential radiochemotherapy of anaplastic glioma with procarbazine, lomustine, and vincristine or temozolomide. *J Clin Oncol* 27:5874-5880.

64. Wrensch M, Kelsey KT, Liu M, Miike R, Moghadassi M, Sison JD, Aldape K, McMillan A, Wiemels J, Wiencke JK (2005) ERCC1 and ERCC2 polymorphisms and adult glioma. *Neuro-oncol* 7: 495–507.
65. Wrensch M, Jenkins RB, Chang JS, Yeh RF, Xiao Y, Decker PA, Ballman KV, Berger M, Buckner JC, Chang S, Giannini C, Halder C, Kollmeyer TM, Kosel ML,LaChance DH, McCoy L, O'Neill BP, Patoka J, Pico AR, Prados M, Quesenberry C, Rice T, Rynearson AL, Smirnov I, Tihan T, Wiemels J, Yang P, Wiencke JK (2009) Variants in the CDKN2B and RTEL1 regions are associated with high-grade glioma susceptibility. *Nat Genet* 41, 905–8.
66. Xiao A, Wu H, Pandolfi PP, Louis DN, Van Dyke T (2002) Astrocyte inactivation of the pRb pathway predisposes mice to malignant astrocytoma development that is accelerated by PTEN mutation. *Cancer Cell* 1:157–168.
67. Yan H, Parsons DW, Jin G, McLendon R, Rasheed BA, Yuan W, Kos I, Batinic-Haberle I, Jones S, Riggins GJ, Friedman H, Friedman A, Reardon D, Herndon J, Kinzler KW, Velculescu VE, Vogelstein B, Bigner DD (2009) IDH1 and IDH2 mutations in gliomas. *N Engl J Med* 360:765–73.
68. Yang P, Kollmeyer TM, Buckner K, Bamlet W, Ballman KV, Jenkins RB (2005) Polymorphisms in GLTSCR1 and ERCC2 are associated with the development of oligodendrogliomas. Cancer 103: 2363–2372.

Chapter – 2

Increased β-Catenin/Tcf signaling in pilocytic astrocytomas: A comparative study to distinguish pilocytic astrocytomas from low-grade diffuse astrocytomas

2.1. Introduction

Astrocytomas are tumors that are alleged to arise from precursors of astrocytes – supportive cells of the brain having star-like shape and they are the most common of primary brain tumors. They are classified into four different malignancy grades according to World Health Organization (WHO) classification. Grade III (anaplastic astrocytoma) and IV (glioblastoma multiforme – GBM) astrocytomas are the fast growing tumors, and are also called high-grade tumors. Grades I (pilocytic astrocytoma) and II (diffuse astrocytoma) astrocytomas are the slowest growing tumors, and are also called low-grade astrocytomas.

Pilocytic astrocytoma is more common in the ages 5-14 years and the second among age group between 0-4 years and 15-19 years, although it constitutes only 6% of all gliomas (CBTRUS, 2012). Pilocytic astrocytoma occurs equally in males and females, and 75% of occurrence is reported in the ages of 6 to 13 years-old (Louis et al, 2007). These tumors are slow-growing, indolent, well circumscribed tumors and associated with excellent prognosis and 10 year survival rates range from 90 to 96.8% (Giannini and Scheithauer, 1997; Kleihues and Cavenee, 2000; CBTRUS, 2005; Burkhard et al, 2003). However, 10-20% of patients suffer with recurrence of growing residual lesions and in 2-3% of the patients residual tumor may disseminate through the spinal cord (Jones, 2011). This type of tumor behaviour is more frequent in adults and older patients, which explains the difference in the 10-year survival (Johnson, 2012). In general, the prognosis between children and adults is significantly different. While 5-year survival of children and young adults is >90%, in the group of 60+ years patients it is only 52% (Johnson, 2012). Even though main location of pilocytic astrocytoma is the cerebellum, with more than 60% of the cases occurring in cerebellar hemispheres, however, it can arise all through the neuraxis, including hypothalamic region, the optic-chiasmatic tract and spinal cord, with some cases involving the whole spinal cord which have worse outcome (Fernandez, 2003). The clinical signs and symptoms of pilocytic astrocytoma depends upon its location in neuraxis and affected area. As the most common location is the cerebellum, headache and neck pain, vomiting, posture disturbance and visual abnormalities are usually common (Burger, 1994; Abdollahzadeh, 1994). In supratentorial tumors, the occurrence of seizures may be seen and is related to cortical involvement (Burger, 1994). Occurrence of pilocytic astrocytoma in the hypothalamic area may affect hormonal functions leading to diabetes insipidus, obesity, hyperkinesis, irritability and accelerated growth and involvement of the optical pathway is related to visual loss or visual-field deficits

(Koeller, 2004). Histologically these tumors are well characterized with the areas showing compact biphasic pattern, oligodendroglial morphology, glomeruloid vasculature, heterogeneity in cellular density, cellular pleomorphism, microglial distribution, microcystic areas, Rosenthal fibers, and eosinophilic granular bodies (Tanaka et al, 2008; Tibbetts et al, 2009).

Diffuse astrocytoma (grade II) is a well-differentiated and slow growing tumor, but shows a consistent tendency to recur after surgical resection, and this is often associated with progression to a higher grade of malignancy, that is, anaplastic astrocytoma (WHO grade III) and eventually secondary glioblastoma (WHO grade IV) (Louis, 2007; Ohgaki, 2005). Diffuse astrocytomas commonly occur in young adults (~34 years), characterized by high degree of cellular differentiation, slow growth and diffuse infiltration into neighbouring structures and absence of microvascular proliferation, necrosis and single mitoses may or may not be present. They are predominantly composed of a microcystic tumor matrix within which are embedded fibrillary neoplastic astrocytes with mild nuclear atypia and a low cellular density. There is occasional occurrence of gemistocytes in a diffuse astrocytoma. More frequently they occur in cerebral hemispheres and show biphasic distribution, with one peak in childhood (6-12 years) and the other peak in early adulthood (26-46 years) (Tonn, 2006). Patients with diffuse astrocytoma exhibit clinical symptoms like headache and seizures in 30-50% cases. Depending on the size of the tumor and its location other features may also be present, e.g. hydrocephalus, focal neurological dysfunction including personality change.

However, there are serious clinical problems in distinguishing grade II tumors from grade I tumors especially in the case of diffuse fibrillary astrocytomas showing the features of increased cellular and nuclear pleomorphism. Due to huge discrepancy in histopathological appearance, the diagnosis of pilocytic astrocytoma is usually challenging, especially in minute biopsies, and is greatly dependent upon correlation with neuro-radiological aspects and most of the times pathologists misdiagnose pilocytic astrocytomas as higher-grade tumors at primary diagnosis (Aldape, 2000). In this aspect, clinical correlation and use of immuno-histochemical markers can help in better defining the diagnosis.

2.1.1. Immunohistochemical markers

Current markers fail to delineate between pilocytic astrocytoma and diffuse astrocytomas. For example, Glial Fibrillary Acidic Protein (GFAP) which is a cytoplasmic

intermediate filament helps in differentiating pilocytic astrocytoma from other gliomas such as ependymomas and oligodendrogliomas but not from diffuse astrocytoma. Other immunohistochemical markers like Ki67 and galectin-3 (gal-3) to some extent help in diagnosis of pilocytic astrocytomas. Ki67 is a non-histone nuclear protein expressed in all stages except G0 and early G1 phase of the cell cycle (Burger, 1986). Ki67 permits accurate estimation of proliferation index in neoplasms. Pilocytic astrocytomas show low proliferation index of around 2% (Bowers et al, 2003) compared to diffuse astrocytoma which is >2% (Neder et al, 2004). But sometimes even pilocytic astrocytomas show proliferation index as high as 4.4% (Roessler et al, 2002) thereby questioning the use of Ki67 as a diagnostic marker. Galectin-3 is a carbohydrate-binding protein that binds exactly to β-galactosides sugars. This protein plays vital role in various biological processes, such as cellular proliferation, apoptosis, transcriptional regulation, intracellular signaling, adhesion and migration (Park et al, 2008). Gal-3 expression is found to be present in both cytoplasm and nucleus of neoplastic cells. Though numerous studies have tried to correlate the amount of gal-3 expression to the clinical behavior of pilocytic astrocytoma, but no prognostic significance has been proved. Still, as gal-3 expression is an obvious finding in pilocytic astrocytomas, to some extent this marker may be useful in distinguishing it from other astrocytoma grades and its diagnosis (Park et al, 2008; Borges et al, 2011).

Since there is no perfect marker to differentiate pilocytic astrocytoma from diffuse astrocytoma, the genetic characteristics of pilocytic astrocytoma have recently been the focus to better understand the behaviour of this tumor. Molecular pathways altered in pilocytic and diffuse astrocytoma are different. The growth factors like epidermal growth factor receptor (EGFR) and platelet derived growth factor receptor (PDGFR) involved in invasion and malignant progression are highly expressed in diffuse astrocytoma compared to pilocytic astrocytoma (Huang et al, 2005; Rorive et al, 2006). Moreover, tumor suppressor genes like *TP53* and *PTEN* are highly altered in diffuse astrocytoma, whereas they are normally expressed in pilocytic astrocytoma (Beatriz et al, 2007). There are other genes and pathways which are altered in pilocytic astrocytoma. For example, there is loss of *NF1* gene expression resulting in the activation of RAS-RAF-MERK-ERK molecular pathway or the mTOR/AKT pathway in pilocytic astrocytomas (Jones et al, 2011). Besides, an oncogene *BRAF* is constitutively activated in 80% of pilocytic astrocytoma cases (Riemenschneider et al, 2010). But these alterations are not specific to pilocytic astrocytomas and can be detected in various other brain tumors like pleomorphic xanthoastrocytoma, ganglioglioma. So understanding the molecular

components that are specifically altered and responsible for the progression of pilocytic astrocytoma may be important in its distinction from diffuse astrocytoma and its treatment.

2.1.2. Wnt/β-catenin/Tcf signaling pathway

Wnt signaling is a major developmental pathway involved in neural stem cell self-renewal and differentiation (Zechner et al, 2003). The Wnt pathway components affect major developmental properties like embryonic induction, generation of cell polarity, and the specification of cell fate (Logan et al, 2004), tissue homeostasis and cancer. Besides, this pathway is involved in the nervous system development (Lie et al, 2005) and alteration in this pathway may lead to development of central nervous system (CNS) malignancy. In general the Wnt signaling components are divided into upstream players, central player and downstream affecters. The upstream players are Wnt ligands, a member of the Frizzled (Fzd) family and either one of two single-span transmembrane proteins, low density-lipoprotein receptor related proteins (LRP5 and LRP6) (Jeannet and He, 2000). Wnt signaling proteins binds specifically to Frizzled (Fzd) receptor complexes on the surface of target cells and form Fzd/LRP coreceptor complex activating canonical Wnt signaling pathway (Pinson et al, 2000; Tamai et al, 2000; Wehrli et al, 2000). The central player of the canonical signaling pathway is β-catenin (*CTNNB1)*, a cytoplasmic protein whose stability is regulated by the ‘‘destruction complex’’. In this complex the Axin and APC proteins form a scaffold that facilitates β-catenin phosphorylation by CK1α and GSK3β. Phosphorylated β-catenin is subsequently recognized and ubiquitinylated, resulting in its proteasomal degradation (Moon et al, 2004; Polakis, 2000). The resulting low level of β-catenin allows the DNA binding Tcf/Lef proteins to interact with transcriptional co-repressors to block target genes expression in the nucleus (Brown et al, 1998; Barker and Clevers, 2006). In presence of Wnt ligand, formation of Dvl-Fzd complexe takes place and subsequent phosphorylation of LRP by CK1γ facilitates relocation of Axin to the membrane and consequent inactivation of the destruction box (Cliffe et al, 2003; Pinson et al, 2000). This allows β-catenin to accumulate and enter the nucleus, where it interacts with the members of the Tcf/Lef family. In the nucleus β-catenin converts the Tcf/Lef proteins into potent transcriptional activators by displacing transcriptional repressor groucho/TLE proteins and recruiting an array of co-activator proteins including CBP, TBP, BRG1, BCL9/PYG, Legless, Mediator and Hyrax. This ensures efficient activation of Tcf target genes such as c-myc, n-myc, cyclinD1, c-jun, MMP7, VEGF, IL-8 etc (He et al, 1998; Shiina et al, 2003; Shtutman et al, 1999). The over view of Wnt signaling pathway is shown in fig. 2.1.

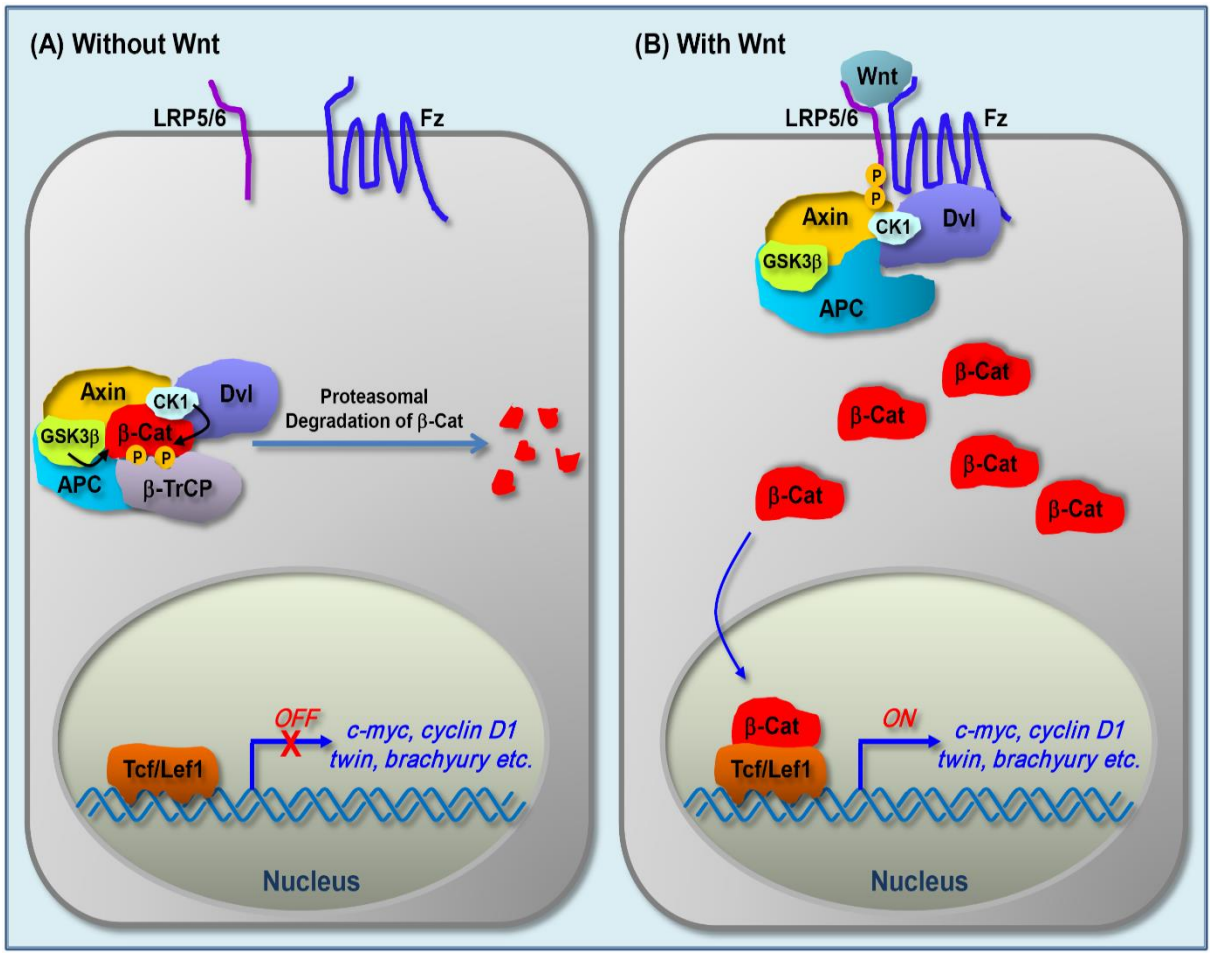

Fig. 2.1. Wnt/β-catenin signaling pathway. Schematic diagram for the core components and signal transduction of Wnt/β-catenin pathway. (A) In the absence of Wnt, GSK3β and CK1 phosphorylate β-catenin degradation complex which includes APC and Axin. The phosphorylated β-catenin is recognized by β-TrCP and subsequently degraded by proteasomal pathway. As a result, TCF/LEF1 suppresses the expression of target genes. (B) In the presence of Wnt, binding of Wnt to Fz and its co-receptor LRP5/6 leads to phosphorylation of LRP6. Axin, itself alone or whole β-catenin degradation complex including Axin, translocates to the phosphorylated LRP5/6, which leads to stabilization of cytoplasmic β-catenin. The stabilized β-catenin translocates into the nucleus and interacts with TCF/LEF1, which in turn enhances the expression of target genes (Kim and Jho, 2014).

Recent studies have reported aberrant activation of Wnt signaling pathway in malignant progression of gliomas. Sareddy et al., have shown that Wnt/β-catenin/Tcf signaling pathway is constitutively activated in astrocytic tumors of humans and expression of Wnt pathway components both at mRNA and protein level were positively correlating with the histological malignancy of the tumor (Sareddy et al, 2009). In another study patients with reduced β-catenin

expression levels tend to be associated with a better prognosis than those with high levels (Zhang et al, 2010). Further, siRNA mediated down regulation of Wnt2 and β-catenin supressed malignant glioma growth both *in vitro* and *in vivo* by decreasing PI3K/p-AKT expression (Pu et al, 2009).

However, the status of Wnt pathway in pilocytic astrocytomas is not well understood. Therefore, in this study, we investigated Wnt signaling pathway components β-catenin, Lef1, Tcf4 and c-Myc in a panel of pilocytic astrocytoma samples and compared with diffuse astrocytomas of all grades.

2.2. Materials and Methods

2.2.1. Sample collection

Total 47 astrocytic tumor samples were collected from patients who underwent surgical resection at Nizam Institute of Medical Sciences (Hyderabad, India) and Krishna Institute of Medical Sciences (Secunderabad, India). The tumors were classified histopathologically according to the WHO classification: 15 pilocytic astrocytoma (PILO; grade I), 8 diffuse astrocytomas (DA; grade II), 7 anaplastic astrocytomas (AA; grade III), and 17 glioblastoma multiforme (GBM; grade IV). The case details of astrocytoma patients are summarized in table 2.1. Three normal brain specimens consisting of periventricular region were obtained from patients with temporal lobe epilepsy and these specimens were histologically normal as confirmed by neuropathologist. All samples were obtained from patients after taking the informed consent from patients or their relatives. A part of the surgically removed samples were immediately snap frozen in liquid nitrogen and then stored at -80°C until analysis. The remaining samples were fixed with formalin and embedded in paraffin. These fixed samples were used for routine H&E staining, as well as for immunohistochemical analyses.

Table 2.1. Clinical characteristics of astrocytoma patients

No	Age	Sex	Grade	Location
Control 1	16	M	TLE	Periventricular
Control 2	12	F	TLE	Periventricular
Control 3	28	M	TLE	Periventricular
1	7	M	I	Optic pathway
2	14	M	I	Cerebellum

No	Age	Sex	Grade	Location
3	7	M	I	Cerebellum
4	18	F	I	Thalamus
5	5	M	I	Septum
6	11	F	I	Brainstem
7	12	M	I	Temporal lobe
8	7	M	I	Vermis
9	13	F	I	Cerebellum
10	28	F	I	Cerebellum
11	10	M	I	Cerebellum
12	3	F	I	Temporal lobe
13	9	F	I	Cerebellum
14	12	M	I	Cerebellum
15	24	M	I	Thalamus
16	34	F	II	Fronto-temporal
17	35	M	II	Frontal
18	27	M	II	Fronto-temporal
19	30	M	II	Frontal
20	16	M	II	Frontal
21	60	M	II	Parietal
22	37	F	II	Tempero-frontal
23	40	M	II	Frontal
24	29	M	III	Frontal
25	62	F	III	Parietal
26	35	M	III	Frontal
27	37	M	III	Frontal
28	30	F	III	Frontal
29	45	F	III	Fronto-temporal
30	43	M	III	Frontal
31	45	M	IV	Parietal
32	36	F	IV	Frontal
33	16	M	IV	Frontal
34	52	M	IV	Frontal
35	20	M	IV	Frontal

No	Age	Sex	Grade	Location
36	19	M	IV	Tempero-parietal
37	27	M	IV	Frontal
38	48	M	IV	Temporal
39	15	M	IV	Frontal
40	58	F	IV	Fronto-tempero-parietal
41	61	M	IV	Frontal
42	50	M	IV	Corpus callosal
43	55	M	IV	Frontal
44	5	M	IV	Multiple intra cranial
45	30	M	IV	Frontal
46	40	M	IV	Parietal
47	34	M	IV	Temporal

2.2.2. Preparation of soluble cell lysates

Deep frozen samples were thawed gradually and homogenized by using dounce homogenizer in 5 volumes of RIPA (radioimmunoprecipitaiton assay) buffer containing 50 mM Tris-HCl (pH 8.0), 150 mM NaCl, 1 mM EDTA, 0.4% deoxy-cholate, 1% NP-40 containing protease inhibitors including 1 mM phenyl methyl sulfonyl fluoride (PMSF) and phosphatase inhibitors including 10 mM β-glycerophosphate, 10 mM NaF, 0.3 mM Na3VO4 and 0.3 mM aprotinin. The lysates were sonicated for 2 min and then centrifuged at 14,000g for 15 min at 4^{o}C. The supernatant (whole tissue lysate) was collected and frozen at -80^{o}C before use. Protein concentrations were determined by Lowry method.

2.2.3. Western blotting

Equal amount of proteins (75 μg) were resolved on 10% SDS-polyacrylamide gels and then transferred on to nitrocellulose membranes. After, blocking the membranes in 5% milk solution for 1 h at room temperature, blots were probed with β-catenin, Tcf4, Lef1, c-Myc and β-actin primary antibodies (Cell Signaling Technology, Beverly, MA, USA) for overnight at 4°C. Blots were again incubated with secondary antibodies conjugated to alkaline phosphatase (ALP) for 1 h at room temperature and developed with BCIP-NBT solution (Genei Pvt Ltd, Bangalore, India). Blots were analysed quantitatively using scion image software (NIH).

2.2.4. Immunohistochemistry

Immunohistochemical studies were performed on formalin-fixed, paraffin-embedded specimens. Briefly, sections were deparaffinized in xylene and passed through graded alcohols and further rehydrated in phosphate buffered saline (PBS). Antigen unmasking was carried out by micro waving the sections for 10-14 min in 10 mM citrate buffer (pH 6.0). Sections were then treated with 3% H2O2 for 10 min to inhibit endogenous peroxidase followed by incubation with serum for 1 h at room temperature in a humid chamber. The sections were then incubated overnight at 4^{o}C with primary antibodies against β-catenin (1:100 dilution), Tcf4 (1:100 dilution), Lef1 (1:1000 dilution) and c-Myc (1:100 dilution) as per data sheet in blocking solution. Peroxidase conjugated secondary antibody was used for 1 h incubation time at room temperature followed by TBS washes (3x5 min each). Diaminobenzidine (DAB) in buffer was used till sections develop color. Then sections were counterstained using haematoxylin. Sections were washed with distilled water followed by dehydration in graded alcohols, xylene and mounted with DPX (kit obtained from Biogenex Pvt Limited, India). In each experiment, a negative control was included in which the primary antibody step was skipped and replaced by non-immune serum.

The number of immunostained cells in each grade is evaluated quantitatively in terms of positive staining for β-catenin, Lef1, Tcf4 and c-Myc. The positive areas were selected randomly in tumor section. The staining indices for β-catenin, Tcf4, Lef1 and c-Myc were calculated as the ratio of positive cells in high power microscopic fields (HPF) to all the cells in the HPF. Positivity in vascular proliferative and necrotic regions was carefully omitted.

2.2.5. Statistical Analysis

Statistical analysis was performed using sigma stat version 3.1. All data were represented as mean ± SD obtained from individual patients of each grade and were compared with control. The significant differences of the data were determined using one-way ANOVA. Differences between tumor samples and controls were compared by paired Student's t-test. Values of $P < 0.05$ were considered as statistically significant.

2.3. Results

2.3.1. Elevation of β-Catenin, Lef1, Tcf4 and c-Myc Levels in Pilocytic Astrocytomas and GBM

Aberrant activation of Wnt signaling pathway contributes to the malignant growth of several tumors including gliomas. Sareddy et al, investigated the expression levels of Wnt

pathway components in a panel of 32 diffuse astrocytoma patients and determined that Wnt pathway is abnormally activated in these tumors compared to normal brain samples and positively correlated with the pathological grading of astrocytomas. To evaluate the status of Wnt pathway activity, β-catenin, Lef1, Tcf4 and c-Myc levels were measured by western blotting in a panel of 15 pilocytic astrocytomas and these levels were compared with diffuse astrocytomas. As shown in fig.2.2A, β-catenin, Lef1, Tcf4 and c-Myc levels were upregulated in astrocytoma samples compared to control samples. Quantitative densitometric analysis showed that the β-catenin, Lef1, Tcf4, and c-Myc levels were significantly elevated in pilocytic astrocytomas and GBM when compared to control ($P < 0.05$) (Fig. 2.2B). In addition β-catenin, Lef1, Tcf4 and c-Myc levels also significantly increased in pilocytic astrocytomas and GBM compared to grade II diffuse astrocytomas ($P < 0.05$). The mean increase in protein expression levels of β-catenin in grade I (253.6 ± 5.4), grade II (158.4 ± 6.4), grade III (189.5 ± 8.2), grade IV (326.7 ± 7.4) were statistically significant ($p < 0.05$) when compared to control (9.3 ± 2.12). The mean increase in protein expression levels of Lef1 in grade I (104.6 ± 4.2), grade II (78.2 ± 5.3), grade III (82.3 ± 6.3), grade IV (108.9 ± 7.4) were statistically significant ($p < 0.05$) when compared to control (18.4 ± 5.07). The mean increase in protein expression levels of Tcf4 in grade I (112.4 ± 2.9), grade II (82.2 ± 4.21), grade III (84.6 ± 5.8), grade IV (129.7 ± 8.12) were statistically significant ($p < 0.05$) when compared to control (14.2 ± 2.31). The mean increase in protein expression levels of c-Myc in grade I (121.6 ± 8.09), grade II (45.8 ± 0.9), grade III (47.3 ± 1.04), grade IV (139.7 ± 5.3) were statistically significant ($p < 0.05$) when compared to control (8.7 ± 2.01). Interestingly, the levels of these proteins were differentially expressed in grade I and grade II astrocytic tumors. The mean increase in protein expression levels of β-catenin in grade I (253.6 ± 5.4) were statistically significant ($p < 0.05$) when compared to grade II (158.4 ± 6.4). The mean increase in protein expression levels of Lef1 in grade I (104.6 ± 4.2) were statistically significant ($p < 0.05$) when compared to grade II (78.2 ± 5.3). The mean increase in protein expression levels of Tcf4 in grade I (112.4 ± 2.9) were statistically significant ($p < 0.05$) when compared to grade II (82.2 ± 4.21). The mean increase in protein expression levels of c-Myc in grade I (121.6 ± 8.09) were statistically significant ($p < 0.05$) when compared to grade II (45.8 ± 0.9).

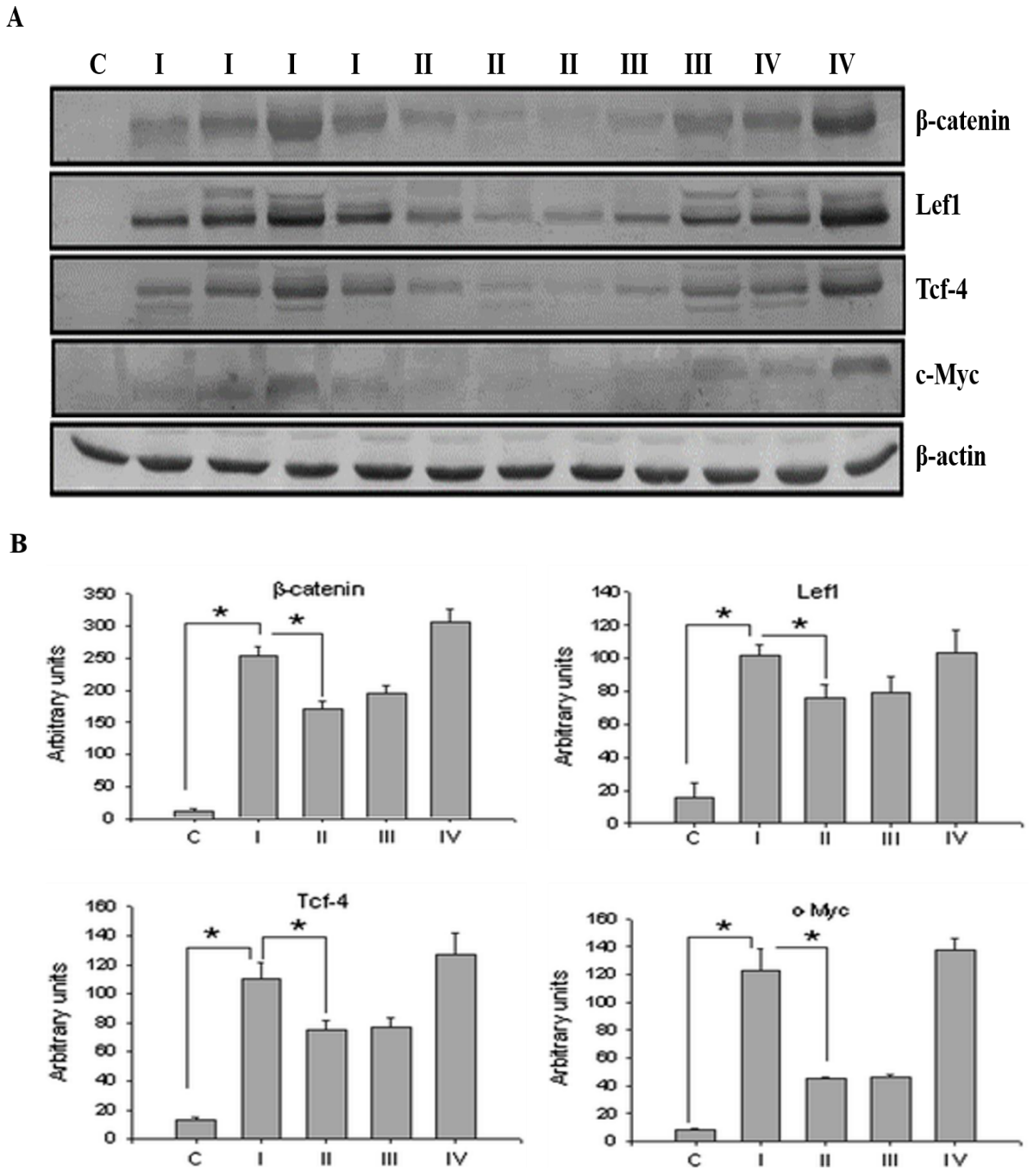

Fig. 2.2. Overexpression of β-catenin, Lef1, Tcf4 and c-Myc in pilocytic astrocytoma and GBM. A. Equal amounts of total cellular protein from astrocytomas of different grades and control sample were subjected to western blotting. β-actin used as loading control. **B.** Quantitative densitometric analysis showed that the levels of β-catenin, Lef1, Tcf4 and c-Myc were significantly higher in pilocytic astrocytomas and GBM than that of diffuse astrocytomas and control brain. I-pilocytic astrocytoma, II-diffuse astrocytoma, III-anaplastic astrocytoma. IV-GBM, C- normal control brain sample. * denotes $P < 0.05$.

2.3.2. Immunohistochemical expression of β-Catenin, Lef1, Tcf4 and c-Myc protein staining indices were higher in pilocytic astrocytomas and GBM

To corroborate with the western blot results, tumor sections from different grades of astrocytoma were immunohistochemically evaluated for the staining of β-catenin, Lef1, Tcf4 and c-Myc. The Ki-67 labelling index was performed on all sections of pilocytic astrocytoma ranged from 0.3% to 2%. Immunohistochemical analysis of β-catenin (Fig. 2.3), Lef1 (Fig. 2.4), Tcf4 (Fig. 2.5) and c-Myc (Fig. 2.6) showed that these proteins were strongly expressed in tumor cells of pilocytic astrocytoma and GBM. The mean labelling indices of β-catenin, Lef1, Tcf4 and c-Myc in pilocytic astrocytoma and GBM were statistically significant ($P < 0.05$) compared to grade II and control tumors. These results clearly manifested the differential expression of Wnt pathway components between pilocytic astrocytomas and diffuse grade II astrocytomas.

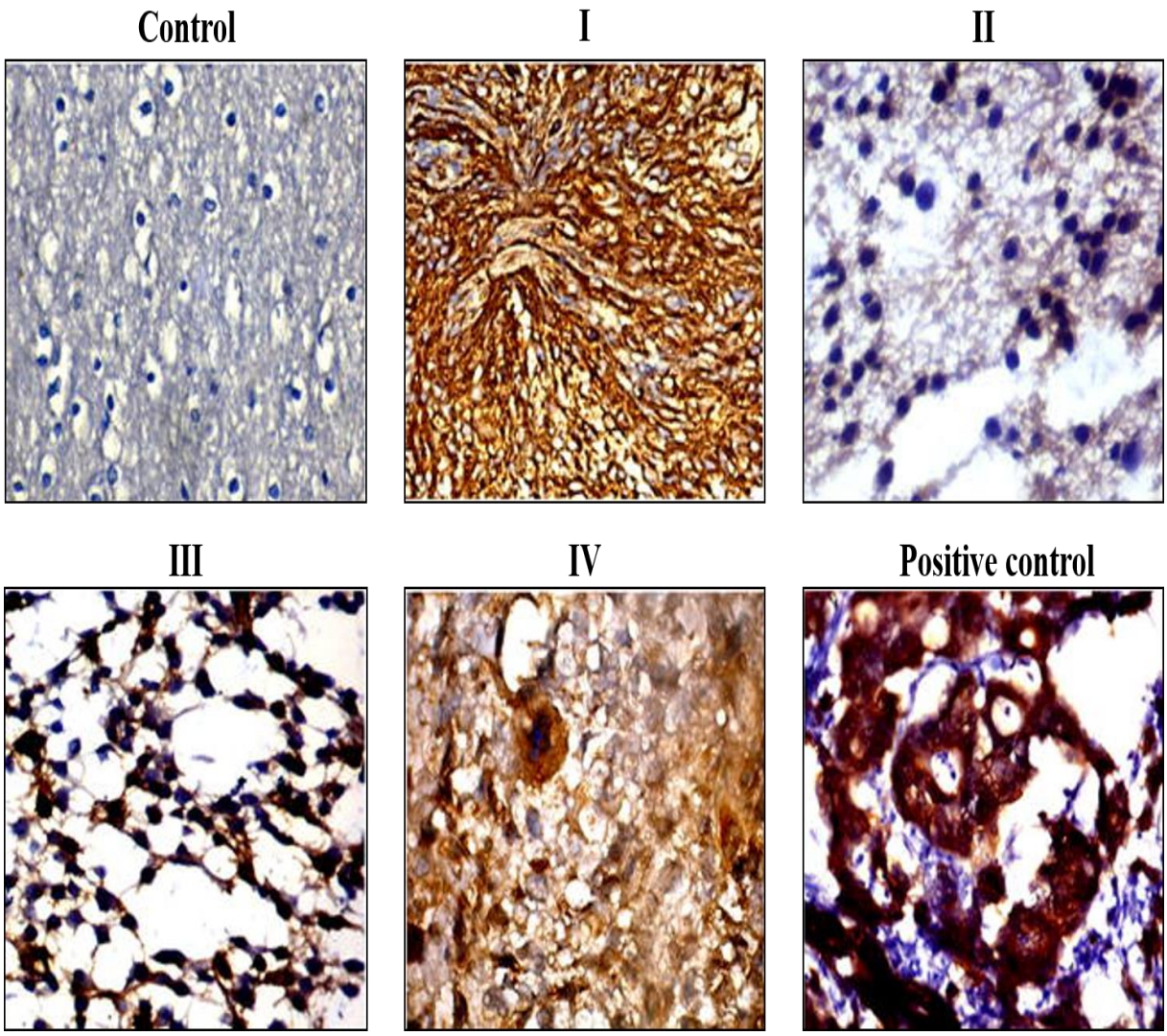

Fig. 2.3. Immunohistochemical analysis of β-catenin. Paraffin embedded tissue sections from control and astrocytomas of different grades were subjected to immunohistochemical analysis. Strong β-catenin immunoreactivity was observed in pilocytic astrocytomas than diffuse grade II tumors. Colon adenocarcinoma tissue section used as positive control. I-pilocytic astrocytoma, II-diffuse astrocytoma, III-anaplastic astrocytoma, IV-glioblastoma multiforme.

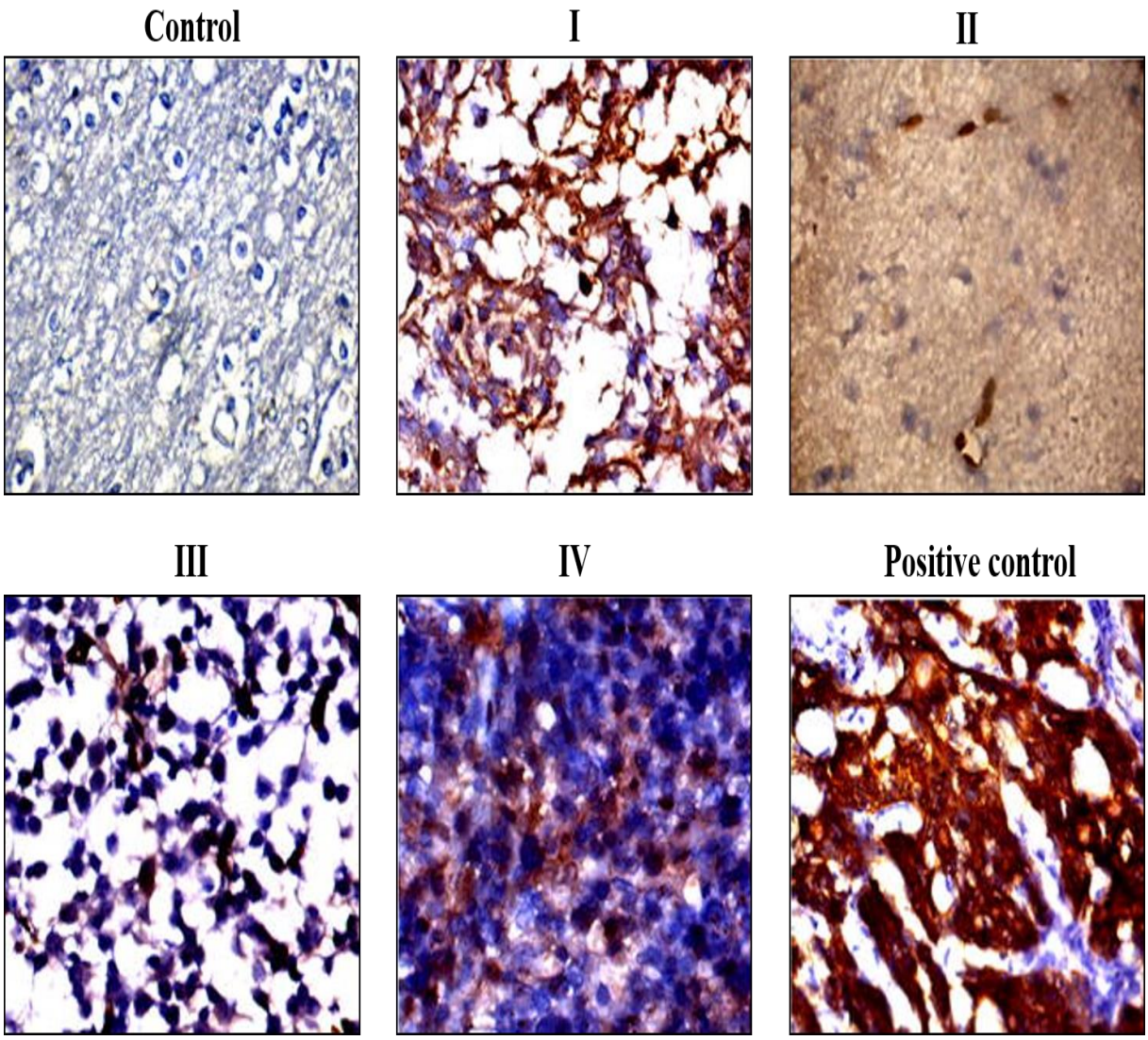

Fig. 2.4. Immunohistochemical analysis of Lef1. Paraffin embedded tissue sections from control and astrocytomas of different grades were subjected to immunohistochemical analysis. Lef1 immunoreactivity was observed in the nucleus of astrocytoma tissues and expression was more in pilocytic astrocytomas and high-grade tumors than diffuse grade II tumors. Colon adenocarcinoma tissue section used as positive control. I-pilocytic astrocytoma, II-diffuse astrocytoma, III-anaplastic astrocytoma, IV-glioblastoma multiforme.

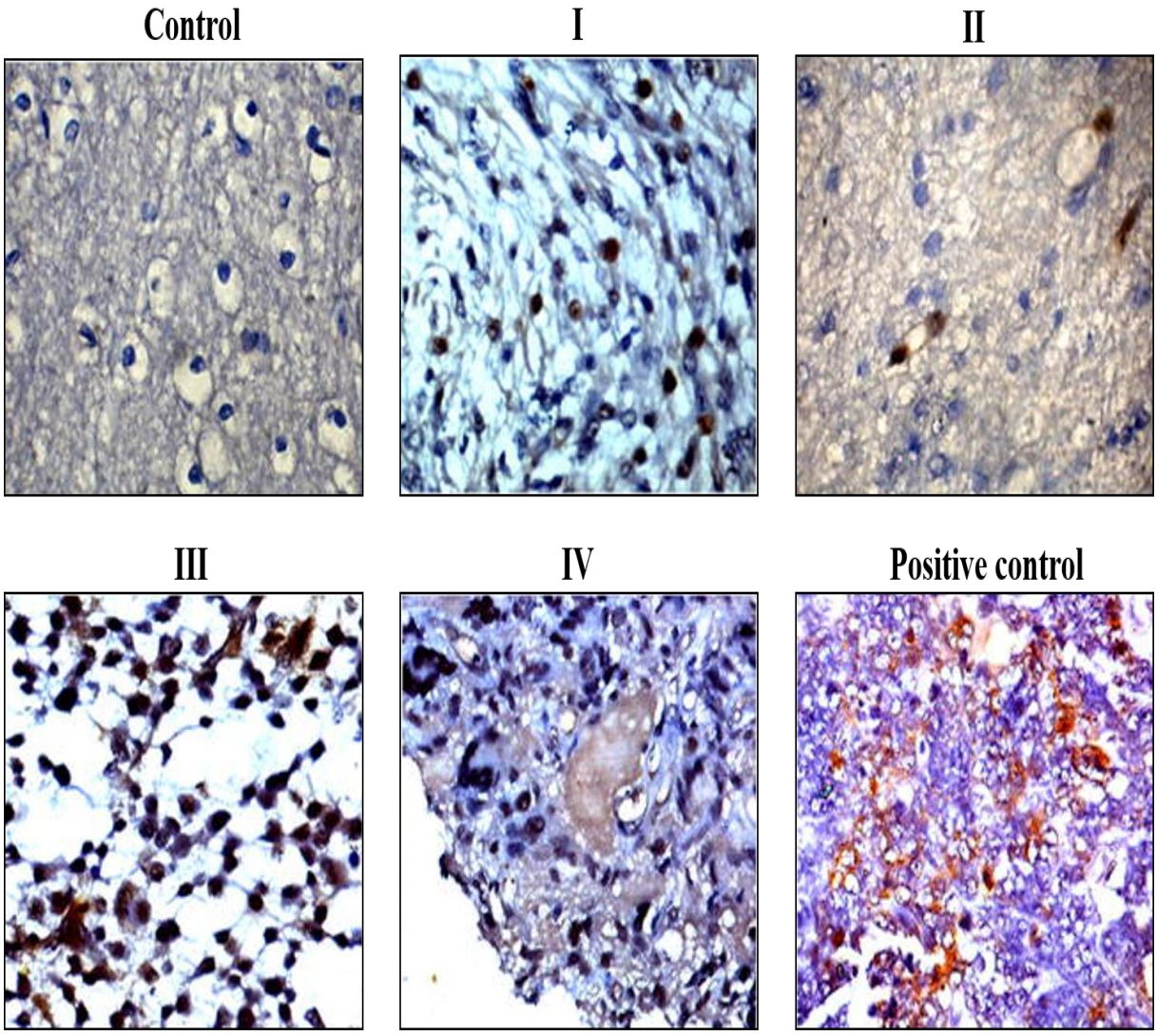

Fig. 2.5. Immunohistochemical analysis of Tcf4. Paraffin embedded tissue sections from control and astrocytomas of different grades were subjected to immunohistochemical analysis. Tcf4 immunoreactivity was observed in the nucleus of astrocytoma tissues and expression was more in pilocytic astrocytomas and high-grade tumors than diffuse grade II tumors. medulloblastoma tissue section used as positive control. I-pilocytic astrocytoma, II-diffuse astrocytoma, III-anaplastic astrocytoma, IV-glioblastoma multiforme.

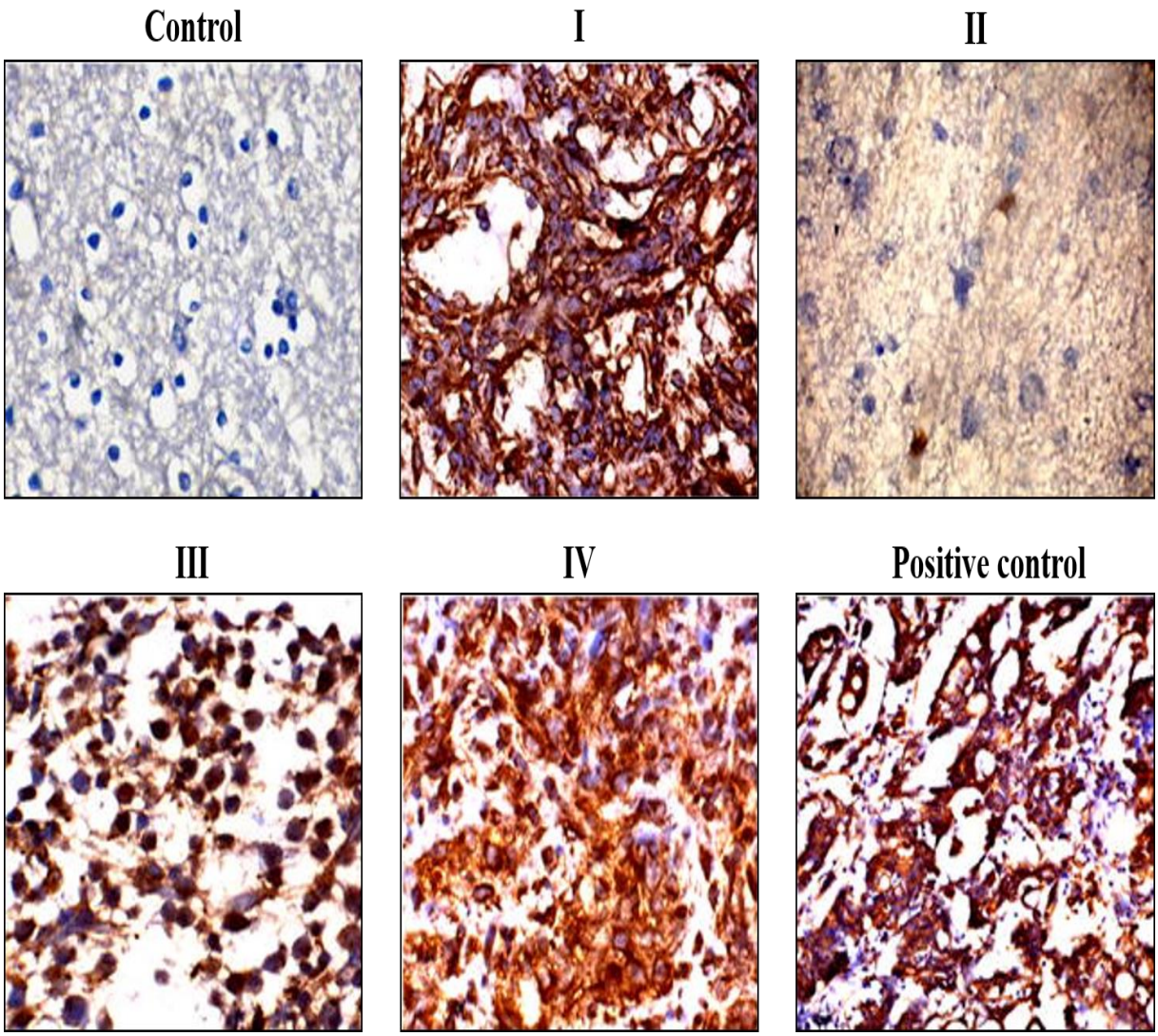

Fig. 2.6. Immunohistochemical analysis of c-Myc. Paraffin embedded tissue sections from control and astrocytomas of different grades were subjected to immunohistochemical analysis. c-Myc immunoreactivity was observed in the nucleus of astrocytoma tissues and expression was more in pilocytic astrocytomas and high-grade tumors than diffuse grade II tumors. Colon adenocarcinoma tissue section used as positive control. I-pilocytic astrocytoma, II-diffuse astrocytoma, III-anaplastic astrocytoma, IV-glioblastoma multiforme.

2.3.3. Strong expression of β-Catenin, Lef1, Tcf4 and c-Myc proteins in vascular endothelial cells of pilocytic astrocytomas and GBM

Vascular proliferations are the most common feature of angiogenesis which is the major factor contributing to tumor aggressiveness. Despite having microvascular proliferations pilocytic astrocytes are slow growing, benign and have well differentiated tumor margins.

Previous reports showed that Wnt signaling pathway plays crucial role in the proliferation and survival of endothelial cells. It has also been shown that β-catenin is expressed in endothelial cells of glial tumors. As shown in Fig. 2.7 microvascular proliferation, a characteristic feature of pilocytic astrocytomas and GBM showed strong positive staining for Wnt pathway components suggesting that these proteins are essential for endothelial cell proliferation, a major event in the abnormal growth of tumors.

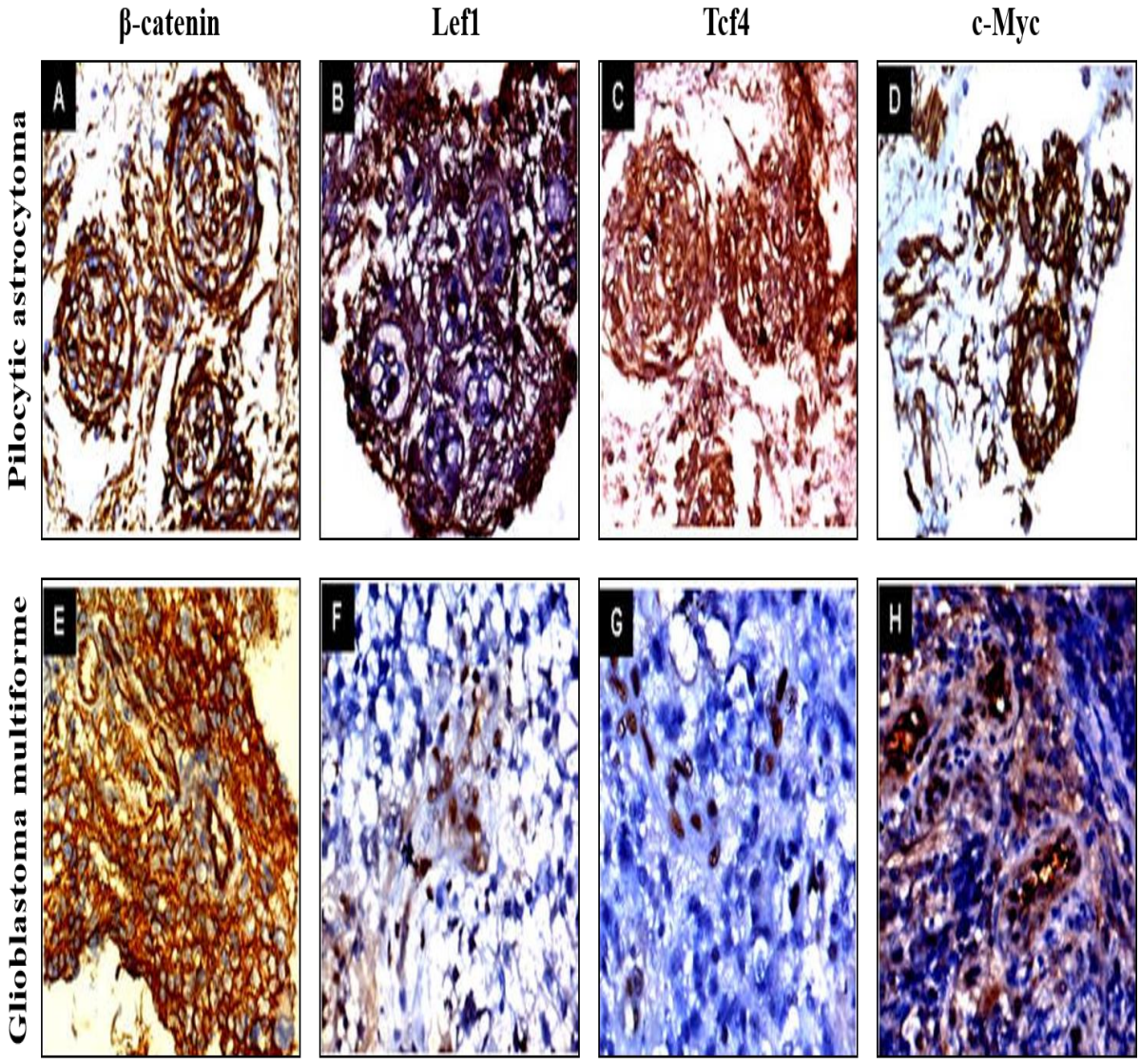

Fig. 2.7. Expression of β-catenin, Lef1, Tcf4 and c-Myc in vascular endothelial cells of pilocytic astrocytoma and GBM. Paraffin embedded tissue sections from pilocytic astrocytoma and GBM subjected to immunohistochemical analysis. Immunohistochemical analysis showed that β-catenin (**A, E**), Lef1 (**B, F**), Tcf4 (**C, G**) and c-Myc (**D, H**) were strongly expressed in endothelial cells of pilocytic astrocytoma (**A, B, C, D**) and GBM (**E, F, G, H**)

2.4. Discussion

The present study demonstrates the distinct protein expression of Wnt pathway components β-catenin, Lef1, Tcf4 and c-Myc in astrocytic tumors, with significantly higher levels in GBMs and pilocytic astrocytoma, in contrast with the low expression in diffuse astrocytoma.

Although considered them as grade I astrocytomas, pilocytic astrocytomas represent a separate clinicopathological entity from other grades of astrocytomas. In general, pilocytic astrocytomas are considered as benign with well-defined circumscribed boundaries. Their tendency towards infiltrative growth is very low when developed in cerebellum, but have worse prognosis when developed in sensitive areas like hypthalamo-chiasmatic and brain stem regions (Garcia et al, 1989; Tchoghandjian et al, 2009). Recently much interest is focused to understand the tumor behaviour of pilocytic astrocytomas. Several studies were conducted to draw a clinical boundary between pilocytic astrocytomas and diffuse astrocytomas and compared their molecular profile. Nevertheless, several complications are present in distinguishing pilocytic astrocytomas from grade II astrocytomas due to lack of proper diagnostic markers and molecular features. So, better understanding of the molecular basis of these tumors is crucial in delineating the characteristic differences of these tumors which are helpful in better characterization of grade I and grade II astrocytic tumors. Present study demonstrated the differential expression of Wnt signaling components β-catenin, Lef1, Tcf4 and c-Myc in astrocytic tumors, with significantly elevated expression in pilocytic astrocytomas and GBM than that of grade II astrocytomas. The oncogenic role of Wnt signaling has been elucidated in almost all human cancers and is essential in proper embryonic development and maintenance of stem cells of both adults and embryos. However, abnormal operation of this pathway leads to the tumor development. Previously, we and others have demonstrated the over activation of the components of this pathway in astrocytic tumors and showed positive correlation with the degree of malignancy. Accumulating evidences suggest that Wnt signaling pathway is activated in endothelial cells and induces the proliferation, survival and promotes angiogenesis via induction of IL-8 (Masckauchan et al, 2005; Levy et al, 2002). It is well known that angiogenesis is the critical event of infiltration and invasion all the tumors. Wnt signaling pathway has been detected in the vasculature *in vivo* (Wright et al, 1999; Maretto et al, 2003). Further evidences supported the role of Wnt pathway in angiogenesis in which transcriptional up regulation of VEGF-A in tumor cells was evident (Zhang et al, 2001). Microvascular proliferation is the characteristic feature of GBM and also pilocytic astrocytomas.

In this study we observed strong expression of Wnt signaling components in the vascular endothelial cells of pilocytic astrocytomas and GBM. Glomeruloid vasculature was evident in pilocytic astrocytomas and all the endothelial cells in these regions strongly expressed Wnt components. However, increased angiogenesis is the key factor in invasion and aggressive behaviour of GBM but pilocytic astrocytomas have benign character with vasculature. Although vascular cells strongly express the Wnt signaling pathway components, pilocytic astrocytomas are relatively non-invasive tumors. The reason behind this property was explained by the report that pilocytic astrocytomas express anti-migratory factors which specifically inhibit tumor invasion. Several studies have evaluated the differential expression of different genes in pilocytic astrocytomas and GBM. It was reported that hedgehog pathway is activated in astrocytomas and differentially expressed among different grades of astrocytomas (Rush et al, 2010). Colin et al, identified some of the differentially expressed genes in pilocytic astrocytomas and GBM using suppression subtractive hybridization (Colin et al, 2006). This study showed that 106 genes overexpressed in pilocytic astrocytomas versus GBM and 80 genes overexpressed in GBM versus pilocytic astrocytomas. The genes that are overexpressed in GBM are related to invasion and angiogenesis whereas genes that are overexpressed in pilocytic astrocytomas are related to metabolism, proteolysis, signal transduction, translation and cell adhesion. Rorive et al, analyzed the microarray studies that were previously conducted on pilocytic and diffuse astrocytomas and compared those studies for identifying molecular markers that were useful to characterize grade I tumors from grade II tumors (Rorive et al., 2006). This analysis revealed that genes differentially expressed in grade I and grade II and vice versa were related to invasion, ECM and adhesion. Furthermore, this study showed the expression of genes that were typically overexpressed in pilocytic astrocytomas, namely TIMP4, C1NH, CHAD, THBS4, IGFBP2 and TLE2 which encode the proteins of antimigratory components. These antimigratory proteins may be responsible for the circumscribed nature of pilocytic astrocytomas as opposed to diffuse astrocytomas that diffusely infiltrate the brain. Another reason of why pilocytic astrocytomas are slow growing tumors came from the studies of Nakamizo et al, who reported that apoptotic ratios in pilocytic astrocytomas were significantly higher than astrocytomas of remaining grades whereas the MIB labeling indices were lower in pilocytic astrocytomas than diffuse astrocytomas and there was a negative correlation between these two parameters (Nakamizo et al, 2002). Further, Klein et al, showed significantly increased indices of microglial proliferation in pilocytic astrocytomas than diffuse astrocytomas (Klein and Roggendorf, 2001). These proliferations constituted 32% of overall proliferations. It has also been shown that Wnt/β-catenin signaling

is activated in active microglia in proinflammatory conditions (Halleskog et al, 2011). Neder et al. reported that galectin-3 is overexpressed in pilocytic astrocytomas and GBM which plays essential roles in adhesion, invasion and migration (Neder et al, 2004). This protein is significantly expressed in pilocytic astrocytomas than grade II astrocytomas and useful for the differentiation of grade I and grade II tumors.

2.5. Conclusion

In conclusion, the present study demonstrates the differential expression of Wnt pathway components in pilocytic and diffuses astrocytomas. Hence this study might be helpful in distinguishing the pilocytic astrocytomas from grade II tumors. The observed high levels of Wnt pathway components in pilocytic astrocytomas remains an open question, because it was proved that high levels of Wnt pathway components in GBM were responsible for its pathogenesis. However, more studies are required to unveil why this pathway is highly expressed in pilocytic astrocytomas and GBM.

2.6. References

1. Abdollahzadeh M, Hoffman HJ, Blazer SI, Becker LE, Humphreys RP, Drake JM, Rutka JT (1994) Benign cerebellar astrocytoma in childhood: experience at the Hospital for Sick Children 1980-1992. *Childs Nerv Syst* 10:380-3.
2. Aldape K, Simmons ML, Davis RL, Miike R, Wiencke J, Barger G, Lee M, Chen P, Wrensch M (2000) Discrepancies in diagnoses of neuroepithelial neoplasms: The San Francisco Bay Area Adult Glioma Study. *Cancer* 88:2342-9.
3. Barker N, Clevers H (2006) Mining the Wnt pathway for cancer therapeutics. *Nat Rev Drug Discov* 5:997–1014.
4. Beatriz M, Lopes S, Scott RV (2007) Tumors of the central nervous system. In: Christopher D.M.Fletcher, ed. Diagnostic Histopathology of Tumors. Philadelphia Elsevier 1653-732.
5. Borges CB, Bernardes ES, Latorraca EF, Becker AP, Neder L, Chammas R, Roque-Barreira MC, Machado HR, de Oliveira RS (2011) Galectin-3 expression: a useful tool in the differential diagnosis of posterior fossa tumors in children. *Childs Nerv Syst* 27:253-7.
6. Bowers DC, Gargan L, Kapur P, Reisch JS, Mulne AF, Shapiro KN, Elterman RD, Winick NJ, Margraf LR (2003) Study of the MIB-1 labeling index as a predictor

of tumor progression in pilocytic astrocytomas in children and adolescents. *Clin Oncol* 21:2968-73.

7. Brown JD, Moon RT (1998) Wnt signaling: why is everything so negative? *Curr Opin Cell Biol* 10:182–187.
8. Burger PC, Scheithauer BW (1994): Tumors of the Central Nervous System. Washington, pp 68, Armed Forces Institute of Pathology, Washington, D.C.
9. Burger PC, Shibata T, Kleihues P (1986) The use of the monoclonal antibody Ki-67 in the identification of proliferating cells: application to surgical neuropathology. *Am J Surg Pathol* 10:611-7.
10. Burkhard C, Di Patre PL, Schuler D (2003) A population-based study of the incidence and survival rates in patients with pilocytic astrocytoma. *J Neurosurg* 98:1170–1174.
11. CBTRUS Statistical Report: Primary Brain and Central Nervous System Tumors Diagnosed in the United States in (2012). Ref Type: Report.
12. CBTRUS: central brain tumor registry of the United States. (2005) http://www.cbtrus.org
13. Cliffe A, Hamada F, Beinz M (2003) A role of Dishevelled in relocating Axin to the plasma membrane during wingless signaling. *Curr Biol* 13:960–966.
14. Colin C, Baeza N, Bartoli C, Fina F, Eudes N, Nanni I, Martin PM, Ouafik L, Figarella-Branger D (2006) Identification of genes differentially expressed in glioblastoma versus pilocytic astrocytoma using supression subtractive hybridization genes expressed in GBM versus PA. *Oncogene* 25:2818–2826.
15. Fernandez C, Figarella-Branger D, Girard N et al (2003) Pilocytic astrocytomas in children: prognostic factors-a retrospective study of 80 cases. *Neurosurgery* 53:544–555.
16. Garcia DM, Latifi HR, Simpson JR, Picker S (1989) Astrocytomas of the cerebellum in children. *J Neurosurg* 71:661–664.
17. Giannini C, Scheithauer BW (1997) Classification and grading of low-grade astrocytic tumors in children. *Brain Pathol* 7:785–798.
18. Halleskog C, Mulder J, Dahlstrom J, Mackie K, Hortobágyi T, Tanila H, Kumar Puli L, Färber K, Harkany T, Schulte G (2011) WNT signaling in activated microglia is proinflammatory. *Glia* 59:119–131.
19. He TC, Sparks AB, Rago C, Hermeking H, Zawel L, da Costa LT, Morin PJ, Vogelstein B, Kinzler KW (1998) Identification of c-MYC as a target of the APC pathway. *Science* 281:1509-1512.

20. Huang H, Hara A, Homma T, Yonekawa Y, Ohgaki H (2005) Altered expression of immune defense genes in pilocytic astrocytomas. *J Neuropathol Exp Neurol* 64:891-901.
21. Jeannet JP, He X (2000) LDL-receptor-related proteins in Wnt signal transduction. *Nature* 407:530–535.
22. Johnson DR, Brown PD, Galanis E, Hammack JE (2012) Pilocytic astrocytoma survival in adults: analysis of the Surveillance, Epidemiology, and End Results Program of the National Cancer Institute. *J Neurooncol* 108:187-93.
23. Jones DT, Gronych J, Lichter P, Witt O, Pfister SM (2012) MAPK pathway activation in pilocytic astrocytoma. *Cell Mol Life Sci* 69:1799-811.
24. Kim M, Jho EH (2014) Cross-talk between Wnt/β-catenin and Hippo signaling pathways: a review. *BMB Reports* 47:540-5.
25. Kleihues P, Cavenee WK (2000) Pathology and genetics of tumors of the central nervous system (world health organization classification of tumors), 2nd edn. IARC, Lyon.
26. Klein R, Roggendorf W (2001) Increased microglia proliferation separates pilocytic astrocytomas from diffuse astrocytomas: a double labeling study. *Acta Neuropathol* 101:245–248.
27. Koeller KK, Rushing EJ (2004) From the archives of the AFIP: pilocytic astrocytoma: radiologic-pathologic correlation. *Radiographics* 24:1693-708.
28. Levy L, Neuveut C, Renard C, Charneau P, Branchereau S, Gauthier F, Van Nhieu JT, Cherqui D, Petit-Bertron AF, Mathieu D, Buendia MA (2002) Transcriptional activation of Interleukin-8 by beta-catenin-Tcf4. *J Biol Chem* 277: 42386–42393.
29. Lie DC, Colamarino SA, Song HJ, Désiré L, Mira H, Consiglio A, Lein ES, Jessberger S, Lansford H, Dearie AR, Gage FH (2005) Wnt signaling regulates adult hippocampal neurogenesis. *Nature* 437:1370-1375.
30. Logan CY, Nusse R (2004) The Wnt signaling pathway in development and disease. *Annu Rev Cell Dev Biol* 20:781-810.
31. Louis DN, Ohgaki H, Wiestler OD, Cavenee WK, Burger PC, Jouvet A, Scheithauer BW, Kleihues P (2007) The 2007 WHO Classification of Tumors of the Central Nervous System. *Acta Neuropathol* 114:97–109.
32. Maretto S, Cordenonsi M, Dupont S, Braghetta P, Broccoli V, Hassan AB, Volpin D, Bressan GM, Piccolo S (2003) Mapping Wnt/ beta-catenin signaling during mouse development and in colorectal tumors. *Proc Natl Acad Sci U S A* 100:3299–3304.

33. Masckauchan TNH, Shawber CJ, Funahashi Y, Li CM, Kitajewski J (2005) Wnt/ beta-catenin signaling induces proliferation, survival and Interleukin-8 in human endothelial cells. *Angiogenesis* 8:43–51.
34. Moon RT, Kohn AD, De Ferrari GV, Kaykas A (2004) WNT and beta-catenin signaling: diseases and therapies. *Nat Rev Genet* 5: 691–701.
35. Nakamizo A, Inamura T, Ikezaki K, Yoshimoto K, Inoha S, Mizoguchi M, Amano T, Fukui M (2002) Enhanced apoptosis in pilocytic astrocytoma: a comparative study of apoptosis and proliferation in astrocytic tumors. *J Neurooncol* 57: 105–114.
36. Neder L, Colli BO, Machado HR, Carlotti CG Jr., Santos AC, Chimelli L (2004) MIB-1 labeling index in astrocytic tumors--a clinicopathologic study. *Clin Neuropathol* 23:262-70.
37. Neder L, Marie SK, Carlotti CG Jr, Gabbai AA, Rosemberg S, Malherios SMF, Siqueira RP, Oba-Shinjo SM, Uno M, Aguiar PH, Miura F, Chammas R, Colli BO, Silva WA, Zago MA (2004) Galectin-3 as an immunohistochemical tool to distinguish pilocytic astrocytomas from diffuse astrocytomas, and glioblastomas from anaplastic oligodendrogliomas. *Brain Pathol* 14:399–405.
38. Ohgaki H, Kleihues P (2005) Population-based studies on incidence, survival rates, and genetic alterations in astrocytic and oligodendroglial gliomas. *J Neuropathol Exp Neurol* 64:479–489.
39. Park SH, Min HS, Kim B, Myung J, Paek SH (2008) Galectin-3: a useful biomarker for differential diagnosis of brain tumors. *Neuropathology* 28:497-506.
40. Pinson KI, Brennan J, Monkley S, Avery BJ, Skarnes WC (2000) An LDL-receptor-related protein mediates Wnt signaling in mice. *Nature* 407:535-538.
41. Polakis P (2000) Wnt signaling and cancer. *Genes Dev* 14: 1837–1851.
42. Pu P, Zhang Z, Kang C, Jiang R, Jia Z, Wang G, Jiang H (2009) Downregulation of Wnt2 and beta-catenin by siRNA suppresses malignant glioma cell growth. *Cancer Gene Ther* 16:351–361.
43. Riemenschneider MJ, Jeuken JW, Wesseling P, Reifenberger G (2010) Molecular diagnostics of gliomas: state of the art. *Acta Neuropathol* 120: 567-84.
44. Roessler K, Bertalanffy A, Jezan H, Ba-Ssalamah A, Slavc I, Czech T, Budka H (2002) Proliferative activity as measured by MIB-1 labeling index and long-term outcome of cerebellar juvenile pilocytic astrocytomas. *J Neurooncol* 58:141-56.
45. Rorive S, Maris C, Debeir O, Sandras F, Vidaud M, Bièche I, Salmon I, Decaestecker C (2006) Exploring the distinctive biological characteristics of pilocytic and low-grade

diffuse astrocytomas using microarray gene expression profiles. *J Neuropathol Exp Neurol* 65:794–807.

46. Rush SZ, Abel TW, Valadez JG, Pearson M, Cooper MK (2010) Activation of the Hedgehog pathway in pilocytic astrocytomas. *Neuro Oncol* 12: 790–798.
47. Sareddy GR, Panigrahi M, Challa S, Mahadevan A, Babu PP (2009) Activation of Wnt/beta-catenin/Tcf signaling pathway in human astrocytomas. *Neurochem Int* 55:307–317.
48. Shiina H, Igawa M, Breault J, Ribeiro-Filho L, Pookot D, Urakami S, Terashima M, Deguchi M, Yamanaka M, Shirai M, Kaneuchi M, Kane CJ, Dahiya R (2003) The human T-cell factor-4 gene splicing isoforms, Wnt signal pathway and apoptosis in renal cell carcinoma. *Clin Cancer Res* 9:2121-2132.
49. Shtutman M, Zhurinsky J, Simcha I, Albanese C, D'Amico M, Pestell R, Ben-Ze'ev A (1999) The cyclin D1 gene is a target of the beta-catenin/ LEF-1 pathway. *Proc Natl Acad Sci U S A* 96:5522-5527.
50. Tamai K, Semenov M, Kato Y, Spokony R, Liu C, Katsuyama Y, Hess F, Saint-Jeannet JP, He X (2000) LDL-receptor-related proteins in Wnt signal transduction. *Nature* 407:530-535.
51. Tanaka Y, Sasaki A, Ishiuchi S, Nakazato Y (2008) Diversity of glial cell components in pilocytic astrocytoma. *Neuropathol* 4:399–407.
52. Tchoghandjian A, Fernandez C, Colin C, El Ayachi I, Voutsinos-Porche B, Fina F, Scavarda D, Piercecchi-Marti MD, Intagliata D, Ouafik L, Fraslon-Vanhulle C,Figarella-Branger D (2009) Pilocytic astrocytoma of the optic pathway: a tumor deriving from radial glia cells with a specific gene signature. *Brain* 132:1523–1535.
53. Tibbetts KM, Emnett RJ, Gao F, Perry A, Gutmann DH, Leonard JR (2009) Histopathological predictors of pilocytic astrocytoma event-free survival. *Acta Neuropathol* 117:657–665.
54. Tonn J, Westphal M (2006) Neuro-oncology of CNS tumors. Springer Verlag ISBN:3540258337.
55. Wehrli M, Dougan ST, Caldwell K, O'Keefe L, Schwartz S, Vaizel- Ohayon D, Schejter E, Tomlinson A, DiNardo S (2000) arrow encodes an LDL-receptor-related protein essential for Wingless signaling. *Nature* 407:527-530.
56. Wright M, Aikawa M, Szeto W, Papkoff J (1999) Identification of a Wnt-responsive signal transduction pathway in primary endothelial cells. *Biochem Biophys Res Commun* 263:384–388.

57. Zechner D, Fujita Y, Hulsken J, Muller T, Walther I, Taketo MM, Crenshaw EB, 3rd, Birchmeier W, Birchmeier C (2003) beta-Catenin signals regulate cell growth and the balance between progenitor cell expansion and differentiation in the nervous system. *Dev Biol* 258:406–418.
58. Zhang LY, Jiang LN, Li FF (2010) Reduced beta-catenin expression is associated with good prognosis in astrocytoma. *Pathol Oncol Res* 2:253–257.
59. Zhang X, Gaspard JP, Chung DC (2001) Regulation of vascular endothelial growth factor by the Wnt and K-ras pathways in colonic neoplasia. *Cancer Res* 61:6050–6054.

Chapter - 3

Role of hSCRIB as a potential prognostic marker in human astrocytoma patients

3.1. Introduction

Cell polarity is an essential phenomenon in several biological processes that contribute to normal tissue integrity and maturity. Several studies in different genetic models has identified and revealed different roles of polarity complexes in maintenances of stem cell population and their asymmetric division (Knoblich, 2010), T-cell functions like migration in response to chemokines and antigens (Krummel and Macara, 2006) and neuronal cell axon and dendritic specification (Arimura and Kaibuchi, 2007). Cell polarity is also crucial for epithelial cell and tissue polarization for maintenance of multicellular structures and perform normal physiological functions like secretion, absorption and distribution of cytoplasmic and membrane proteins in appropriate positions within the cell in order to conduct proper signals. Unlike epithelial cells which require cell polarity for polarization of cellular components and neurons for axon and dendrite specification, glial cells require cell polarity for migration and myelination. The proteins which regulate these cellular functions are called cell polarity regulators.

3.1.1. Cell polarity regulators and their deregulation in cancer

Proficient research work in organisms like *Caenorhabditis elegans* and *Drosophila melanogaster* has led to discovery of three different polarity complexes which are asymmetrically distributed within the cell. They are Partitioning defective (Par) complex consists of Par3, Par6 and an atypical protein kinase C, Crumbs complex consisting of Crumbs, Pals1 (Protein associated with Lin seven 1) and Pals1-associated tight junction protein (PATJ) and Scribble complex consisting of Scribble, Discs large (Dlg) and Lethal giant larvae (Lgl). Crumbs polarity complex and the Partitioning defective (Par) polarity complex are localized to the apical cortex, whereas members of the Scribble polarity complex are localized at the basolateral regions of the cell (Bilder and Perrimon, 2000; Humbert et al, 2006). Fig. 3.1 illustrates cell polarity complexes.

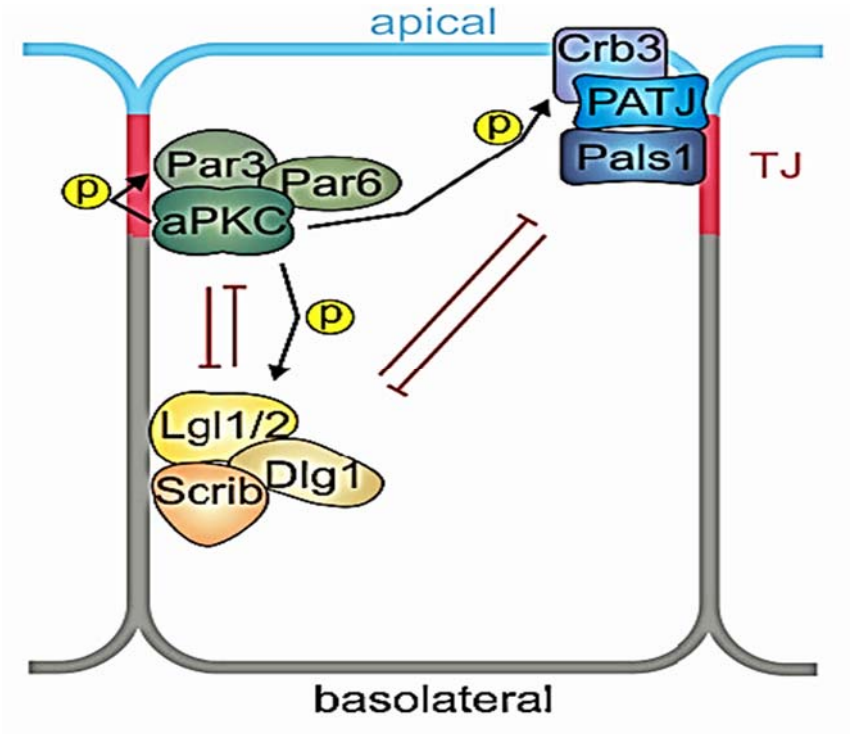

Fig. 3.1. Polarity protein complexes. Three conserved polarity protein complexes i.e. the Par, the Crumbs and the Scribble complex, regulate different modes of cell polarity. In contacting epithelial cells the Par complex is located apically in region where the tight junctions (TJs) are present and consists of Par3, Par6 and aPKC. Also apically localized is the Crumbs complex, consisting of Crb3, Pals1 and PATJ. Mutual exclusion of these apical polarity proteins and the basolaterally localized Scribble complex (comprising Scrib, Dlg1, Lgl1/2) confers apical–basal polarity. (S.I.J. Ellenbroek et al, 2012)

3.1.1a. PAR polarity complex

Par complex was initially identified in *C.elegans* and it consists of two scaffold proteins, PAR6 and PAR3 and an atypical protein kinase C, aPKC. In mammals Par6 protein is encoded by three different genes *PAR6A/C, PAR6B* and *PAR6D/G*, Par3 is encoded by *PAR3A* and *PAR3B* genes and two *aPKC* genes, *aPKCλ*/ι and *aPKCζ* encode two different proteins. Par3 and Par6 interact with each other via their PDZ domains and the interaction between Par 3 protein to aPKC/Par6 is dynamic and aPKC-dependent phosphorylation can expel Par3 from the aPKC/ Par6 unit (Horikoshi et al, 2009). PAR complex is essential for defining the appropriate apicolateral axis and assembly of tight junction proteins at their respective position.

3.1.1b. Crumb polarity complex

Crumbs polarity complex was identified in *Drosophila* and in mammals it consists of transmembrane protein CRB encoded by *CRB1*, *2*, and *3* genes along with two cytoplasmic scaffolding proteins PALS1 and PATJ. CRB1 connect to PDZ domains of Pals1 and PATJ through C-terminal ERLI motif. Pals1 is a member of the membrane-associated guanylate kinase (MAGUK) family, which has a PDZ domain, two L27 domains, a SH3 domain and a guanylate kinase domain. PATJ has 10 PDZ domains and one L27N domain (Tepass and Knust, 1993). CRB complex is involved in formation of tight junctions and differentiation of the apical membrane.

3.1.1c. Scribble (SCRIB) polarity complex

Scribble, Dlg and Lgl were identified in Drosophila as tumor suppressors, in mammals SCRIB (hSCRIB – human scribble) is also called VARTUL. Scribble is a member of LAP family with leucine-rich repeats and PDZ domains, while Dlg in mammals exists in five isoforms and it is a member of the MAGUK family containing PDZ domains. Lgl which exists as Lgl1 and Lgl2 in mammals does not contain PDZ domains but has WD40 domains, which is thought to mediate interactions with phosphorylated serine and tyrosine (Dow et al, 2007).

Interaction among these three complexes dictates them to localize in their respective positions, for example Lgl1 and 2 can compete with Par3 for binding to a module of Par6 and aPKC which in turn phosphorylates Lgl releasing it from the Par6/aPKC dimer, ensuing its localization to the basolateral region of cells (Betschinger et al, 2003). These complexes induce their function by regulating cytoskeleton architecture and there is a substantial data showing direct link with small GTPases of the Rho family. Cdc42, Rac1 and RhoA control the cytoskeletal changes in cells by switching between an active GTP bound state and an inactive GDP-bound state. For example Par3 can bind the Rac-activator Tiam1 during tight junction formation and Par6/Par3 regulates Cdc42-mediated Rac1 activation through Tiam1 in neuronal cells (Nishimura et al, 2005). These multifaceted interactions between polarity proteins and with small GTPases is essential for maintenance of polarity and carrying out normal physiological functions of the cell. For example, glial cells are responsible for myelination of neurons, it requires proper sorting of proteins and lipids and polarized membrane trafficking to organize myelin domains and maintain this highly polarized phenotype (DeBruin and Harauz, 2007). Astrocytes are the cells which carry

out major functions in brain including interactions with neurons and blood vessels (Schipke and Kettenmann, 2004), migration towards inflammation called astrogliosis (Ridet et al, 1997) which requires polarization of astrocytes into front-rear axis. Astrocytes polarize and migrate by interacting with extra cellular matrix components. Upon interaction of ECM with integrin receptors on astorcytes, activates intracellular signaling through small G proteins like Rac and Cdc42 for controlled polarization and orientation (Heasman and Ridley, 2008). Guanine exchange factors are in charge for the GDP–GTP exchange and therefore are the major regulators of small G proteins activity. It has been shown that cell polarity protein Scrib plays a crucial role in astrocyte migration by binding with Rac and Cdc42-specific exchange factor βPIX and controlling the localization of Cdc42 at leading edge of migratory processes (Osmani et al, 2006). Besides Scrib, other evolutionary conserved polarity proteins like Par protein complex is implicated in astrocyte migration. Par6-aPKC complex controls and regulates the microtubule organization during astrocyte migration. The GTP-bound form of Cdc4 binds to Par6 and activates aPKC kinase at leading edge of astrocyte (Etienne-Manneville et al, 2005).

Earlier studies reported that loss of cell polarity was regarded as post effect of cancer, but recent research work led to discovery that cell polarity is lost and responsible for tumorigenesis and its progression. Cell polarity proteins regulate cancer cell properties like proliferation, apoptosis, and epithelial- mesenchymal transition. Studies have shown that Par6 induces growth factor independent proliferation of human mammary epithelial cells by activating MAPK signaling through aPKC and Cdc42/Rac (Muthuswamy et al, 2008). aPKC can regulate cell proliferation through ERK and SRC-3 dependent manner (Castoria et al, 2004 and Yi et al, 2008) and knock down of aPKC in MCF-7 breast cancer cell line inhibited cell proliferation. Down regulation of Scribble induces JNK-dependent cell death (Brumby and Richardson, 2003) and in similar manner inhibition of aPKC increases apoptosis of MDCK cell by activating GSK3β (Kim et al, 2007). Acquisition of mesenchymal property by cancer cells during metastasis is due to change in the cell architecture which is regulated by cell polarity proteins. Research in genetic model *Drosophila* led to discovery that Scribble, DLg, Lgl, Par and Cdc42 cooperate with Rasv12 during invasion (Pagliarini and Xu, 2003). TGFβ signaling has been shown to phosphorylate Par6 protein which leads to RhoA degradation through Smurf1 (Wang et al, 2003). ZEB1, which is a transcriptional

regulator of epithelial mesenchymal transition (EMT), represses the expression of polarity proteins like Crumbs, Lgl2 and PATJ ultimately leading to mesenchymal transition (Aigner et al, 2007). Besides, cancer is a multistep process whereby cells first acquire benign over proliferation due to genetic assaults, followed by inhibition of apoptosis and increased cell proliferation. The conversion of benign to malignant form is accompanied by loss in cell-cell contact and apical basal polarity which ultimately leads to EMT associated with invasion into different parts from the site of cancer. During cancer progression steps, these different polarity complexes are either aberrantly expressed or mislocalised from their respective locations. Genetic studies in model organisms and *in vitro* cell culture has shown that these polarity complexes take apart in diverse hierarchy of human cancer. aPKC is over expressed in various human cancers like non-small cell lung cancer, ovarian cancer and its expression level correlates with over expression of Cyclin E and with their poor prognosis (Regala et al, 2005; Eder et al, 2005). In human esophageal squamous cell carcinoma Par3 gene is homozygously lost with reduced protein expression (Zen et al, 2009). Par6 is regarded as a tumor promoter as it is over expressed in human breast cancer and its interaction with TGFβ receptor implicates its role in EMT (Ozdamar et al, 2005).

However, contribution of Crumb complex for tumor progression is not completely elucidated. Few studies have shown that Crb-3 expression negatively correlates with metastatic behaviour of cells as its decreased expression is associated with increased expression of vimentin and reduced expression of E-cadherin (Bhat et al, 1999). Assembly of Crumb complex leads to phosphorylation of transcription effector molecule of Hippo signaling pathway TAZ/YAP which in turn leads to inhibition of TGF-β-SMAD signaling essential for vimentin expression (Varelas et al, 2010). ZEB1 and SNAIL represses the Crumb complex activity. PATJ and Pals1 are required for tight junction (TJ) assembly. PATJ is targeted for degradation by human papiloma virus (HPV) oncoprotein during development of cervical cancer (Javier, 2008). Till date there is no evidence for role of Pals1 in cancer, however few studies in mice model have shown that Pals1 is essential for survival since its loss results in embryonic lethality.

Scribble complex, regarded as fly tumor suppressor genes and basolateral polarity complex are regulated at different levels in human cancers. Dlg and Lgl proteins are down regulated and mislocalised in tumors of breast, prostate, lung, ovary, cervical and liver. Scribble and Dlg are targeted for degradation by viral oncoproteins from HPV (Thomas et al, 2005), Human Tcell leukemia (HTLV) (Okajima et al, 2008) and their expression levels are correlated with loss of

tissue architecture. Scribble is mislocalised in cervical, colon, endometrial and prostate cancer (Nakagawa et al, 2004; Gardiol et al, 2006; Ouyang et al, 2010; Pearson et al, 2011). In *Drosophila* genetic study, it has been exposed that loss of Scribble function alone is not sufficient to induce tumor, instead Scrib mutant cells expressing oncogenic Raf, Ras or Notch results in loss of apical-basal polarity, neoplastic overgrowth and metastasis (Brumby and Richardson, 2003).

Loss of cell polarity in brain tumors is not well documented and very few works like Klezovitch et al. have shown that loss of cell polarity causes severe brain dysplasia using Lgl1 knockout mice (Klezovitch et al, 2004). However, little is known about the role of cell polarity proteins in glioma or expression level of hSCRIB and its prognostic significance in human gliomas. In the present study we set out to investigate the expression pattern of hSCRIB in human glioma specimens, normal control brain tissues and analyse the relationship between hSCRIB expression and the glioma stage as well as the survival of the patients.

3.2. Materials and methods

3.2.1. Tumor Samples

Total 32 astrocytic tumor samples and 3 control brain samples were collected from patients who underwent surgical resection at Nizam Institute of Medical Sciences and Krishna Institute of Medical Sciences (Hyderabad, India). The tumors were classified histopathologically according to the WHO classification: 8 diffuse astrocytomas (DA; grade II), 7 anaplastic astrocytomas (AA; grade III), and 17 glioblastoma multiforme (GBM; grade IV). The case details of astrocytoma patients were summarized in table 3.1. All samples were obtained from patients after taking the informed consent form patients or their relatives. A part of the surgically removed samples were immediately snap frozen in liquid nitrogen and then stored at -80°C until analysis. The remaining samples were fixed with formalin and embedded in paraffin. These fixed samples were used for routine H&E staining, as well as for immunohistochemical analyses.

Table 3.1. Clinical characteristics of astrocytoma patients

NO.	AGE	SEX	WHO GRADE	LOCATION	SURVIVAL DAYS	OUT COME
1.	34	F	II	Fronto-tlemporal	**1465**	**Alive**
2.	35	M	II	Frontal	**1465**	**Alive**
3.	27	M	II	Fronto-temporal	**1465**	**Alive**
4.	30	M	II	Frontal	**1465**	**Alive**
5	16	M	II	Frontal	**1465**	**Alive**
6.	60	M	II	Parietal	**412**	**Dead**
7.	37	F	II	Tempero-frontal	**1465**	**Alive**
8.	40	M	II	Frontal	**1465**	**Alive**
9.	29	M	II	Frontal	**345**	**Dead**
10.	62	F	III	Parietal	**1465**	**Alive**
11.	35	M	III	Frontal	**326**	**Dead**
12.	37	M	III	Frontal	**1465**	**Alive**
13.	30	F	III	Frontal	**419**	**Dead**
14.	45	F	III	Fronto-temporal	**986**	**Dead**
15.	43	M	III	Frontal	**1021**	**Dead**
16.	45	M	IV	Parietal	**1465**	**Alive**
17.	36	F	IV	Frontal	**446**	**Dead**
18.	16	M	IV	Frontal	**321**	**Dead**
19.	52	M	IV	Frontal	**496**	**Dead**
20.	20	M	IV	Frontal	**462**	**Dead**
21.	19	M	IV	Tempero-parietal	**56**	**Dead**
22.	27	M	IV	Frlontal	**120**	**Dead**
23.	48	M	IV	Temporal	**175**	**Dead**
24.	15	M	IV	Frontal	**32**	**Dead**
25.	58	F	IV	Fronto-tempero-parietal	**93**	**Dead**
26.	61	M	IV	Frontal	**18**	**Dead**

27.	50	M	IV	Corpus callosal	**39**	**Dead**
28.	55	M	IV	Frontal	**172**	**Dead**
29.	5	M	IV	Multiple intra cranial	**113**	**Dead**
30.	30	M	IV	Frontal	**1465**	**Alive**
31.	40	M	IV	Parietal	**59**	**Dead**
32.	34	M	IV	Temporal	**213**	**Dead**

3.2.2. Western Blotting

Western blotting was performed as described previously. Briefly, frozen tissues were homogenized in RIPA (radioimmunoprecipitaiton assay) buffer containing 50 mM Tris-HCl (pH 8.0), 150 mM NaCl, 1 mM EDTA, 0.4% deoxy-cholate, 1% NP-40 containing protease inhibitors including 1 mM phenylmethylsulfonylfluoride (PMSF) and phosphatase inhibitors including 10 mM β-glycerophosphate, 10 mM NaF, 0.3 mM Na_3Vo_4 and 0.3 mM aprotinin using dounce homogenizer and sonicated for 2 min and then centrifuged at 14,000 g for 15 min at 4^0C. The supernatant was collected as whole cell lysates and protein concentrations were determined by Lowry method. Equal amount of proteins (75 µg) were resolved on 6% SDS-polyacrylamide gels and then transferred on to nitrocellulose membranes. After blocking the nitrocellulose paper in non-fat dry milk (5%) in Tris Buffered Saline (TBS) (10mM Tris (pH 7.5), 150 mM NaCl) for 1 h at room temperature, the membranes were incubated for 12 h in primary antibodies at 4^0C. Blots were again incubated with secondary antibodies conjugated to alkaline phosphatase (ALP) (anti-rabbit and anti-mouse IgG conjugated to ALP obtained from Genei Pvt Ltd, Bangalore, India), for 1-2 h at room temperature. Before and after incubation of blots with secondary antibodies, blots were washed with TBS and TBST (TBS containing 0.1% Tween-20). Immunoreactivity was visualized by incubating the blots with BCIP-NBT solution (Genei Pvt Limited, Bangalore, India). The primary antibodies used in these experiments included rabbit polyclonal antibody against hSCRIB (obtained from Cell Signaling Technology, Beverly, MA, USA) and rabbit polyclonal antibody against β-actin (Sigma-Aldrich, USA).

3.2.3. Immunohistochemistry

Immunohistochemical studies were performed on formalin-fixed, paraffin-embedded specimens. Briefly, sections were deparaffinized in xylene and passed through graded alcohols and further rehydrated in phosphate buffered saline (PBS). Antigen unmasking was carried out by micro waving the sections for 10-14 min in 10 mM citrate buffer (pH 6.0). Sections were then treated with 3% H_2O_2 for 10 min to inhibit endogenous peroxidase followed by incubation with serum for 1 h at room temperature in a humid chamber. The sections were then incubated overnight at 4^{o}C with primary antibodies against hSCRIB (1:50 dilution) as per data sheet in blocking solution. Peroxidase conjugated secondary antibody was used for 1 h incubation time at room temperature followed by TBS washes (3x5 min each). Diaminobenzidine (DAB) in buffer was used till sections develop color. Then sections were counterstained using haematoxylin. Sections were washed with distilled water followed by dehydration in graded alcohols, xylene and mounted with DPX (kit obtained from Biogenex Pvt Limited, India). In each experiment, a negative control was included in which the primary antibody step was skipped and replaced by non-immune serum. The number of immunostained cells in each grade is evaluated quantitatively in terms of positive staining for hSCRIB. The positive areas were selected randomly in tumor section. The staining indices for hSCRIB was calculated as the ratio of positive cells in high power microscopic fields (HPF) to all the cells in the HPF.

3.2.4. Immunofluorescent analysis

As described in immunohistochemical analysis in the previous section, after deparafinization, rehydration and cooking, tissue sections were blocked with 5% serum for 1 h at room temperature in a humid chamber. Then incubated the sections in a cocktail of two primary antibodies (mouse polyclonal GFAP obtained from Sigma Chemicals, USA, and rabbit polyclonal hSCRIB antibodies) at 1:50 dilution overnight at 4^{0}C. The sections were subsequently washed and incubated in a mixture consisting FITC and TRITC secondary antibodies (Genei Pvt Limited, Bangalore, India) at 1:250 dilution for 1 h at room temperature. The sections were washed and mounted using 90% glycerol and visualized using a Leica confocal microscope.

3.2.5. RNA isolation and quantitative real-time PCR

Total RNA was isolated from astrocytic tumor tissues (grade II, grade III and grade IV) using TRI reagent (Sigma Chemicals, USA). Briefly, frozen tissues (50–100 mg) were grounded in liquid nitrogen and homogenized in 1 ml of TRI reagent for RNA isolation following manufacturer's instructions. Purified total RNA was dissolved in DEPC treated water and stored at -80^{0}C before use. Five micrograms of RNA was treated with DNase I and reverse transcribed to cDNA using oligo (dT) 18 primer and M-mLV reverse transcriptase enzyme (Invitrogen, Sandiego, CA, USA) as per the protocol recommended by manufacturer. The amplification conditions were initial denaturation at 94^{0}C for 3 min followed by 30 cycles of 94^{0}C for 1 min; 58^{0}C for 45 s; 72^{0}C for 45 s. Real-time monitoring of polymerase chain reactions (PCRs) was performed using the 7500 Fast Real-Time PCR System (Applied Biosystems) and the SYBR green dye (Applied Biosystems), which binds preferentially to double- stranded DNA. Fluorescence signals, which are proportional to the concentration of the PCR product, are measured at the end of each cycle and immediately displayed on a computer screen, permitting real time monitoring of the PCR. The reaction is characterized by the point during cycling when amplification of PCR products is first detected, rather than the amount of PCR product accumulated after a fixed number of cycles. The higher the starting quantity of the template, earlier the significant increase in fluorescence. The threshold cycle is defined as the fractional cycle number at which fluorescence passes a fixed threshold above the baseline. PCR amplification was conducted using the described primer sets (table 3.2). All primers were synthesised by Eurofins Genomics India Pvt Ltd. The PCR profile consisted of initial melting step of 2 min at 94^{0}C, followed by 40 cycles of 15 s at 94^{0}C, 1 min at 60^{0}C, and a final elongation step of 10 min at 72^{0}C. Fluorescence data were converted into cycle threshold measurements using the system software and exported to Microsoft Excel. hSCRIB mRNA levels were compared to GAPDH. Thermal dissociation plots were examined for biphasic melting curves, indicative of whether primer-dimers or other nonspecific products could be contributing to the amplification signal.

Similarly real time quantification of other cell polarity genes was conducted using the described primer sets (table 3.2) and were compared to GAPDH.

TABLE 3.2. Primer sets (F- forward primer, R- reverse primer)

GENE	PRIMER SEQUENCE	AMPLICON SIZE
hSCRIB F hSCRIB R	5’ ATG GCT TCA CTC AGC TGC GCA G 3’ 5’ TTG CCT CCC AGA TCC AGC TGT TC 3’	198
Lgl F Lgl R	5’ AGA TCT ATG GTG CAC CTG GCG TG 3’ 5’ GGT GGA CAA TCT CCC AGA GAT GC 3’	210
Dlg F Dlg R	5’ AGC AAA AGA TGC AGC GGA GTC TG 3’ 5’ CAA AGA CCA TGG GGA AAG GCT 3’	192
CRB1 F CRB1 R	5’ATC AAG GCA GAC ACT GCG AC 3’ 5’CAA GGT TGA CTG GCA CAC TC 3’	225
CRB2 F CRB2 R	5’ATG GCT TCC AGT GTC ACT GC 3’ 5’GAC CCC AGA CTC GAA GAT AG 3’	230
Pals1 F Pals1 R	5’ TGC GTC AGA GGC TCA TGA AC 3’ 5’ CCA GAG TTG ATC ACT TGC CG 3’	210
Patj F Patj R	5’TGA GAC TGA TTG TGG CCA GG 3’ 5’CCT GTC TGG AGT CTT CCA TC 3’	200
PAR3 F PAR3 R	5’ AAT GCT CGC TCG TCT CTG AG 3’ 5’ CTC GAG CAC TGA AAG GCA CT 3’	186
PAR6 F PAR6 R	5’ TCC TCA GTC ATA GAC GTG GAC 3’ 5’ GAC CTC GAG GAT CTC ATC AC 3’	194
aPKCi F aPKCi R	5’TGT GTA CCA GAA CGT CCT GG 3’ 5’GCC GCC CAC ATT CAA TTG TG 3’	206
aPKCζ F aPKCζ R	5’AGA TGG AGG AAG CTG TAC CG 3’ 5’TTG TCG TCT ACT GGA GGC TC 3’	182
GAPDH F GAPDH R	5′-ACCACAGTCCATGCCATCAC-3′ 5′-ACACGGAAGGCCATGCCAGTG-3′	348

3.2.6. Statistical analysis

All computations were carried out using the software of SPSS version13.0 for Windows (SPSS Inc, IL, USA). The rank sum test was used to analyse the ranked data. The measurement data were analysed by one-way ANOVA. Randomized block design ANOVA was used to analyse

the statistical difference among different tissue types. In the analysis of glioma morbidity for all patients, we used the Kaplan-Meier estimator and univariate Cox regression analysis to assess the marginal effect of each factor. Spearman's analysis was carried out to analyse the correlation between hSCRIB mRNA and protein expression levels. The differences between groups were tested by log-rank analyses. Differences were considered statistically significant when $P<0.05$.

3.3. Results

3.3.1. Expression level of hSCRIB protein in patients with malignant gliomas and normal brain tissue specimens by immunohistochemical assay and survival analysis

hSCRIB protein expression was studied in a total of 32 glioma specimens of which 9 were low grade (grade II) and 23 were high grade (grade III – IV). About three control brain tissues served as control. Based on immunohistochemistry analysis, positive staining for hSCRIB was observed in cytoplasm and to a lesser degree in nuclei of cancer cells. Among the glioma specimens, 21 (65.62%) glioma specimens were positively stained, and 11 (34.37%) glioma specimens were negatively stained. Whereas, all the three control tissue showed positive staining for hSCRIB, we also found significant decrease of hSCRIB expression (Fig.3.2) in glioma when compared with normal brain tissues ($P<0.05$).

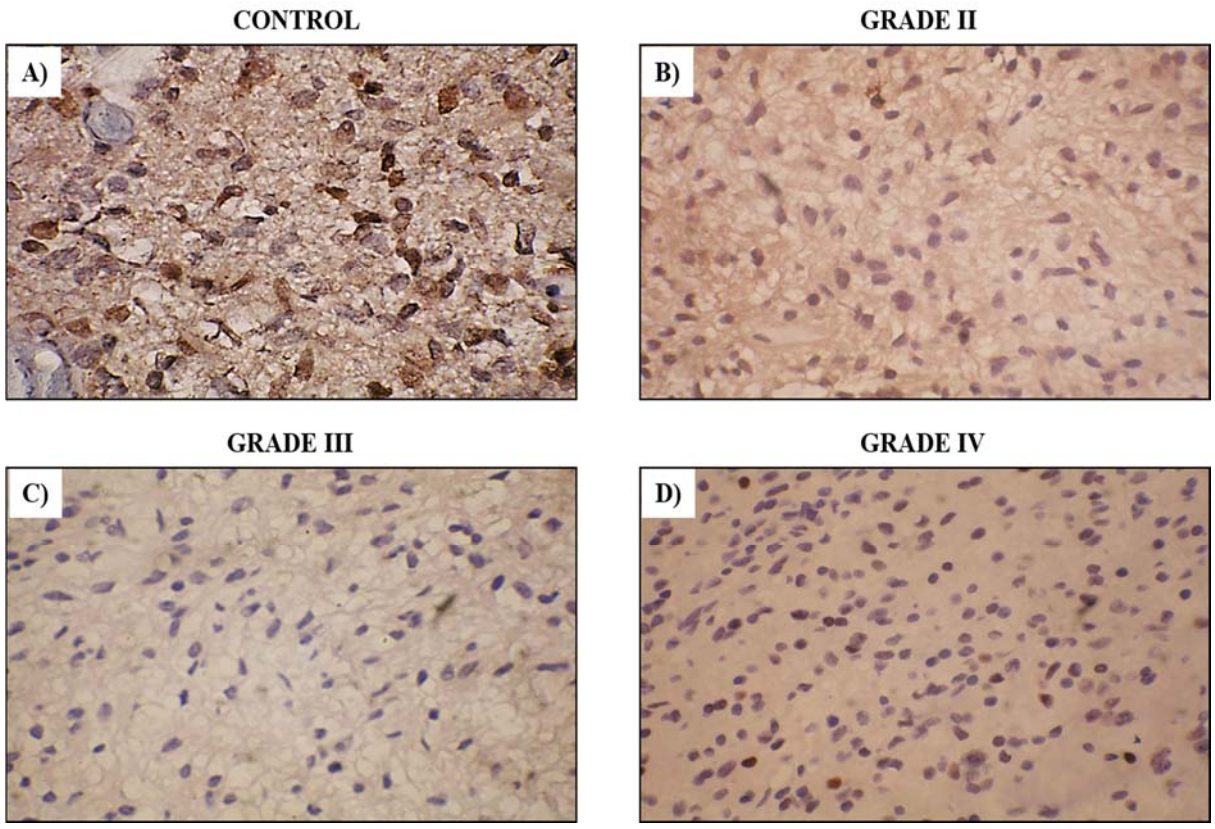

Fig. 3.2. Immunohistochemical staining of hSCRIB in astrocytomas. Paraffin embedded astrocytoma sections were prepared from astrocytoma specimens. Sections were incubated with hSCRIB primary antibody (1:50 dilution) overnight at 4^0C and peroxidase conjugated secondary antibody for 1 h at room temperature. Immunoreactivity was visualized by diaminobenzidine and sections were counterstained using haematoxylin. Positive staining of hSCRIB was seen in A-control sample and is more abundant than B-Diffuse astrocytoma; C-Anaplastic astrocytoma; D-GBM tumors.

Further, in order to confirm the cell type and sub cellular distribution of hSCRIB, immunofluorescence was performed. Double immunofluorescence analysis showed that hSCRIB was delocalised and less expressed in GFAP expressing tumor cells compared to control GFAP expressing cells (Fig. 3.3).

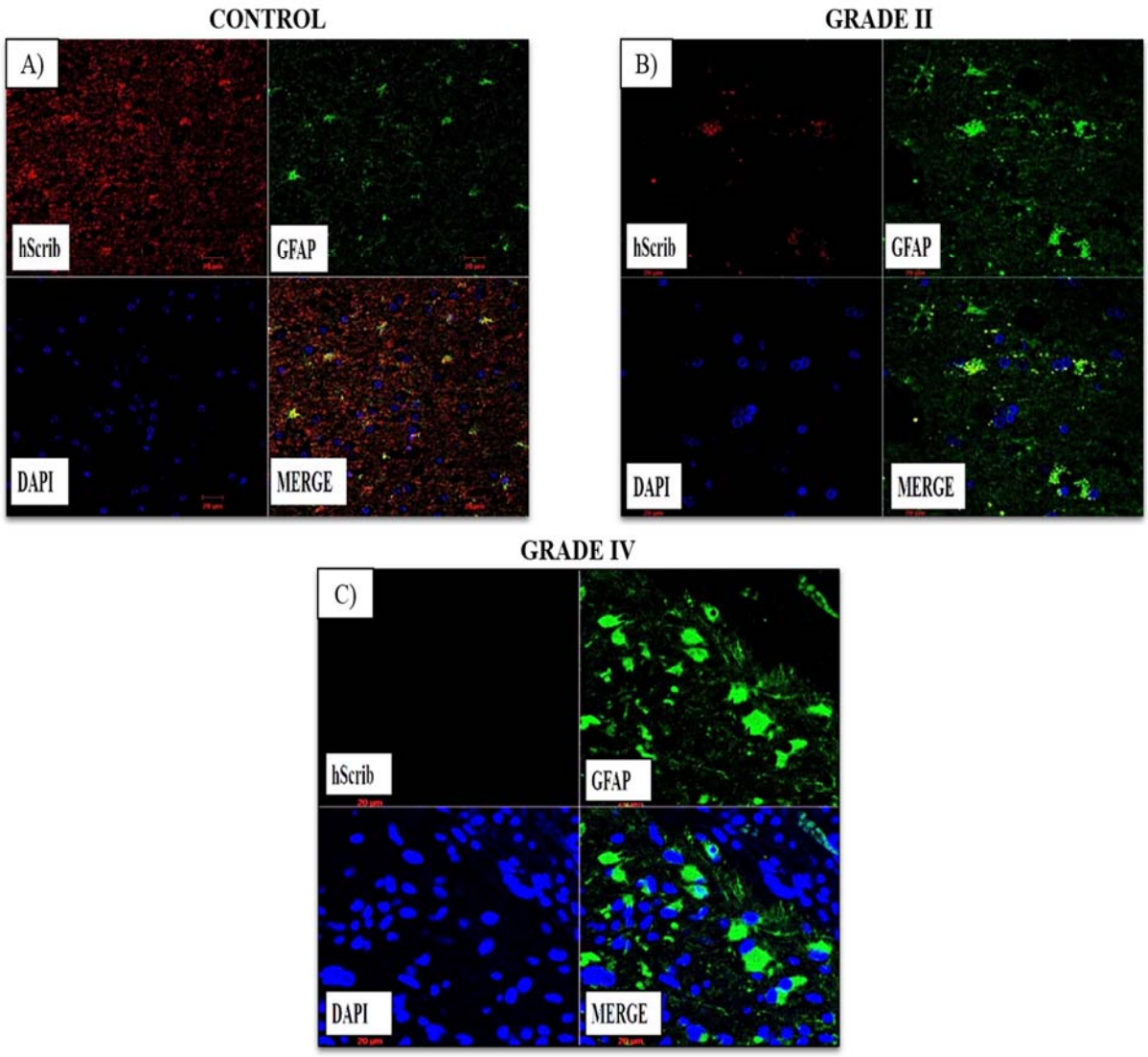

Fig. 3.3. Co-localization of hSCRIB and GFAP. Paraffin-embedded astrocytoma sections were prepared from astrocytoma specimens. Sections were incubated with anti-rabbit hSCRIB and anti-mouse-GFAP specific primary antibodies (1:100 dilution) overnight at 4^0C and anti-rabbit-TRITC and anti-mouse-FITC secondary antibodies were used for 1 h at room temperature. DAPI was used for the detection of nuclei and fluorescence was captured under Leica confocal microscope. Representative figure demonstrates the altered localisation and loss of hSCRIB expression in glioma grades compared to control.

Based on the hierarchical scores of the immunohistochemical staining, we analyzed the relationship between hSCRIB staining and clinical factors. hSCRIB expression was not

significantly affected by gender and age (both P>0.05) of the patients. In contrast, the hSCRIB expression was closely associated with WHO grade, with expression decreasing from grade II to IV (P<0.05; Table II). Moreover, we reviewed clinical information of the glioma patients with hSCRIB-positive or -negative tumors. During the follow-up period, 21 of the 32 glioma patients (65%) had died (13 from the hSCRIB-negative group and 8 from the hSCRIB-positive group). As determined by the log-rank test, the survival rate of patients with tumors having hSCRIB staining was longer than those with hSCRIB-negative staining tumors (P<0.001) (Fig. 3.4).

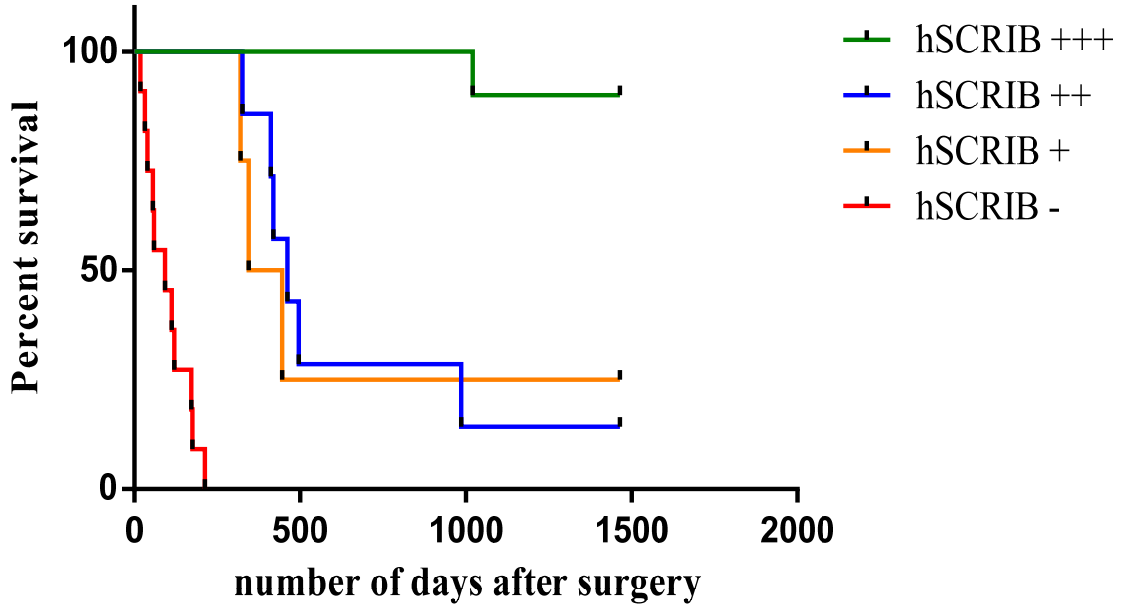

Fig. 3.4. Kaplan-Meier curves indicating the overall survival rates in the glioma patients sub-grouped according to hSCRIB protein expression (-, +, ++, +++ representing negative staining, weak positive staining, moderate positive staining and strong positive staining of hSCRIB respectively).

The median survival time of patients with strong positive (+++) expression of hSCRIB could not be defined by statistical analysis because all patients survived better than the overall median level, and survival time of patients with moderate positive (++), weak positive (+) and negative (-) expression of hSCRIB were 462 days, 395.5 days and 93 days respectively (log-rank test: P <0.05). Furthermore, we observed that hSCRIB expression was not significantly affected by the gender and age (both p > 0.05) of the patients. In contrast, the hSCRIB expression was closely correlated

with WHO grade. Multivariate analysis using Cox PH model demonstrated that the hazard rate is significantly affected by grade of glioma ($p < 0.008$) (table 3.3).

Table 3.3. hSCRIB expression in human astrocytoma tissues with different clinico-pathological features

Clinicopathological features	No. of cases	hSCRIB -	hSCRIB +	hSCRIB ++	hSCRIB +++	P value
WHO grade						
II	9	0	1	1	7	<0.008
III	6	0	0	3	3	
IV	17	11	3	3	0	
Age						
< 55	26	12	4	4	6	NS
≥ 55	6	4	1	0	1	
Gender						
M	25	13	5	1	6	NS
F	7	2	0	3	2	

-, negative staining; +, weak positive staining; ++, moderate positive staining; +++, strong positive staining. P-value was estimated using the Kruskal-Wallis test.

2.3.2. Quantitative analysis of hSCRIB protein expression based on WHO grade in gliomas

From western blot analysis, we found that hSCRIB protein expression tended to decrease from control tissue to glioma tissue (Fig. 3.5a). Also, hSCRIB expression was highest in grade II and lowest in grade IV (Fig. 3.5a). Densitometry analysis showed that percentage of hSCRIB expression in grade II (85.6 ± 3.21), grade III (48.4 ± 3.25), grade IV (10.8 ± 1.76) tumors were statistically significant ($P < 0.05$) when compared with that of control and showed negative correlation with degree of histological malignancy (Fig. 3.5b). These results are in concordance

with the findings of the immunohistochemistry analysis and indicate a close correlation of hSCRIB protein expression with WHO tumor grade.

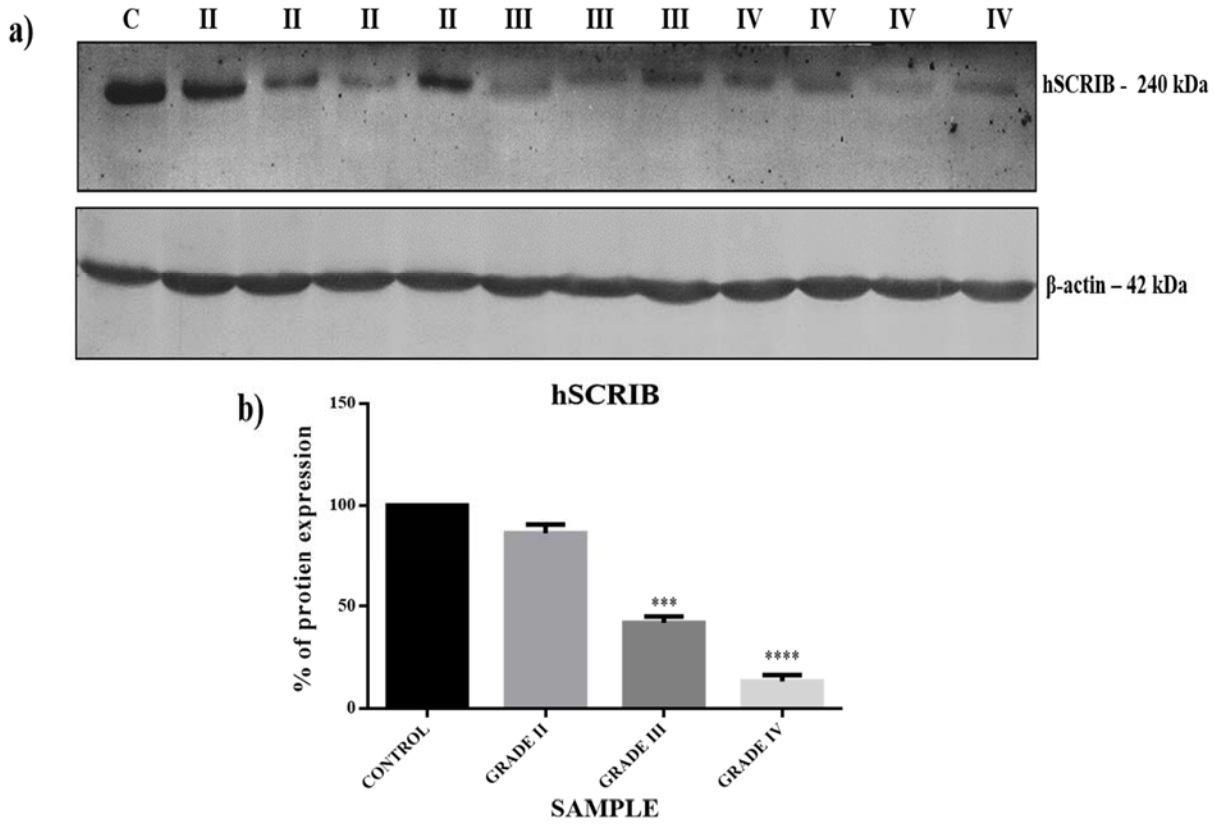

Fig. 3.5. hSCRIB protein expression in glioma as determined by western blotting. (a) hSCRIB protein expression in representative gliomas of different World Health Organization tumor grades and normal brain tissue (as control), relative to actin expression (loading control). **(b)** Mean expression of hSCRIB in gliomas of each grade and normal brain tissue, as determined by densito-metric analysis of western blotting. These were, normalized against expression of actin as a loading control. The data are presented as mean ± SD of relative protein expression levels in tumors and control. Statistical significance was calculated using paired t-test between c-control (n = 3) and GRADE II (n = 8) (no significant difference), GRADE III (n = 7) (*** represents P<0.0033) and GRADE IV (n = 17) gliomas (**** represents P<0.0001).

3.3.3. Quantitative analysis of hSCRIB mRNA expression in glioma by RT-PCR

We studied the mRNA expression of *hSCRIB* normalized to *GAPDH* by real-time PCR. As shown in fig. 3.6, there was an obvious decrease in the expression of hSCRIB mRNA from the control normal brain tissues to glioma tissues ($P<0.05$). We further analyzed the expression of hSCRIB mRNA in various WHO tumor grades. Notably, hSCRIB mRNA expression decreased with advancement of WHO grade II to IV ($P<0.01$). There was a significant positive correlation between the expression of hSCRIB mRNA and protein expression levels from the same glioma tissues ($rs=0.854$, $P<0.001$).

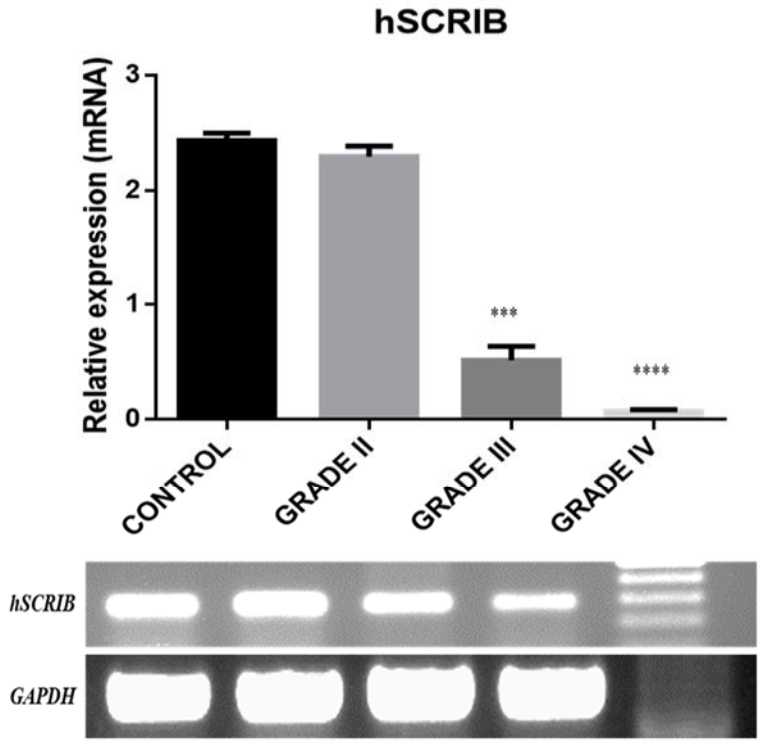

Tissue	No. of cases	2^-ΔΔCt
CONTROL	3	2.439
GRADE II	9	2.299
GRADE III	6	0.513
GRADE IV	17	0.072

Fig. 3.6. Relative mRNA levels of *hSCRIB* expression in glioma of different World Health Organization tumor grades and normal brain tissue as determined by real-time PCR. We determined the mRNA expression of *hSCRIB* normalized to *GAPDH* and as shown in above table, there was a conspicuous decrease in the expression of hSCRIB mRNA from the control brain tissues to glioma tissues (*$P < 0.05$).

Further, we analysed the mRNA levels of other cell polarity genes like SCRIB complex (Lgl, Dlg), CRUMB complex (CRB1, CRB2, Pals1, Patj) and PAR complex (PAR3, PAR6, aPKCi, aPKCζ)

in glioma tissue and compared to control brain tissue. Real time PCR analysis showed that SCRIB complex and CRUMB complex mRNA expression levels were lower in glioma tissues compared to control brain tissue and their expression decreased with increase in the tumor grade (Fig. 3.7, Fig. 3.8). Whereas, PAR complex mRNA expression levels were higher in glioma tissues compared to control brain tissue and their expression increased with increase in the tumor grade (Fig. 3.9).

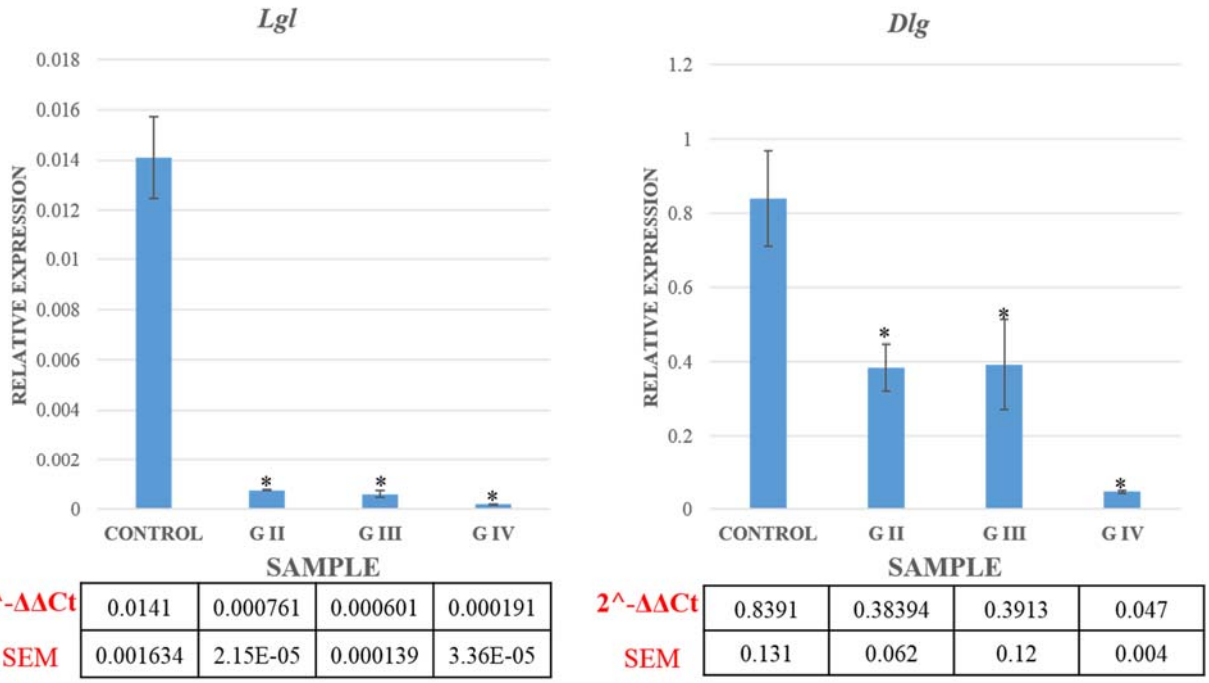

2^-ΔΔCt	0.0141	0.000761	0.000601	0.000191
SEM	0.001634	2.15E-05	0.000139	3.36E-05

2^-ΔΔCt	0.8391	0.38394	0.3913	0.047
SEM	0.131	0.062	0.12	0.004

Fig. 3.7. Total RNA was isolated form human glioma samples and subjected to RT-qPCR using the primers specific for *Lgl* and *Dlg*. *GAPDH* used as an internal control. All data presented are mean ± SEM. *p<0.05, t test.

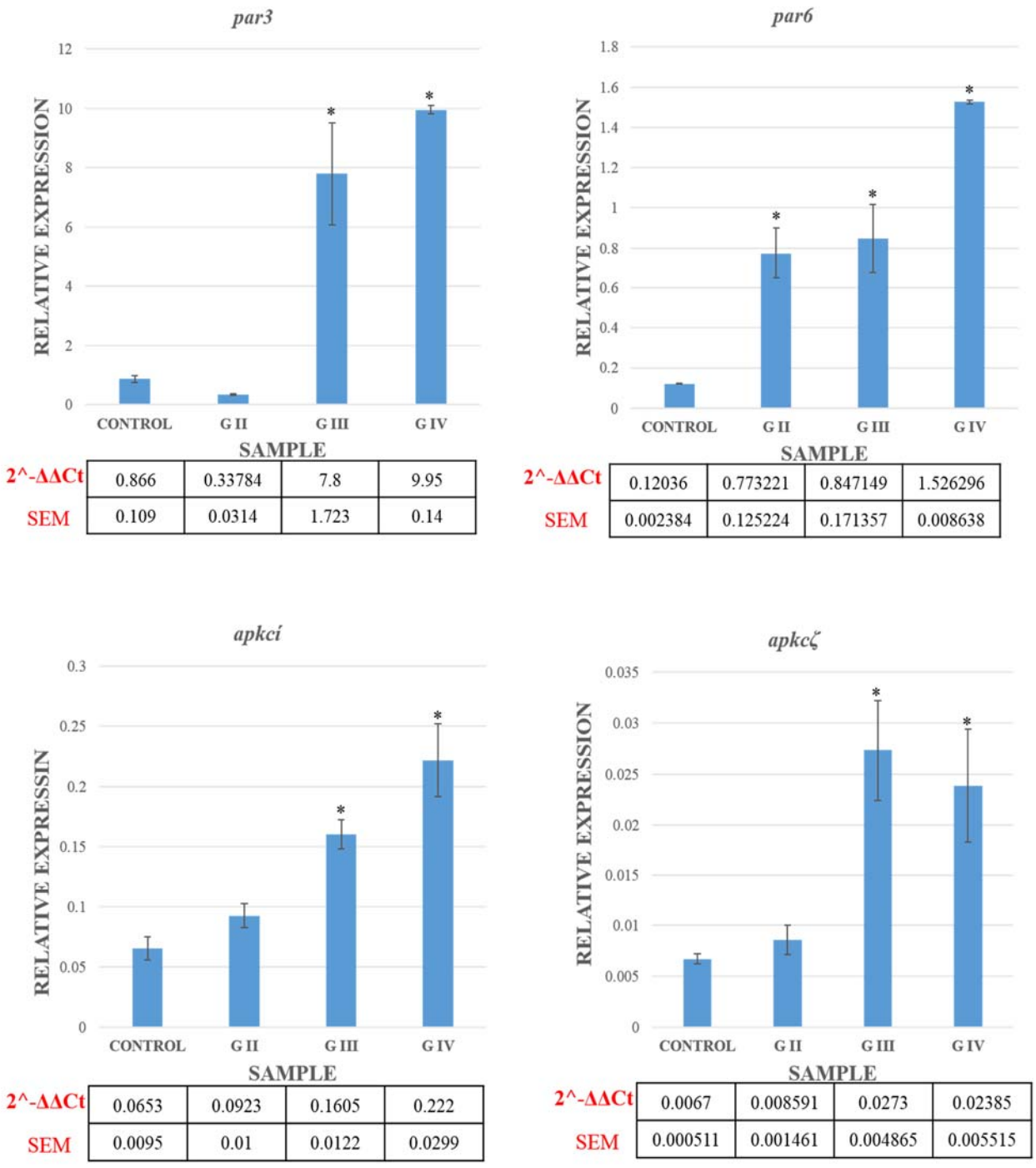

Fig. 3.8. Total RNA was isolated form human glioma samples and subjected to RT-qPCR using the primers specific for *par3, par6, apkcí* and *apkcζ. GAPDH* used as an internal control. All data presented are mean ± SEM. *p<0.05, t test.

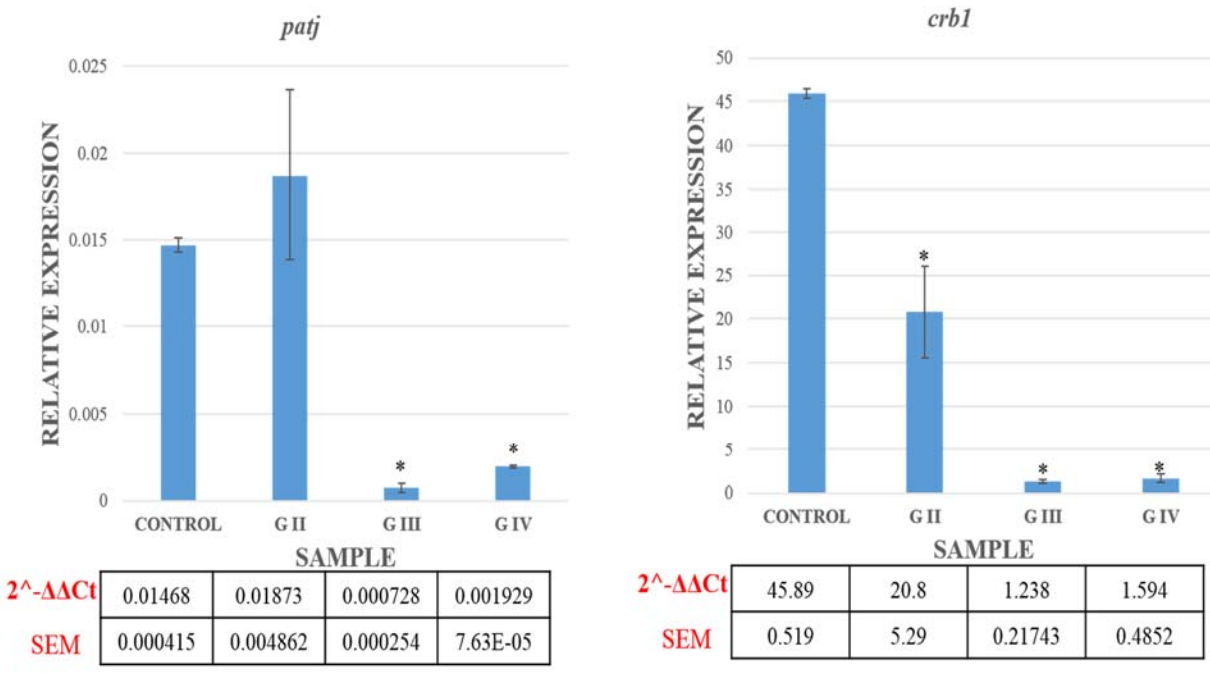

2^-ΔΔCt	0.01468	0.01873	0.000728	0.001929
SEM	0.000415	0.004862	0.000254	7.63E-05

2^-ΔΔCt	45.89	20.8	1.238	1.594
SEM	0.519	5.29	0.21743	0.4852

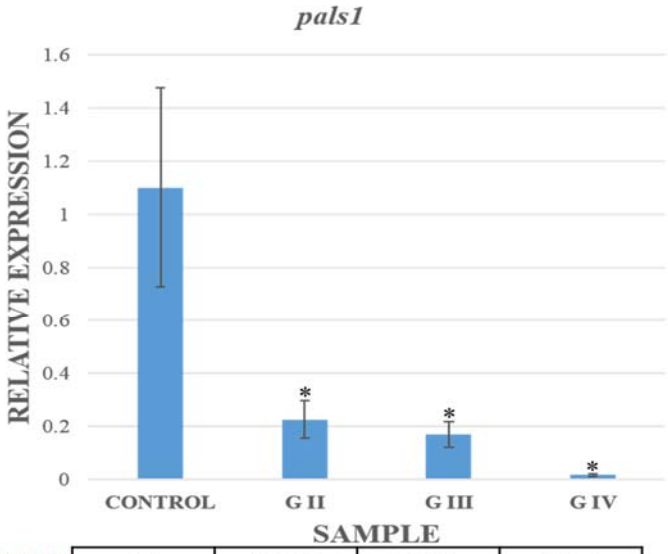

2^-ΔΔCt	1.1	0.226	0.17	0.017
SEM	0.374	0.0699	0.0485	0.0048

Fig. 3.9. Total RNA was isolated form human glioma samples and subjected to RT-qPCR using the primers specific for *patj, crb1* and *pals1*. *GAPDH* used as an internal control. All data presented are mean ± SEM. *p<0.05, t test.

3.4. Discussion

In the current study, we investigated the expression of hSCRIB in 32 cases of human glioma and three human normal brain tissue and compared the expression with tumor grade and the survival rates of patients. Our data demonstrated that hSCRIB protein decreased in glioma compared to normal brain tissue. hSCRIB mRNA expression also reduced in glioma compared with control normal brain tissue. We found a decreased trend of both hSCRIB protein level and mRNA level from WHO grade II to WHO grade IV glioma. These results suggest that the transcriptional repression of human SCRIB might participate in the carcinogenesis and progression of glioma. hSCRIB may have an important role during the genesis or progression of glioma. Further, real time PCR analysis of other cell polarity complex genes showed that expression of SCRIB and CRUMB complex genes decreased whereas expression of PAR complex genes increased with increase in the tumor grade compared to control brain tissue.

Decades of research revealed that the generation of an epithelial tumor requires the cooperation of mutations in various oncogenes or tumor suppressor genes (Hanahan and Weinberg, 2000). For the formation of an invasive tumor from a normal epithelial cell, mutations affecting at least six cellular processes are required—the so-called 'hallmarks of cancer'. They are: (1) continued cell proliferation, (2) evasion of apoptosis (cell death), (3) loss of differentiation, (4) invasion/ metastasis, (5) continued telomere elongation and (6) sustained angiogenesis. Although not initially documented in relation to the hallmarks of cancer, for epithelial cells to exhibit invasive/metastatic properties, they must undergo an EMT to sever cell–cell and cell– extracellular matrix adhesions, thereby enabling them to metastasize from the primary tumor (Thiery, 2002). EMT is related to the loss of cell polarity, specifically the loss of adherens junction function.

The organised polarity of cells is a hallmark of the epithelia. Loss of polarity and tissue architecture is a common feature of cancer tissues. However, neither the mechanisms by which cell and tissue architecture is deregulated nor the role of tissue architecture during cancer are well understood. Recently, Bilder et al (Bilder and Perrimon, 2000) identified the basolateral protein scribble that determines the localisation of the apical epithelial determinants. Loss of scribble mutation leads to loss of apical-basolateral polarity and leads to the overgrowth of imaginal discs, follicle epithelia, and larval brain in *Drosophila* (Bilder et al, 2000a). Scribble is localised at the septate junction in *Drosophila*, which is the analogue of the vertebrate tight junction. In scribble mutants, the adherens junctions are distributed around the cell periphery. Looking at its amino-

acid sequence, scribble has four PDZ domains named for its occurrence in the PSD-95, Discs-Large, and ZO-1 proteins), and it could have four different binding partners through four PDZ domains simultaneously. *Drosophila* scribble and hScrib have the conserved amino-acid sequence, especially in LRRs and PDZ domains, which propose an identical function for these two homologues. In addition, scribble has 16 canonical leucine-rich repeats (LRRs), another protein–protein interaction motif. These proteins are grouped as LAP (LRR and PDZ domain) proteins (Bilder et al, 2000b).

Scribble or hSCRIB overexpression and mislocalization are observed, with very low levels of scribble detected in invasive projections of tumors. In mammals, loss of SCRIB induces dysplastic growth *in vivo*, identifying loss of expression as a tumor suppressive mechanism. Although the precise mechanism of tumor suppression is unclear, SCRIB is known to inhibit apoptosis in a β-PIX (PAK-interacting exchange factor b)/Rac/JNK pathway-dependent manner, and promote proliferation in a Ras/MAPK dependent manner in mammary and prostate epithelia, respectively (Zhan et al, 2008; Pearson et al, 2011). Conversely, overexpression of SCRIB in mammary epithelial cells promotes epithelial differentiation by suppressing expression of epithelial mesenchymal transition regulators in a Ras/MAPK-dependent manner (Elsum et al, 2013). Conditional deletion of SCRIB in the corneal epithelium decreases E-cadherin expression and promotes mesenchymal transition, suggesting that SCRIB is required for maintaining epithelial cell identity (Yamben et al, 2013). In addition, SCRIB also regulates the Hippo signaling pathway (Skouloudaki et al, 2009), and signal transducer and activator of transcription (STAT) (Werme et al, 2008). SCRIB interacts with the Akt phosphatase PHLPP1 (Li et al, 2011), the planar cell polarity protein VANGL1 (Anastas et al, 2012), and the neuronal nitric oxide synthase adaptor protein NOS1AP (Richier et al, 2010) to regulate cancer cell migration and axon morphogenesis. In addition to changes in SCRIB gene expression, hSCRIB protein is mislocalized from cell–cell junctions in multiple human cancers, including breast, prostate, and colon. In prostate cancer, hSCRIB mislocalization is correlated with poor patient survival (Pearson et al, 2011). Mislocalization of other polarity proteins, including LGL and DLG, has also been associated with cancer progression (Huang and Muthuswamy, 2010), suggesting that mislocalization of polarity proteins is likely to have important implications for cancer in addition to changes in gene expression levels. However, it is not known if mislocalization of SCRIB is a consequence or a cause for cancer. In addition, a link between Scribble deregulation and the cytoplasmic

accumulation of β-catenin has been proposed, implicating Scribble in the APC/β-catenin pathway. Interestingly, Scribble has been shown to bind APC (Takizawa et al, 2006) and, in some contexts, β-catenin. Links have also been described between Scribble and E-cadherin; Scribble was found to colocalize with E-cadherin in the normal cervical epithelium, but in lobular breast cancer, in which E-cadherin is commonly downregulated, a loss of Scribble was observed at high frequency (Navarro et al, 2005). Scribble is also lost, but at a lower frequency, in breast ductal carcinomas, which maintain E-cadherin expression. An important observation which needs to be resolved is that the Scribble locus at 8q24.3 is frequently amplified in breast and ovarian tumors (Naylor et al, 2005; Kim et al, 2007). Collectively, the connections between hSCRIB and several pathways involving oncogenes and tumor suppressors, strongly suggest that it may play a role in the carcinogenesis of different types of tumor.

The present results confirm that hSCRIB shows decreased expression during glioma progression. We further analysed the correlation of hSCRIB expression and survival rates of patients. The survival rate of patients with strong positive or moderate positive staining tumors for hSCRIB was higher than the survival rates of patients with tumors showing hSCRIB-negative or weak positive staining. In our study, Kaplan-Meier analysis of the survival curves showed a significantly worse overall survival for patients whose tumors had low hSCRIB levels, indicating that low hSCRIB protein level is a marker of poor prognosis for patients with glioma. Moreover, multivariate analysis showed that decreased expression of hSCRIB may be a marker of worse outcome independent of known clinical prognostic indicators such as age, gender and grade. These data indicate that low expression of hSCRIB is correlated with a worse outcome of patients with glioma. Thus, hSCRIB may be an independent predictor of survival for glioma patients. In our study, which consisted of 32 cases of glioma and three normal brain samples, hSCRIB expression was analysed by immunohistochemistry, real-time PCR and western blot analysis. Thus, using a comprehensive methodology and a detailed clinical follow-up in our study the results were consistent and reliable.

3.5. Conclusion

In conclusion, our comprehensive analysis indicated that decreased expression of hSCRIB appears to be intimately involved in the pathogenesis of gliomas, and the activity of hSCRIB may contribute to maintaining an undifferentiated state of glioma cells. On the basis of these findings,

we assume that loss of hSCRIB may favour the progression of glioma cell transformation. However, further study is required to determine the precise role of hSCRIB and the mechanism of hSCRIB transcriptional regulation in gliomas.

3.6. References

1. Aigner K, Dampier B, Descovich L, Mikula M, Sultan A, Schreiber M, Mikulits W, Brabletz T, Strand D, Obrist P, Sommergruber W, Schweifer N, Wernitznig A,Beug H, Foisner R, Eger A (2007) The transcription factor Zeb1 ([Delta]Ef1) promotes tumor cell dedifferentiation by repressing master regulators of epithelial polarity. *Oncogene* 26:6979–6988.
2. Anastas JN, Biechele TL, Robitaille M, Muster J, Allison KH, Angers S, Moon RT (2012) Aprotein complex of SCRIB, NOS1AP and VANGL1 regulates cell polarity and migration, and is associated with breast cancer progression. *Oncogene* 31:3696–708.
3. Arimura N, Kaibuchi K (2007) Neuronal polarity: from extracellular signals to intracellular mechanisms. *Nat Rev Neurosci* 8: 194–205.
4. Betschinger J, Mechtler K, Knoblich JA (2003) The Par complex directs asymmetric cell division by phosphorylating the cytoskeletal protein Lgl. *Nature* 422:326-330.
5. Bhat MA, Izaddoost S, Lu Y, Cho KO, Choi KW, Bellen HJ (1999) Discs Lost, a novel multi-PDZ domain protein, establishes and maintains epithelial polarity. *Cell* 96:833-845.
6. Bilder D, Birnbaum D, Borg JP, Bryant P, Huigbretse J, Jansen E, Kennedy MB, Labouesse M, Legouis R, Mechler B, Perrimon N, Petit M, Sinha P (2000) Collective nomenclature for LAP proteins. *Nat Cell Biol* 2:E114.
7. Bilder D, Li M, Perrimon N (2000a) Cooperative regulation of cell polarity and growth by Drosophila tumor suppressors. *Science* 289:113–116.
8. Brumby AM, Richardson HE (2003) *scribble* mutants cooperate with oncogenic Ras or Notch to cause neoplastic overgrowth in *Drosophila. EMBO J* 22:5769–5779.
9. Castoria G, Migliaccio A, Di Domenico M, Lombardi M, De Falco A, Varricchio L, Bilancio A, Barone MV, Auricchio F (2004) Role of atypical protein kinase C in estradiol-triggered G1/S progression of Mcf-7 cells. *Mol Cell Biol* 24:7643–7653.
10. Debruin LS, Harauz G (2007). White matter rafting- membrane microdomains in myelin. *Neurochem Res* 32: 213-228.

11. Dow LE, Kauffman JS, Caddy J, Zarbalis K, Peterson AS, Jane SM, Russell SM, Humbert PO (2007) The tumor-suppressor Scribble dictates cell polarity during directed epithelial migration: regulation of Rho GTPase recruitment to the leading edge. *Oncogene* 26:2272–2282.
12. Eder AM, Sui X, Rosen DG, Nolden LK, Cheng KW, Lahad JP, Kango-Singh M, Lu KH, Warneke CL, Atkinson EN, Bedrosian I, Keyomarsi K, Kuo WL, Gray JW,Yin JC, Liu J, Halder G, Mills GB (2005) Atypical PKCiota contributes to poor prognosis through loss of apical-basal polarity and cyclin E overexpression in ovarian cancer. *Proc Natl Acad Sci U S A* 102:12519-12524.
13. Ellenbroek SI, Iden S, Collard JG (2012) Cell polarity proteins and cancer. *Seminars in Cancer Biology* 22: 208– 215.
14. Elsum IA, Martin C, Humbert PO (2013) Scribble regulates an EMT polarity pathway through modulation of MAPK-ERK signaling to mediate junction formation. *J Cell Sci* 126:3990–9.
15. Etienne-manneville S, Manneville JB, Nicholls S, Ferenczi M, Hall A (2005) Cdc42 and Par6-PKCζ regulate the spatially localized association of Dlg1 and APC to control cell polarization. *J Cell Biol* 170:895-901.
16. Gardiol D, Zacchi A, Petrera F, Stanta G, Banks L (2006) Human discs large and scrib are localized at the same regions in colon mucosa and changes in their expression patterns are correlated with loss of tissue architecture during malignant progression. *Int J Cancer* 119:1285–1290.
17. Hanahan D, Weinberg RA (2000) The hallmarks of cancer. *Cell* 100:57–70.
18. Heasman SJ, Ridley AJ (2008) Mammalian Rho GTPases: new insights into their functions from in vivo studies. *Nat Rev Mol Cell Biol* 9:690-701.
19. Horikoshi Y, Suzuki A, Yamanaka T, Sasaki K, Mizuno K, Sawada H, Yonemura S, Ohno S (2009) Interaction between PAR-3 and the aPKC–PAR-6 complex is indispensable for apical domain development of epithelial cell. *J Cell Sci* 122:1595–1606.
20. Huang L, Muthuswamy SK (2010) Polarity protein alterations in carcinoma: a focus on emerging roles for polarity regulators. *Curr Opin Genet Dev* 20:41–50.
21. Humbert PO, Dow LE, Russell SM (2006) The Scribble and Par complexes in polarity and migration: friends or foes? *Trends Cell Biol* 16:622–630.

22. Javier RT (2008) Cell polarity proteins: common targets for tumorigenic human viruses. *Oncogene* 27:7031-7046.
23. Kim M, Datta A, Brakeman P, Yu W, Mostov KE (2007) Polarity proteins Par6 and APKC regulate cell death through GSK-3beta in 3d epithelial morphogenesis. *J Cell Sci* 120:2309–2317.
24. Klezovitch O, Fernandez TE, Tapscott SJ, Vasioukhin V (2004) Loss of cell polarity causes severe brain dysplasia in Lgl1 knockout mice. *Genes Dev* 18:559-71.
25. Knoblich JA (2010) Asymmetric cell division: recent developments and their implications for tumor biology. *Nat Rev Mol Cell Biol* 11:849–860.
26. Krummel MF, Macara I (2006) Maintenance and modulation of T cell polarity. *Nat Immunol* 7:1143–1149.
27. Li X, Yang H, Liu J, Schmidt MD, Gao T (2011) Scribble-mediated membrane targeting of PHLPP1 is required for its negative regulation of Akt. *EMBO Rep* 12:818–24.
28. Nakagawa S, Yano T, Nakagawa K, Takizawa S, Suzuki Y, Yasugi T, Huibregtse JM, Taketani Y (2004) Analysis of the expression and localisation of a LAP protein, human scribble, in the normal and neoplastic epithelium of uterine cervix. *Br J Cancer* 90:194–199.
29. Navarro C, Nola S, Audebert S, Santoni MJ, Arsanto JP, Ginestier C, Marchetto S, Jacquemier J, Isnardon D, Le Bivic A, Birnbaum D, Borg JP (2005) Junctional recruitment of mammalian Scribble relies on E-cadherin engagement. *Oncogene* 24:4330–4339.
30. Nishimura T, Yamaguchi T, Kato K, Yoshizawa M, Nabeshima Y, Ohno S, Hoshino M, Kaibuchi K (2005). PAR-6-PAR-3 mediates Cdc42-induced Rac activation through the Rac GEFs STEF/Tiam1. *Nat Cell Biol* 7:270-277.
31. Nolan ME, Aranda V, Lee S, Lakshmi B, Basu S, Allred DC, Muthuswamy SK (2008) The polarity protein Par6 induces cell proliferation and is over expressed in breast cancer. *Cancer Res* 68:8201–8209.
32. Okajima M, Takahashi M, Higuchi M, Ohsawa T, Yoshida S, Yoshida Y, Oie M, Tanaka Y, Gejyo F, Fujii M (2008) Human T-cell leukemia virus type 1 Tax induces an aberrant clustering of the tumor suppressor Scribble through the PDZ domain-binding motif dependent and independent interaction. *Virus Genes* 37:231–240.
33. Osmani N, Vitale N, Borg JP, Etienne-manneville S (2006) Scrib controls Cdc42 localization and activity to promote cell polarization during astrocyte migration. *Curr Biol* 16:2395-2405.

34. Ouyang Z, Zhan W, Dan L (2010) hScrib, a human homolog of *Drosophila* neoplastic tumor suppressor, is involved in the progress of endometrial cancer. *Oncol Res* 18:593–599.
35. Ozdamar B, Bose R, Barrios-rodiles M, Wang HR, Zhang Y, Wrana JL (2005) Regulation of the polarity protein Par6 by TGFbeta receptors controls epithelial cell plasticity. *Science* 307:1603-1609.
36. Pagliarini RA, Xu T (2003) A genetic screen in Drosophila for metastatic behavior. *Science* 302:1227–1231.
37. Pearson HB, Perez-Mancera PA, Dow LE, Ryan A, Tennstedt P, Bogani D, Elsum I, Greenfield A, Tuveson DA, Simon R, Humbert PO (2011) SCRIB expression is deregulated in human prostate cancer and its deficiency in mice promotes prostate neoplasia. *J Clin Invest* 121:4257–4267
38. Regala RP, Weems C, Jamieson L, Khoor A, Edell ES, Lohse CM, Fields AP (2005) Atypical protein kinase C iota is an oncogene in human non-small cell lung cancer. *Cancer Res* 65:8905-8911.
39. Richier L, Williton K, Clattenburg L, Colwill K, O'Brien M, Tsang C, Kolar A, Zinck N, Metalnikov P, Trimble WS, Krueger SR, Pawson T, Fawcett JP (2010) NOS1AP associates with Scribble and regulates dendritic spine development. *J Neurosci* 30:4796–805.
40. Ridet JL, Malhotra SK, Privat A, Cage FH (1997) Reactive astrocytes: cellular and molecular cues to biological function. *Trends Neurosci* 20:570-577.
41. Schipke CG, Kettenmann H (2004). Astrocyte responses to neuronal activity. *Glia* 47:226-232.
42. Skouloudaki K, Puetz M, Simons M, Courbard JR, Boehlke C, Hartleben B, Engel C, Moeller MJ, Englert C, Bollig F, Schäfer T, Ramachandran H, Mlodzik M,Huber TB, Kuehn EW, Kim E, Kramer-Zucker A, Walz G (2009) Scribble participates in Hippo signaling and is required for normal zebrafish pronephros development. *Proc Natl Acad Sci U S A* 106:8579–84.
43. Takizawa S, Nagasaka K, Nakagawa S, YanoT, Nakagawa K, Yasugi T, Takeuchi T, Kanda T, Huibregtse JM, Akiyama T, Taketani Y (2006) Human scribble, a novel tumor suppressor identified as a target of high-risk HPV E6 for ubiquitin-mediated degradation, interacts with adenomatous polyposis coli. *Genes Cells* 11:453–464.
44. Tepass U, Knust E (1993) Crumbs and stardust act in a genetic pathway that controls the organization of epithelia in *Drosophila melanogaste.* *Dev Biol* 159:311–326.

45. Thiery JP (2002) Epithelial–mesenchymal transitions in tumor progression. *Nat Rev Cancer* 2:442–454.
46. Thomas M, Massimi P, Navarro C, Borg JP, Banks L (2005) The hScrib/Dlg apico-basal control complex is differentially targeted by HPV-16 and HPV-18 E6 proteins. *Oncogene* 24:6222–6230.
47. Varelas X, Samavarchi-tehrani P, Narimatsu M, Weiss A, Cockburn K, Larsen BG, Rossant J, Wrana JL (2010) The Crumbs complex couples cell density sensing to Hippo-dependent control of the TGF-β-SMAD pathway. *Dev Cell* 6:831-44.
48. Wang HR, Zhang Y, Ozdamar B, Ogunjimi AA, Alexandrova E, Thomsen GH, Wrana JL (2003) Regulation of cell polarity and protrusion formation by targeting Rhoa for degradation. *Science* 302:1775–1779.
49. Werme K, Wigerius M, Johansson M (2008) Tick-borne encephalitis virus NS5 associates with membrane protein Scribble and impairs interferon- stimulated JAK-STAT signaling. *Cell Microbiol* 10:696–712.
50. Yamben IF, Rachel RA, Shatadal S, Copeland NG, Jenkins NA, Warming S, Griep AE (2013) Scrib is required for epithelial cell identity and prevents epithelial to mesenchymal transition in the mouse. *Dev Biol* 384:41–52.
51. Yi P, Feng Q, Amazit L, Lonard DM, Tsai SY, Tsai MJ, O'Malley BW (2008) Atypical protein kinase C regulates dual pathways for degradation of the oncogenic coactivator Src-3/Aib1. *Mol Cell* 29:465–476.
52. Zen K, Yasui K, Gen Y, Dohi O, Wakabayashi N, Mitsufuji S, Itoh Y, Zen Y, Nakanuma Y, Taniwaki M, Okanoue T, Yoshikawa T (2009) Defective expression of polarity protein PAR-3 gene (PARD3) in esophageal squamous cell carcinoma. *Oncogene* 28:2910-2918.
53. Zhan L, Rosenberg A, Bergami KC, Yu M, Xuan Z, Jaffe AB, Allred C, Muthuswamy SK (2008) Deregulation of Scribble promotes mammary tumorigenesis and reveals a role for cell polarity in carcinoma. *Cell* 135:865–78.

Chapter - 4

Role of SAPK/JNK signaling pathway in tumorigenesis and tumor progression of N-ethyl-N-nitrosourea induced transplacental rat glioma model

4.1. Introduction

Gliomas are the most common primary intracerebral neoplasms. Despite recent advances in treatment modalities such as surgical techniques, radiation therapy, chemotherapy and targeted gene therapy, their prognosis remains poor. Glioblastoma multiforme (GBM) is the most common and highly recurrent tumor of gliomas. GBMs include two subtypes. Primary GBMs arise `*de novo*' and secondary GBMs develop due to accumulation of mutations in lower grade gliomas. EGFR amplification, LoH 10q, $p16^{Ink4A}$ deletion and PTEN mutations are the common genetic alterations associated with primary GBMs whereas p53 mutations and PDGFR amplifications are frequent in secondary GBMs (Kleihues et al, 1999; Holland, 2001; Simmons et al, 2001; Ohgaki et al, 2007). These genetic alterations disrupt the cell cycle arrest pathways or activate various signal transduction pathways. Mutation of the p53, retinoblastoma (RB) and PTEN, deletion of $p16^{Ink4A}$, activation of the Ras and Akt pathways, and amplification of CDK4 and EGFR contribute to the development of gliomas (Cavenee, 1992; Hayashi et al, 1997).

4.1.1. N-ethyl-N-nitrosourea (ENU) induced rat glioma model

The possibility of having experimental models of brain tumors allows for testing therapies applicable to human brain tumors. There is a major need of animal models in experimental neuro-oncology that can be used to assess the efficacy of innovative approaches for the treatment of brain tumors. There are several reasons for modelling of gliomas, which include: 1) determining which genetic alterations identified in human gliomas are the actual etiological events in the formation of gliomas by mimicking those genetic alterations in mice. 2) Accurate animal models are powerful tools to investigate important aspects of glioma biology that cannot be studied in cell culture systems, such as angiogenesis, invasion, and metastasis. There are numerous approaches for modelling gliomas. To date, four major approaches have been successfully employed: 1) chemical mutagen-induced models, 2) germline genetic modification-induced models, 3) xeno or allograft transplantation-induced models, and 4) somatic genetic modification-induced models. In very few cases radiation induced brain tumor models is employed. Each of these strategies has characteristic features that have advantages or disadvantages depending on the application. Among DNA viruses, both adenoviruses and papovaviruses have been shown to induce brain tumors in animals. RNA viruses causing experimental brain tumors consistently belong to the retrovirus group. On the other hand, the hetero-transplantation of human brain tumors into immune-deprived animals

has gained great interest after the development of the nude mouse model. It is known that human meningiomas and glioblastomas can grow after subcutaneous transplantation into the nude mouse, maintaining its original morphology. However, at present, diverse chemical agents provide the best models of experimental neurocarcinogenesis.

4.1.1a. Chemical neurocarcinogenesis

The discovery of chemical carcinogens has stimulated neuro-oncology research because, after systemic application, these compounds induce a high incidence of tumors in the central nervous system (CNS) and peripheral nervous system (PNS). Druckrey et al, has demonstrated the ability of N-methyl-N-nitrosourea (MNU) in inducing CNS tumors (Druckrey et al, 1969). N-nitroso-compounds in particular nitrosamides are not only carcinogenic but also toxic, teratogenic and mutagenic (Magee, 1969). Some of these compounds occasionally induce tumors in the CNS of adult animals, but they represent powerful neuro-oncogenic agents when administered transplacentally or during the early stages of postnatal life. Compounds, such as N-propyl-N-nitrosourea, N-butyl-N-nitrosourea, N-dimethyl-N-nitrosourea, and N-Trimethyl- N-nitrosourea, have been used in literature to induce CNS tumors. However, at present, N-ethyl-N-nitrosourea (ENU) is considered the best chemical agent to induce experimental brain tumors, because it is capable of inducing a high incidence of tumors, with known latency and morphology. These carcinogens would induce glioma formation by inducing mutations in simultaneous multiplication of cells of different origin (Zimmerman, 1969).

4.1.1b. Mechanism of tumor induction in chemical neurocarcinogenesis

Most carcinogenic compounds are precarcinogens which are converted in the host. The final product of this transformation is an electrophilic group that is capable of reacting with various cell constituents. Upon metabolism these carcinogens are converted into carbonium ion and nitrogen ion whereby they react with –SH, –OH or –NH groups of proteins or nucleic acids. These compounds exhibit biological effects as alkylating metabolites which are formed during processing *in vivo*. Alkylation of guanine in DNA has been observed with ethyl and methyl nitrosourea and observed to persist for longer time duration in brain than in liver (Wechsler et al, 1969; Goth and Rajewsky, 1974; Kleihues and Margison, 1974). Recent studies suggest the possibility that the induction of neural tumors by nitrosourea compounds may be related to a deficiency in DNA repair mechanisms in the Nervous System (Goth and Rajewsky, 1974). In the non-target organs for carcinogenic action, the O6-alkylation excision is repaired during replication, or alteration remains in the sequence of DNA bases.

4.1.1c. Factors influencing the tumor induction by chemical neurocarcinogenesis

Several factors like species, age of animal, dose and mode of administration of carcinogen and immunological factors influence the incidence, distribution, histology of tumors, and survival time of animals. For example, male Sprague-Dawley rats treated with methyl nitroso urea only develop brain tumors, while male Fischer rats show a high incidence of PNS tumors (Swenberg et al, 1972). In adult animals, repeated doses of the carcinogen is needed to obtain a high incidence of neurogenic tumors. In perinatal carcinogenesis, however, a single dose is sufficient to induce tumors in the nervous system, approximately in 90-100% of the experimental animals. The prenatal administration of these compounds increases the neurospecific carcinogenic effect. Even the amount of carcinogen influence the rate of tumor occurrence. For example, number of tumors transplacentally induced by ENU can vary between 100% and 63% when the carcinogen dose is reduced from 80 mg / kg to 5 mg / kg body weight. Regarding the role of immunological factors in development of nervous system tumors, there is very little data. Delinger et al, (1973) studied the effect of the suppression of cell mediated immunity in carcinogenesis with methyl nitroso urea in Fischer rats. They used a treatment with anti-lymphocyte serum and observed no change in the incidence of neurogenic tumors.

These carcinogens induce tumors in different parts of brain. For example, these tumors are located preferably in periventricular region, in subcortical white matter of the cerebral hemispheres, and hippocampus. The periventricular tumors usually develop around lateral ventricles, including caudate nucleus and corpus callosum. In the spinal cord, tumors are normally at cervical and lumbar segments. After histological studies, the experimental brain tumors induced by ENU are classified as: 1) Mixed gliomas (oligodendro-astrocytomas). 2) Anaplastic gliomas, tumors that show great cellular pleomorphism with high mitotic activity and regressive changes. 3) Glioependymomas, tumors with ependymoma features that contained pleomorphic glial cells. 4) Gliosarcomas, containing neoplastic glial cells and mesodermal cells (Wechsler et al, 1969; Druckrey et al, 1970; Koestner et al, 1971; Swenberg et al, 1972). Neoplasms produced by methyl nitroso urea (MNU) and ethyl nitroso urea (ENU) have morphological and biological similarities to naturally occurring neural tumors in human and animals. An ethyl group in nitrosourea results in a relative specificity of nervous system tumors by transplacental route of administration, whereas methyl side chain results in high yields of these tumors after intravenous administration in the mature animal. MNU has to be given in small repeated doses to adults to obtain highest incidence, whereas ENU exerts its maximal carcinogenic action transplacentally or in neonatal application.

4.1.1d. ENU induced glioma development in rat

ENU induced rat glioma model has allowed the study of several aspects of tumor behaviour, such as microvascular organization (Yoshimura et al, 1998), dedifferentiation (Jang et al, 2004), gene mutations (O'Neill, 2000), microcirculation, angiogenesis (Bulnes et al, 2007) and experimental therapeutic agents (Kish et al, 2001). The ENU-induced glioma rat model is a well-established animal model for studying the natural development of glioma and is representative model for human glioma because of its location and also of its similar molecular and genetic alterations.

ENU induces tumors by acting on the NPC which persists in the ventricular and subventricular region (Leonard et al, 2001). During brain development, neuronal proliferation and differentiation precede the glial development. Hence, ENU injected at 18th day of gestational period is likely to show effect on glial cells that are actively proliferating and makes them susceptible to ENU action. ENU induced glioma rat model is an appropriate model to study stage specific alterations during tumor progression and it also provides latent period, which gives lucid perception of pathological changes in tumor development (Schiffer et al, 1980; Trosko, 2001). However, transplacental neurocarcinogenesis induced by ENU, is an ideal model for the study of glial tumors, because essentially 100% of offspring's develop neural tumors several months after a single maternal exposure in the late embryonic period (Druckrey et al, 1966; Koestner, 1990). Since ENU decomposes rapidly *in vivo* (Goth and Rajewsky, 1974), the interaction between the carcinogen and the relevant cellular macromolecules is brief and allows for a sequential study of tumor development. However, there is a latency period that it is the time between birth and the first neurological manifestations. This period has generally been estimated between 5 or 6 months. When animals are killed during this period of time, tumor lesions can be observed with different levels of development. The first "early neoplastic proliferations" appear about two months after birth. These lesions represent early stages of tumor development, and are generally located in the white matter at the level of the lateral ventricles, and the angle of the ventricle, between the caudate nucleus and corpus callosum, or in the subcortical white matter. The tumors that develop from these microtumors retain their morphology, including proliferation centres, but occasionally may have an increased cellular pleomorphism. At four-five months, they show a polymorphic aspect. In many proliferative centres, the cells develop a cytoplasm showing a clear appearance of astrocytes, which subsequently can be gemistocytic. In these neoplasms a central zone showing avascular necrosis, and a peripheral vascular zone can be observed. In most vessels, hyperplasia at level of endothelial cells (Nishio et al, 1983), and an increase in

the number of capillaries can be seen. In contrast to sections of untreated rats, H&E staining sections of ENU induced glioma rats show cells with apoptotic features and marked cellularity including mitotic figures and bizarre pleomorphic cells and increased cellularity in sub ventricular region. General scheme of tumor development after transplacental ENU administration is represented in fig. 4.1.

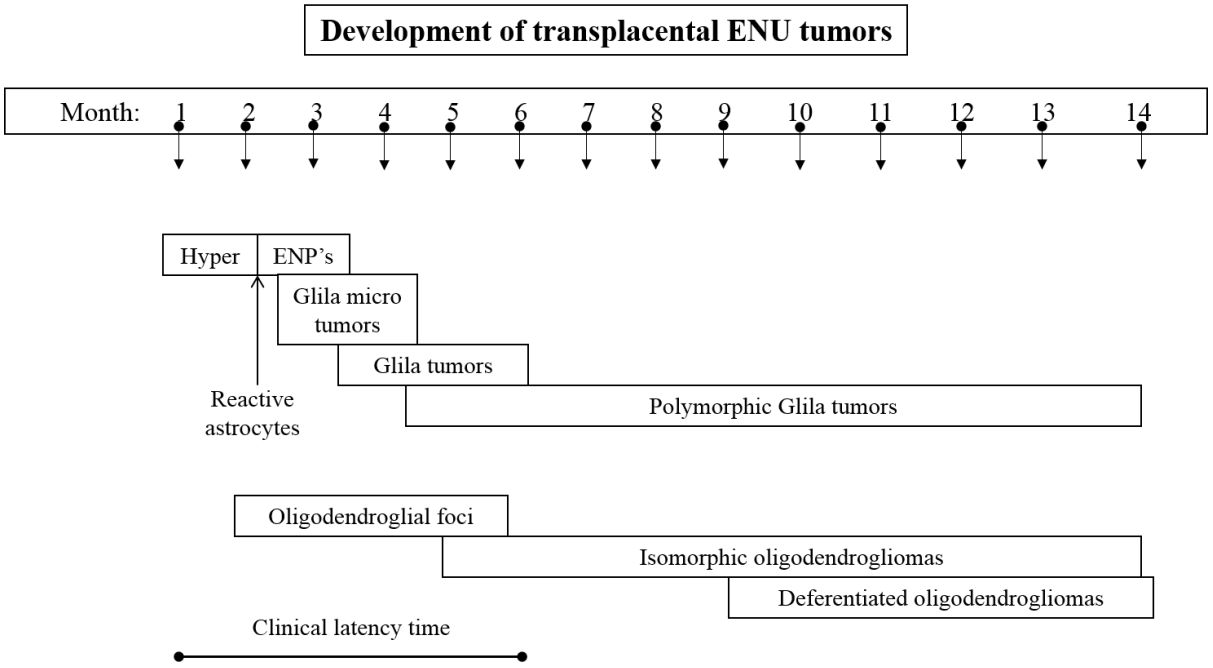

Fig. 4.1. General scheme of tumor development after transplacental ENU. (Schiffer et al, 1980).

4.1.2. JNK pathway

The mitogen-activated protein kinase (MAPK) cascades are evolutionary conserved, intracellular signal transduction pathways that respond to various extracellular stimuli and control a large number of fundamental cellular processes including growth, proliferation, differentiation, motility, stress response, survival and apoptosis (Shaul and Seger, 2007; Raman et al, 2007; Pimienta and Pascual, 2007). MAPK family includes three modules: Extracellular signal regulated kinase cascade, c-jun N-terminal kinase cascade and p38 MAPK cascade.

The c-Jun N-terminal kinase (JNK) group of mitogen-activated protein kinases (MAPKs) is activated in mammalian cells by environmental stress, pro-inflammatory cytokines, and mitogenic stimuli. The c-Jun NH_2-terminal kinase (JNK) is activated by the cytokine tumor necrosis factor (TNF). This pathway is implicated in the regulation of AP-1-dependent gene

expression by TNF. JNK enzymes phosphorylate transcription factors such as c-Jun, ATF-2, and JunD, which participate in formation and activation of the AP-1 complex (Karin and Gallagher, 2005). JNK family members include JNK1, JNK2 and JNK3, each of which has multiple isoforms that are generated through alternative splicing events (Gupta et al, 1996). JNK1 and JNK2 are ubiquitously expressed, while JNK3 is principally expressed in neural tissue (Davis, 2000). Biochemical and genetic studies demonstrate that JNK regulates the activities of many transcription factors and is involved in cell death, proliferation, and differentiation as well as cells response to stress such as ultraviolet light and proinflammatory molecules. The mechanism of activation of JNK is mediated by dual phosphorylation within kinase subdomain VIII on the motif Thr-Pro-Tyr. This phosphorylation is mediated by the MAP kinase kinases MKK4 and MKK7. These MAP kinase kinases serve as signaling molecules that integrate a wide array of stimuli into the activation of JNK signaling pathway. The diversity of mediators upstream of MKK4 and MKK7 may allow JNK pathway activation by a range of external stimuli such as tumor necrosis factor (TNF) and interleukin-1 (Dong et al, 2002).The JNK cascade was initially identified as a regulator of the transcription factor c-Jun, and a mediator of intra- or extra-cellular stresses, which gave it its other name, stress-activated protein kinase (SAPKs) cascade (Davis, 1994).Upon activation, the stress and other stimuli transmit their signals to small GTPases such as CDC42 and Rac1, which activate the MAP3K level kinases either directly or via MAP4Ks. Alternatively, the MAP3Ks and MAP4Ks of the cascade can be directly activated also by stimulated interaction with adaptor proteins such as TRAF (Bradley and Pober, 2001). A large number of MAP4Ks (Dan et al, 2001) and MAP3Ks (Craig et al, 2008) has been identified thus far, and each of these seems to transmit signal of the cascade by binding to distinct scaffold proteins under distinct conditions (e.g. JIPs (Whitmarsh, 2006). Upon activation, kinases at MAP3K tier transmit signals further by phosphorylating Thr and Ser residues in activation loop, and thereby activating kinases at MAPKK level (MKK4 and MKK7 (Wang et al, 2007). In turn, these kinases activate the three components at the MAPK level (JNK1-3; 46 and 54 kDa; JNKs) by direct phosphorylationof Tyr and Thr residues in their activation loop's Thr-Pro-Tyr motif). JNK activation may influence important cellular consequences, such as alterations in gene expression (Xie et al, 2005; Zachos et al, 1999), cell death (Guessan et al, 2005; Tamanini et al, 2003), viral replication, persistent infection or progeny release (Rahaus et al, 2004), or altered cellular proliferation (Lan et al, 2004).

The oncogenic role of JNK signaling pathway is well established in several cancers but little is known in glioma development. It has been documented that JNK pathway is activated

in astrocytic tumors in direct association with WHO grade of malignancy but not in normal brain tissues, suggesting a role for JNK in biology of astrocytic tumors including their most malignant form, glioblastoma (Antonyak et al, 2002; Assimakopoulou et al, 2007; Li et al, 2008). A study using the serum-cultured U87 cell line showed that JNK is indeed involved in the growth of bulk-cultured glioblastoma cells as well as xenografts derived from them, the results also showed that such JNK involvement is modest (Cui et al, 2006). However, JNK2α, a JNK isoform is constitutively activated through an auto phosphorylation mechanism independently of upstream activating signals, is reportedly expressed in majority of human glioblastomas (Cui et al, 2006). Recently Ken-ichiro Matsuda et.al, have shown that JNK pathway is activated in small sub population of cells called stem like glioblastoma cells (Matsuda et al, 2012). Thus, targeting JNK pathway either upstream or downstream of JNK may be essential to control the pathway in glioblastoma cells.

In the present study we wanted to investigate role of JNK signaling pathway in progression of ENU-induced rat gliomas and *in vitro* targeting rat C6 glioma cell proliferation using small molecule inhibitor SP600125 (anthra [1.9-cd] pyrazole-6(2H)-one), which has been reported to be a potent and selective inhibitor of JNK1,-2 and -3 with more than >20 fold selectivity over other related MAP kinases (Bennett et al, 2002).

4.2. Materials and methods

4.2.1. Screening of the vaginal smears for time specific gestation in rats

Prior to the experimentation, institutional ethical clearance was obtained as per the national ethical committee guidelines (CPCSEA-2011). Female Wistar rats weighing about 250 g were screened regularly at daily interval by using methylene blue dye method for the pattern of vaginal smears to detect the different stages of estrus cycle. When the rats showed estrus smear pattern, they were allowed for mating and the day following mating with appearance of diestrus pattern of vaginal smear indicated zero-day of pregnancy.

4.2.2. Induction of experimental transplacental glioma

All the experiments on animals were approved by the institutional ethics committee. ENU (Sigma Aldrich, St Louis, MO, USA) was freshly prepared by dissolving 10 mg/ml in 0.9% saline and adjusted pH to 4.5 with crystalline ascorbic acid. ENU injections were performed as described earlier (Bhaskara et al, 2006; Sareddy et al, 2009). In this study 6 pregnant Wistar rats were injected with single transplacental dose of (75 mg/kg body weight)

of ENU on 18th day of gestational period and rats receiving injections of saline at the same day of gestation under similar conditions were used as control.The sample group containing total of 44 glioma rats was sacrificed at postnatal day (P) 90, 16rats at (P) 135 and 16 rats at (P) 180 days representing different levels/grades of tumor malignancy and used for western blot and histopathological analyses. For histological studies we examined the coronal section of glioma rat brains encompassing the anterior corpus callosum to the posterior hippocampus.

4.2.3. Western blotting

Rat brain tissues were homogenized in 5 volumes of RIPA (radioimmunoprecipitaiton assay) buffer containing 50 mM Tris-HCl (pH 8.0), 150 mM NaCl, 1 mM EDTA, 0.4% deoxy-cholate, 1% NP-40 containing protease inhibitors including 1 mM phenylmethylsulfonylfluoride (PMSF) and phosphatase inhibitors including 10 mM β-glycerophosphate, 10 mM NaF, 0.3 mM Na3Vo4 and 0.3 mM aprotinin. The lysate was sonicated for 2 min and centrifuged at 14,000g for 15 min at 4^{o}C. The supernatant was collected as whole tissue lysate and frozen at -80^{o}C before use. Protein concentrations were determined by Lowry method. 75 μg of cellular protein were mixed with SDS sample buffer, boiled for 5 min and subjected to electrophoresis on 10% SDS-polyacrylamide gels and transferred onto nitrocellulose membranes. After blocking the nitro cellulose paper in non-fat dry milk (5%) in Tris Buffered Saline (TBS) (10mM Tris (pH 7.5), 150 mM NaCl) for 1 h at room temperature, membranes were incubated for 12 h with primary antibody pMKK4, pJNK, JNK, pc-jun and β-actin (Cell Signalling Technologies, Beverly, MA, USA) for overnight at 4^{0}C. Then membranes were incubated with secondary antibodies conjugated to alkaline phosphatase (ALP) (anti-rabbit and anti-mouse IgG conjugated to ALP obtained from Genei Pvt ltd, Bangalore, India), for 1-2 h at room temperature. Before and after incubation with secondary antibodies, membranes were washed with TBS and TBST (TBS containing 0.1% Tween- 20). Immunoreactivity was visualized by incubating the membranes with BCIP-NBT solution (Genei Pvt Limited, Bangalore, India). Membranes were analyzed quantitatively using image J software (NIH).

4.2.4. Immunohistochemistry

Immuno histochemical studies were performed on formalin-fixed, paraffinembedded specimens. Briefly, sections were deparaffinised in xylene and passed through graded alcohols and further rehydrated in phosphate buffered saline (PBS). Antigen unmasking was carried out by micro waving the sections for 10-14 min in 10mM citrate buffer (pH 6.0). Sections were

then treated with 3% H2O2 for 10 min to inhibit endogenous peroxidase followed by incubation with blocking serum for 1 h at room temperature in a humid chamber. The sections were then incubated overnight at 4ºC with primary antibodies against pMKK4, pJNK and pc-jun for 1 h at room temperature followed by incubation with peroxidase conjugated secondary antibody for 1 h at room temperature. After washing in TBS, diaminobenzidine (DAB) in buffer was applied till sections develop colour. Then, sections were washed with distilled water followed by dehydration in graded alcohols, xylene and mounted with DPX (kit obtained from Biogenex Pvt Limited, India). In each experiment, a negative control was included in which the primary antibody step was skipped and replaced by non-immune serum.

4.2.5. Cell culture

C6 glioma cell line was obtained from National Center for Cell Science (NCCS), Pune, India. C6 cells were cultured in RPMI media, supplemented with 10% FBS, 100 IU/ml penicillin and 100µg/ml streptomycin in a humidified atmosphere with 5% $C0_2$ at 37°C.

4.2.6. Cell viability, Clonogenic assays and Western Blotting

The growth inhibitory effect of SP600125 on C6 cells was assessed by trypan blue exclusion assay. C6 cells were plated ($1x10^5$/well) in a 6-well plate and treated with vehicle (0.1% DMSO) or 20µM of SP600125 for 24 h, 48 h and 72 h. Then, number of trypan blue-excluding viable cells was counted using light microscope. Clonogenic assays were performed by plating 500 C6 cells in a 100-mm dish and treated with SP600125 or vehicle (0.1% DMSO) for 48 h. Then cells were allowed to grow for 7 days and stained with 0.5% methylene blue in 50% methanol. Colonies that contain more than 50 cells were counted (Du et al, 2004). All treatments were performed in triplicate and results expressed as mean ± S.D.

Besides, C6 cells were treated with vehicle (0.1%DMSO), 10µM, 15 µM and 20 µM SP600125 for 12 h and the cells were lysed in RIPA buffer followed by sonication and centrifugation at 14,000 rpm for 15 min. The supernatant was collected as whole cell lysate and subjected to western analysis for JNK, pJNK, pc-jun and β-actin as described earlier.

4.2.7. Statistical analysis

All data are represented as mean ± S.D. Differences between tumors and controls were compared by paired Student's t-test (n = 44). *P* values <0.05 were considered as statistically significant.

4.3. Results

4.3.1. Identification of vaginal smears pattern representing different stages of the estrus cycle

Time specific gestation is essential for the administration of ENU during the critical gestation time period of the rats. Appearance of different patterns of vaginal cells followed in a cyclic manner among the rats. Estrus stage was indicated by the presence of large cornified (degenerative cells which lost nuclei) epithelial cells with few nucleated cells. Metestrus was observed after ovulation and consists of large cornified epithelial cells mixed with polymorphonuclear leukocytes. Presence of polymorphonuclear leukocytes exclusively along with few nucleated epithelial cells was classified as diestrus stage, which was known as period of inactivity. Mixture of round nucleated epithelial cells and presence of few leukocytes in the smear will indicate proestrus stage. Proestrus stage is known to be as preparatory period of next estrous cycle. Vaginal cell patterns of different stages are presented in fig. 4.2.

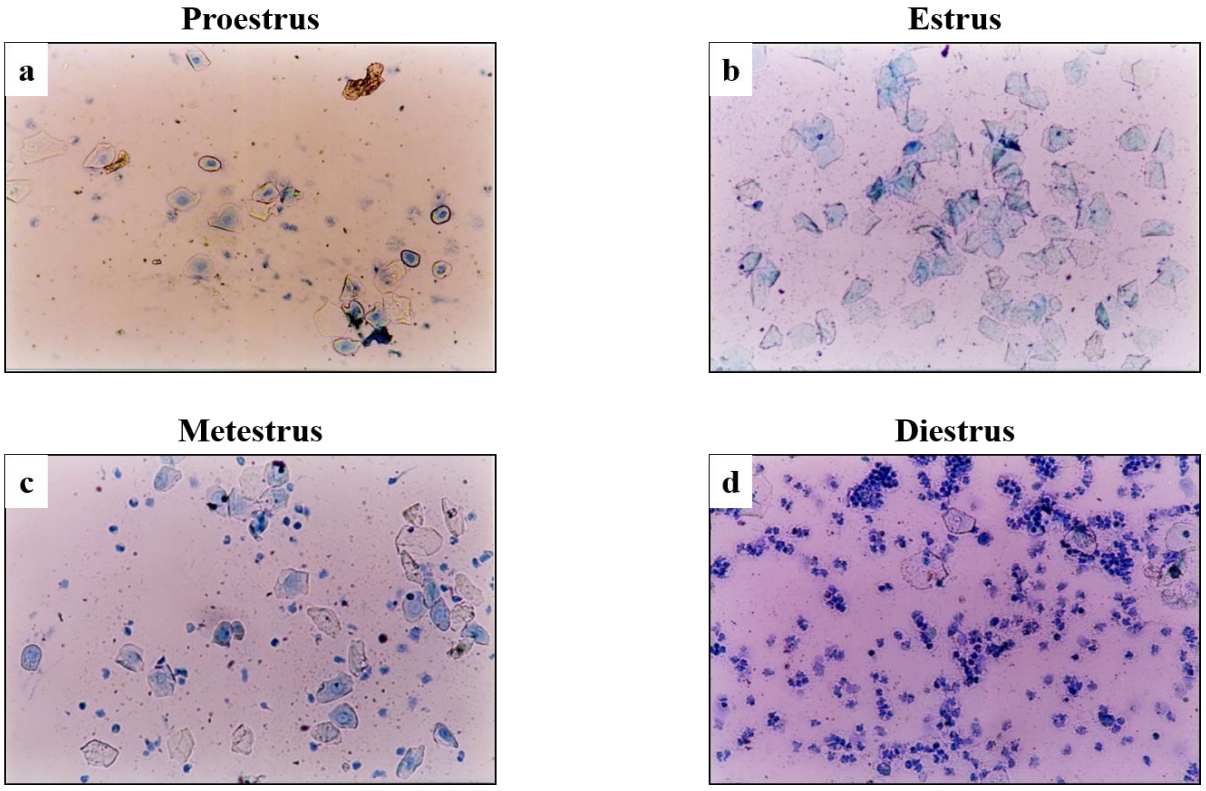

Fig. 4.2. (a) Rat vaginal smear showing mixture of round nucleated epithelial cells and with few leukocytes, which lasts for 12 h. This pattern is referred to as proestrus stage of the cycle. **(b)** Rat vaginal smear showing presence of exclusively a large cornified epithelial cells with few nucleated epithelial cells, which lasts for 12 h. This pattern is referred to as estrus stage of

the cycle. **(c)** Rat vaginal smear showing presence of large cornified epithelial cells mixed with polymorphonuclear leukocytes, which lasts for 21 h. This pattern is referred to as metestrus stage of the cycle. **(d)** Rat vaginal smear showing presence of exclusively a large number of polymorpho nuclear leukocytes through the smear, which lasts for 60–70 h. This pattern is referred to as diestrus.

4.3.2. Screening the glioma rats with neurological symptoms indicating growth of brain or spinal cord tumors

Clinical examination should include observation on state of consciousness and behaviour, grooming state, gait, head posture, visual and tactile placing reactions, bladder function, appearance of eyes, response of limbs to stimuli, and palpation of cranium and spine. In the present study, rats were suffering due to the corneal erosion observed from the birth, weight loss, shaggy and loss of fur along with discoloration of skin, rats were also observed to be aggressive or depressive. Animals with neurological symptoms indicating growth of brain tumors were used for the present experimentation.

4.3.3. Increased expression of pMKK4, pJNK and pc-Jun with tumor malignancy

The protein levels of pMKK4, an upstream activator of JNK, were significantly elevated in glioma rats compared to saline treated control rats ($P<0.05$) (Fig.4.3a and b). Immunohistochemical analysis showed pMKK4 positivity in tumor cells of 90, 135 and 180 day glioma rats (Fig. 4.3c). MKK4 is phosphorylated and activated by Raf kinases in response to growth factor and stress stimuli which further phosphorylates and activates JNK resulting in its nuclear translocation. In the present study, the levels of pJNK were significantly increased in brain tissues of glioma bearing rats compared to controls ($P<0.05$) (Fig. 4.4a and b). Further, immunohistochemical analysis revealed its cytoplasmic and nuclear positivity in tumor cells of 90, 135 and 180 day brain sections of glioma bearing rat (Fig. 4.4c). In contrast, un-phosphorylated JNK levels were unchanged in brain tissue of control and glioma bearing rats. In nucleus, pJNK mediates its effects through phosphorylating and activating c-Jun. In this study, levels of pc-jun were significantly increased in brain tissues of glioma bearing rats in comparison to control rats ($P<0.05$) (Fig. 4.5a and b). Further, immunohistochemical analysis revealed its nuclear positivity for pc-jun in tumor cells of glioma bearing rats (Fig. 4.5c).

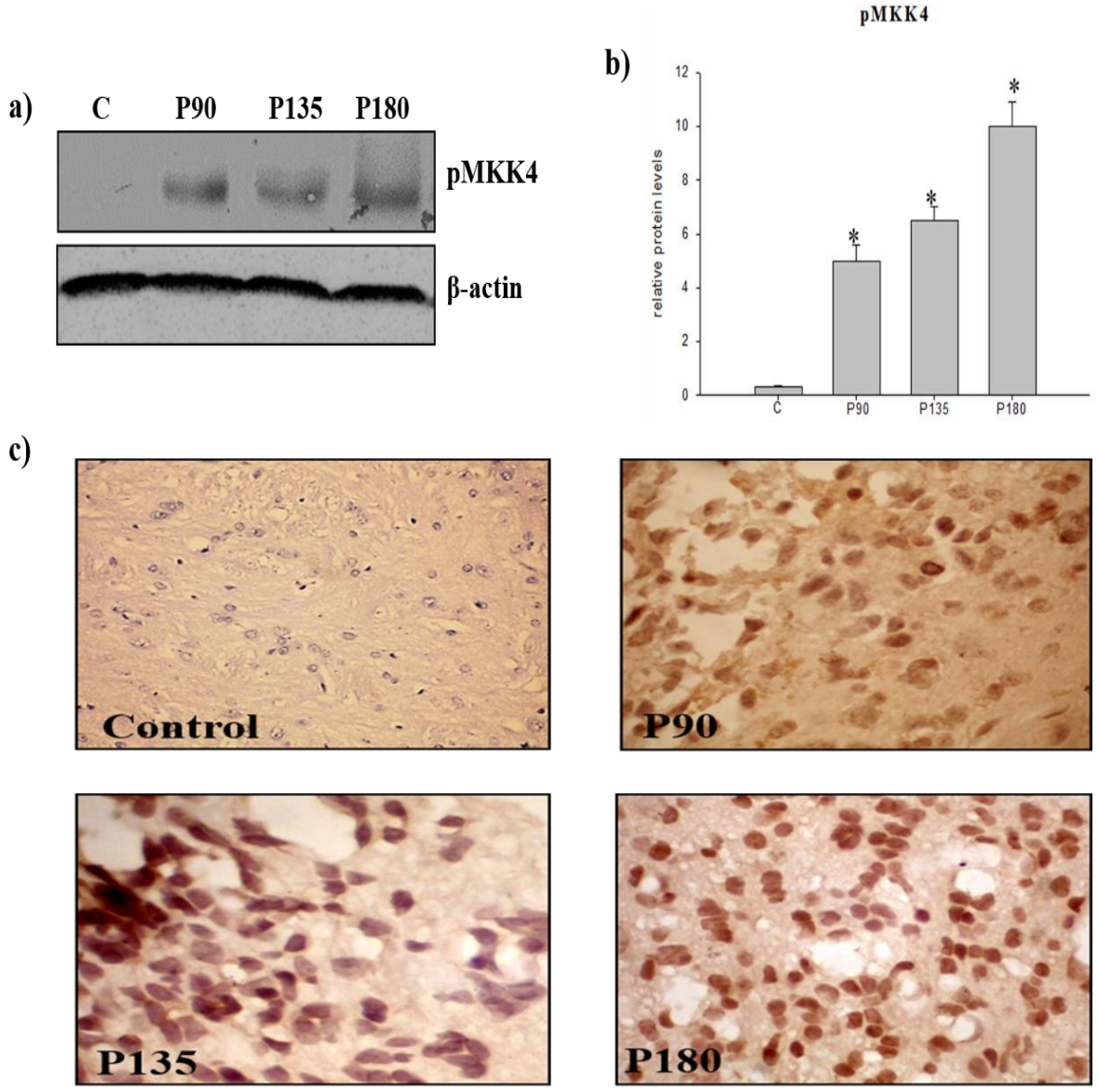

Fig. 4.3. Overexpression of pMKK4 in gliomas. **(a)** Whole cell lysates extracted from glioma rat brains were resolved on 10% SDS gels and subjected to western blot analysis. β-actin used as loading control. **(b)** Quantitative densitometric comparison of pMKK4 protein levels between controls and glioma rats. Data presented are mean ± SD from three independent experiments (*$p < 0.05$ indicate significant difference relative to the corresponding control). **(c)** Paraffin embedded sections prepared from glioma rat brains were incubated with anti-rabbit-pMKK4 primary antibody overnight at 4^0C and peroxidase conjugated secondary antibody for 1 h at room temperature. Then, immunoreactivity was visualized by diaminobenzidine (control, P90, P135 and P180: "P" indicates post natal age in days of glioma rats).

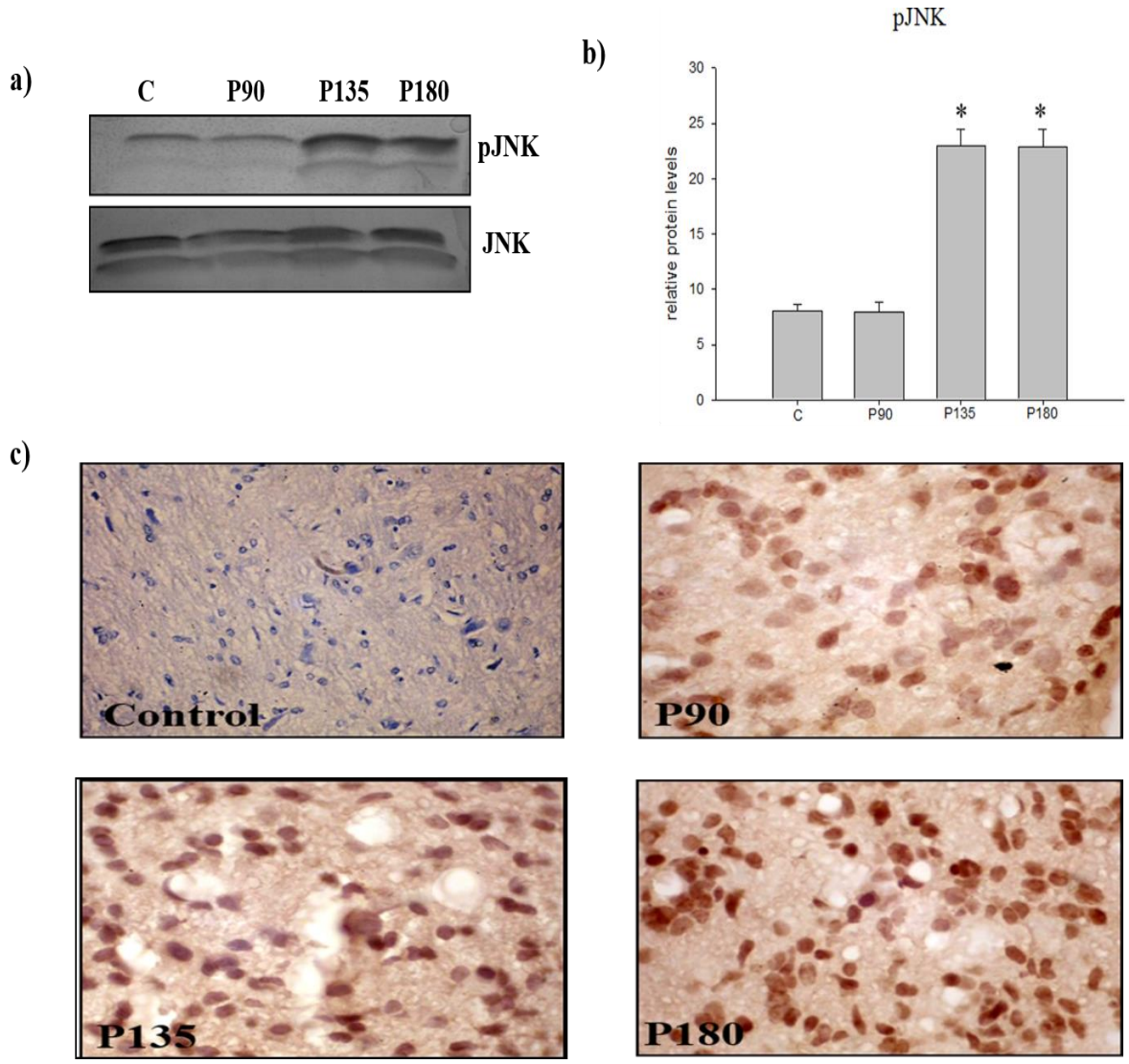

Fig. 4.4. Overexpression of pJNK in gliomas. **(a)** Whole cell lysates extracted from glioma rat brains were resolved on 10% SDS gels and subjected to western blot analysis. JNK used as loading controls. **(b)** Quantitative densitometric comparison of pJNK protein levels between tumor sections of control and glioma rats. Data presented are mean ± SD from three independent experiments (*p < 0.05 indicate significant difference relative to the corresponding control). **(c)** Paraffin embedded sections prepared from glioma rat brains were incubated with anti-rabbit-pJNK primary antibody overnight at 4^0C and peroxidase conjugated secondary antibody for 1 h at room temperature. Then, immunoreactivity was visualized by diaminobenzidine (control, P90, P135 and P180: "P" indicates post natal age in days of glioma rats).

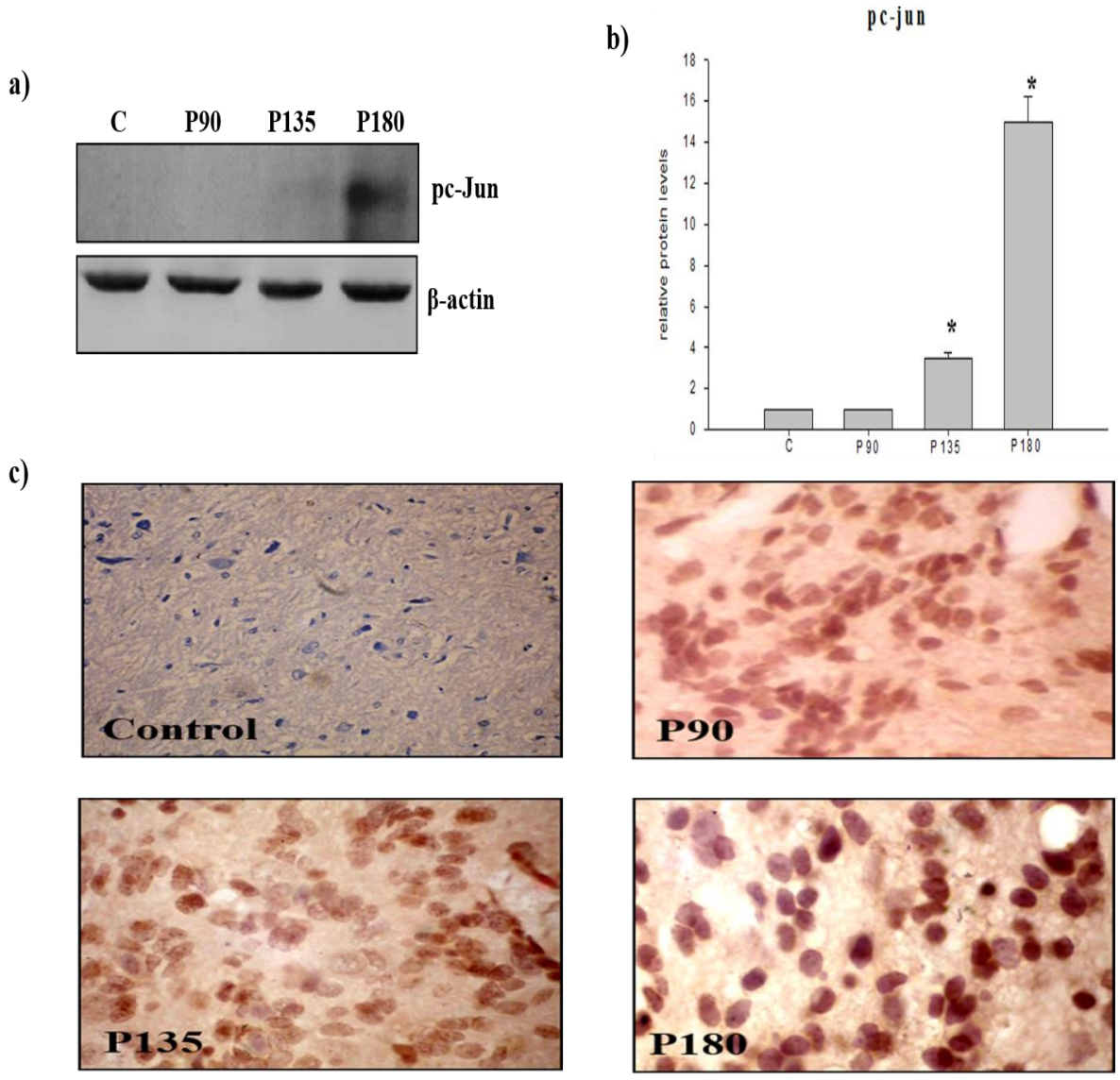

Fig. 4.5. Overexpression of pc-Jun in gliomas. **(a)** Whole cell lysates extracted from glioma rat brains were resolved on 10% SDS gels and subjected to western blot analysis. β-actin used as loading control. **(b)** Quantitative densitometric comparison of pc-Jun protein levels between controls and glioma rats. Data presented are mean ± SD from three independent experiments (*$p < 0.05$ indicate significant difference relative to the corresponding control). **(c)** Paraffin embedded sections prepared from glioma rat brains were incubated with anti-rabbit-pc-Jun primary antibody overnight at 4^0C and peroxidase conjugated secondary antibody for 1 h at room temperature. Then, immunoreactivity was visualized by diaminobenzidine (control, P90, P135 and P180: "P" indicates post natal age in days of glioma rats).

4.3.4. SP600125 inhibited C6 cell viability with decreased expression of JNK modules

In order to confirm the role of JNK signaling in glioma malignancy, we conducted studies with specific peptide JNK inhibitor SP600125 in C6 rat glioma cell lines. Treatment with SP600125 resulted in the significant inhibition of C6 cell proliferation in a time dependent manner (P<0.05) (Fig. 4.6a). Further, we performed clonogenic assays by plating 100 C6 cells in 100mm culture dishes and treated with SP600125 for 48 h and allowed to grow for 8 days. The clonogenic efficiency of C6 cells was significantly inhibited (P<0.05) following SP600125 treatment (Fig. 4.6b). Likewise, C6 cells treated with different concentrations (10µM, 15 µM and 20 µM) of SP600125 decreased the expression level of pJNK and pc-Jun in dose dependent manner compared to vehicle (0.1% DMSO) treatment (Fig. 4.6c). These results clearly suggest that SP600125 reduces the proliferation of C6 glioma cells by inhibiting the JNK signaling pathway.

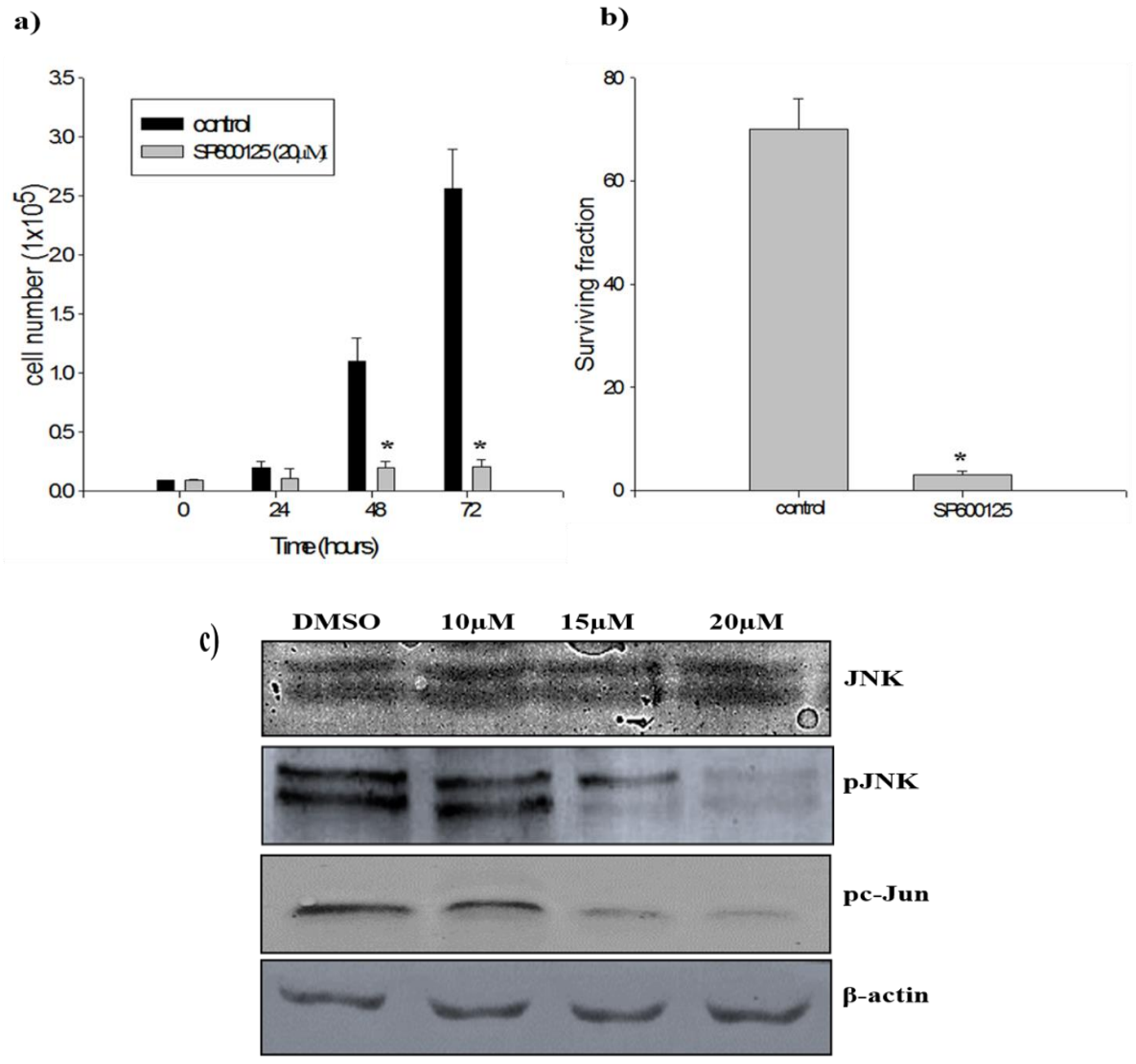

Fig. 4.6. Effect of SP600125 on proliferation of C6 glioma cell lines. **(a)** C6 cells were seeded in 6 well plates and treated with vehicle (0.1% DMSO) or 20 μM SP600125 and total viable cell numbers determined at daily intervals. Day "0" represents the starting condition of cells before addition of the inhibitor. Data presented are mean ± SD and are representative of three independent experiments (*$p < 0.05$). **(b)** 500 C6 cells were seeded in 100 mm culture dishes and treated with either vehicle (0.1% DMSO) or 20 μM SP600125. 8 days later colonies were stained with methylene blue and those containing 50 cells or greater were counted. Data presented are mean ± SD and are representative of three independent experiments (*$p < 0.05$). **(c)** Whole cell lysates were prepared from vehicle (0.1% DMSO) and SP600125 treated C6 cells and subjected to western analysis with JNK, pJNK and pc-Jun antibodies. β-actin served as internal control. Blots are representatives of three independent experiments.

4.4. Discussion

The chemical mechanism of tumor induction by ENU is well known and the model is very well established animal model to study tumor biology (Zook et al, 2000). Although used extensively in the 1970s and 1980s, ENU model has been abandoned for long time by glioma biologists on the basis that ENU is not a common cause of gliomas (which occur spontaneously), produces nonspecific genetic damages, and results in a diverse number of glioma types that creates too much heterogeneity for systemic study. However, each of these points can be answered. Thus, although vast majority of gliomas appear to rise "spontaneously", this does not exclude the possibility that the process was initiated by a prior exposure. As, in fact, it was shown by several epidemiological studies that exposure to chemical and radiological agents as important risk factors in glioma development (Wrensch et al, 2002). The ENU model accurately reflects the scenario of the apparent spontaneous development of gliomas because there is no way to distinguish the ENU-induced rat from an uninduced littermate until the former suddenly becomes symptomatic of glioma in middle age. The long latency between the administration of ENU which is cleared immediately and the appearance of brain tumors in offspring suggest that tumors develop through a multi-step process. ENU induces tumors by acting on the neural precursor cells (NPC) which persists in the ventricular and subventricular region (Leonard et al, 2001). From birth to one month of extra uterine life there is no difference between treated and control rats in the ventricular region, cortex, periventricular white matter and subeppendymal layer. After 30th day diffused cellular hyperplasia can be observed in the paraventricular white matter and reactive astrocytes appear.

These lesions further grow and become early neoplastic proliferation (ENP) (Schiffer et al, 1980). These ENP centers or oligodendroglial foci appear at the end of second month of extra uterine life and continue to appear till $3_{1/2}$ months and subsequently progress to "micro tumors" and then "tumors" at different stages of tumor development. Circumscribed necrosis and endothelial cell proliferations appear at $5_{1/2}$ months (Schiffer et al, 1978). In terms of the chromosomal aberrations produced, ENU produces N- and O-ethylation that damages DNA. Targeted cells then apply repair mechanisms. Subsequently, the insult and repair mechanisms result in a random mutagenesis including deletions, substitutions, and translocations (Shibuya et al, 1993; Alvarez et al, 2003; Beranek, 1990). Thus, a wide range of abnormalities can be noted, several of which are quite representative of the clinical situation. Finally although many types of primary tumors occur after ENU exposure, they resemble those encountered clinically. The WHO classification lists >17 tumors that can be clinically classified as gliomas based on their morphological characteristics (Kleihues et al, 2000). The ENU-induced tumors are composed of similar glial type of cells that can fit within such subgroups by using clinical neuropathological strategies. Furthermore, macroscopic tumors frequently contain hemorrhage and necrosis that are characteristic of the most malignant GBM (Zook et al, 2000). Thus, although a variability of glioma types is encountered in this model, they all have analogies to human histological findings (Jang et al, 2008). In the present study, we studied the stage specific alterations of JNK signaling at initiation (P90), promotion (P135) and progression stages (P180) of tumor development.

Till now, many molecules and pathways have been described as possible areas in the control of gliomas (Tabatabai et al, 2011). Nevertheless, none of these areas have been demonstrated as feasible targets of drugs meeting above necessities. Growth factors and growth factor receptors have shown to play an important role in neoplastic transformation of central nervous system tumors (Nieder et al, 2003). Over expression of PDGFR and EGFR and their ligands are common features of GBMs. These ligands and receptors activate Ras pathway, a major oncogenic signaling pathway, which activates the MAPK signaling cascades. Several lines of evidence suggest that ERK pathway is primarily activated by growth factors and ERK pathway activation associated with several human cancers (Reddy et al, 2003). Previously we reported the overexpression of growth factor receptors EGFR and PDGFR in human and ENU-induced rat gliomas and also showed the elevation of ERK signaling in human as well as ENU-induced rat gliomas (Bhaskara et al, 2005; Bhaskara et al, 2006). In addition, EGFR also activates JNK pathway and this activation is associated with several cancers. EGFR activation and PTEN loss are the most frequent events in gliomagenesis and these events act as upstream

modulators of JNK pathway (Rong et al, 2009). On the other hand, JNK2α, a JNK isoform overexpressed in most of the human glioblastomas is activated through an auto-phosphorylation mechanism independent of upstream activating signals (Cui et al, 2006). The JNK signaling pathway is primarily implicated in apoptosis in response to several stress stimuli. However, under certain physiological conditions, JNK plays a protective role and controls cell survival, cell proliferation, cell transformation, tumor progression and embryonic morphogenesis. Several lines of evidences suggest role of JNK signaling in cell growth and proliferation. Most of cultured cells have basal JNK activity and it is activated in response to growth factors (Kyriakis et al, 1994; Nieder et al, 2003). JNK pathway is required for transformation by Ras and other oncogenes and fibroblasts become partially transformed upon constitutive JNK activation (Rennefahrt et al, 2002). At this juncture we have recognized JNK as a critical regulator of ENU induced glioma progression. It has been reported that JNK pathway is activated in astrocytic tumors and degree of activation correlates with WHO grade of malignancy but not in normal brain tissues, implicating a vital role for JNK in gliomagenesis and its progression including their most malignant form, glioblastoma (Li et al, 2008). In addition, blocking of JNK with antisense oligonucleotides inhibited cell growth of human GBM cells (Potapova et al, 2000). The elevation of JNK signaling in pathogenesis of human brain tumors is reported previously and also found that JNK activation is most common than that of ERK in human astrocytomas (Antonyak et al, 2002; Tsuiki et al, 2003). Therefore, targeting JNK pathway either upstream or downstream of JNK can help us to control glioma growth. To test this hypothesis we used JNK inhibitor SP600125 (Bennett et al, 2002). Several studies have demonstrated the *in vitro* and *in vivo* effects of SP600125, thus it has become the small molecular inhibitor of JNK. In this study we observed that JNK signaling cascade is activated in ENU-induced gliomas compared to controls. Most importantly, use of specific JNK inhibitor SP600125 inhibited the proliferation and clonogenic efficiency of C6 glioma cells with decreased expression of JNK components.

4.5. Conclusion

In conclusion, though the present study does not provide complete evidence about JNK being therapeutic target compared to the candidate molecules described earlier, the *in vitro* study described in this report is consistent with and in support of existing studies, providing further support that JNK is a key regulator of ENU induced glioma progression and JNK might be an attractive target for therapeutic depletion of glioma.

4.6. References

1. Alvarez L, Comendador MA, Sierra LM (2003) Effect of nucleotide excision repair on ENU-induced mutation in female germ cells of Drosophila melanogaster. *Environ Mol Mutagen* 41:270–279.
2. Antonyak MA, Kenyon LC, Godwin AK, James DC, Emlet DR, Okamoto I, Tnani M, Holgado-Madruga M, Moscatello DK, Wong AJ (2002) Elevated JNK activation contributes to the pathogenesis of human brain tumors. *Oncogene* 21:5038–5046.
3. Assimakopoulou M, Kondyli M, Gatzounis G, Maraziotis T, Varakis J (2007) Neurotrophin receptors expression and JNK pathway activation in human astrocytomas. *BMC Cancer* 7: 202.
4. Bennett BL, Sasaki DT, Murray BW, O'Leary EC, Sakata ST, Xu W, Leisten JC, Motiwala A, Pierce S, Santoh Y, Bhagwat SS, Maning AM, Anderson AM, Anderson DW (2002) SP600125, an anthrapyrazolone inhibitor of Jun N-terminal kinase. *Pro Natl Acad Sci U S A* 98:13681-13686
5. Beranek DT (1990) Distribution of methyl and ethyl adducts following alkylation with monofunctional alkylating agents. *Mutat Res* 231:1–30.
6. Bhaskara VK, Manas P, Sundaram C, Prakash BP (2005) Comparative status of activated ERK1/2 and PARP cleavage in human gliomas. *Neuropathology* 25:48-53.
7. Bhaskara VK, Sundaram C, Prakash BP (2006) pERK, pAkt and pBad: a possible role in cell proliferation and sustained cellular survival during tumorigenesis and tumor progression in ENU induced transplacental glioma rat model. *Neurochem Res* 31:1163-1170.
8. Bradley JR, Pober JS (2001) Tumor necrosis factor receptor-associated factors (TRAFs). *Oncogene* 20:6482–6491.
9. Bulnes S, Lafuente JV (2007) VEGF immunopositivity related to malignancy degree, proliferative activity and angiogenesis in ENU induced gliomas. *J Mol Neurosci* 33:163-172.
10. Cavenee WK (1992) Accumulation of genetic defects during astrocytoma progression. *Cancer* 70 (6 Suppl):1788-1793.
11. Craig EA, Stevens MV, Vaillancourt RR, Camenisch TD (2008) MAP3Ks as central regulators of cell fate during development. *Dev Dyn* 237:3102–3114.
12. Cui J, Han SY, Wang C, Su W, Harshyne L, Holgado-Madruga M, Wong AJ (2006) c-Jun NH(2)-terminal kinase 2alpha2 promotes the tumorigenicity of human glioblastoma cells. *Cancer Res* 66:10024–10031.

13. Dan I, Watanabe NM, Kusumi A (2001) The Ste20 group kinases as regulators of MAP kinase cascades. *Trends Cell Biol* 11:220–230.
14. Davis RJ (1994) MAPKs: new JNK expands the group. *Trends Biochem. Sci.* 19:470–473.
15. Davis RJ (2000) Signal transduction by the JNK group of MAP kinases. *Cell* 103:239–252.
16. Dong C, Davis RJ, Flavell RA (2002) MAP kinases in the immune response. *Annu. Rev Immunol.* 20:55–72.
17. Druckrey H, Ivankovic S, Preussmann R (1966) Teratogenic and carcinogenic effects in the offspring after single injection of ethylnitrosourea to pregnant rats. *Nature* 210:1378-1379.
18. Druckrey H, Preussmann R, Ivankovic S (1969) N-nitroso compounds in organotropic and transplacental carcinogenesis. *Ann N Y Acad Sci* 163:676-696.
19. Druckrey H, Schagen B, Ivankovic S (1970) The induction of neurogenic malignancies by single dosage of ENU to newborn and young BD IX rats. *Z Krebsforsch* 74:141-161.
20. Goth R, Rajewsky MF (1974) Persistence of O6-ethylguanine in rat brain DNA: correlation with nervous system-specific carcinogenesis by ethylnitrosourea. *Proc Natl Acad Sci U S A* 71:639–643.
21. Gupta S, Barrett T, Whitmarsh AJ, Cavanagh J, Sluss HK, Derijard B, Davis RJ (1996) Selective interaction of JNK protein kinase isoforms with transcription factors. *EMBO J* 15:2760–2770.
22. Hayashi Y, Ueki K, Waha A, Wiestler OD, Louis DN, von Deimling A (1997) Association of EGFR gene amplification and CDKN2 (p16/MTS1) gene deletion in glioblastoma multiforme. *Brain Pathol* 7: 871-875.
23. Holland EC (2001) Gliomagenesis: genetic alterations and mouse models. *Nat. Rev. Genet.* 2:120-129.
24. Jang T, Litofsky NS, Smith TW, Ross AH, Recht LD (2004) Aberrant nestin expression during Ethylnitrosourea-(ENU)-induced neurocarcinogenesis. *Neurobiol Dis* 15:544-552.
25. Jang T, Sathy B, Hsu YH, Merchant M, Recht B, Chang C, Recht L (2008) A distinct phenotypic change in gliomas at the time of magnetic resonance imaging detection. *J Neurosurg* 108:782–790.
26. Karin M, Gallagher E (2005) From JNK to pay dirt: jun kinases, their biochemistry, physiology and clinical importance. *IUBMB Life* 57: 283–295.

27. Kish PE, Blaivas M, Strawderman M, Muraszko KM, Ross DA, Ross BD, McMahon G (2001) Magnetic resonance imaging of ethylnitrosourea- induced rat gliomas: A model for experimental therapeutics of low-grade gliomas. *J Neurooncol* 53:243–257.
28. Kleihues P, Cavenee WK (2000) Pathology and Genetics of Tumors of the Central Nervous System (World Health Organization Classification of Tumors), 2nd edn. IARC: Lyon.
29. Kleihues P, Marigson GP (1974) Carcinogenicity of N-methyl Nnitrosourea: Possible role of exicision repair of O6 – methylguanine from DNA. *J Nat Cancer Inst* 53:1839-41.
30. Kleihues P, Ohgaki H (1999) Primary and secondary glioblastomas: from concept to clinical diagnosis. *Neuro Oncol.* 1:44-51.
31. Koestner A (1990) Characterization of N-nitrosourea-induced tumors of the nervous system; Their prospective value for studies of neurocarcinogenesis and brain tumor therapy. *Toxicol Pathol* 18:186– 192.
32. Koestner A, Swenberg JA, Wechsler W (1971) Transplacental production with ethylnitrosourea of neoplasms of the nervous system in Spraguer-Dawley rats. *Am. J. Pathol.* 63:37-56.
33. Kyriakis JM, Banerjee P, Nikolakaki E, Dai T, Rubie EA, Ahmad MF, Avruch J, Woodgett JR (1994) The stress-activated protein kinase subfamily of c-Jun kinases. *Nature* 369:156-160.
34. Lan KP, Wang CJ, Hsu JD, Chen KM, Lai SC, Lee HH (2004) Induced eosinophilia and proliferation in Angiostrongylus cantonensis- infected mouse brain are associated with the induction of JAK/STAT1, IAP/NF-kappaB and MEKK1/JNK signals. *J. Helminthol.* 78:311–317.
35. Leonard JR, D'Sa C, Klocke BJ, Rotha KA (2001) Neural precursor cell apoptosis and glial tumorigenesis following transplacental ethylnitrosourea exposure. *Oncogene* 20:8281–8286.
36. Li JY, Wang H, May S, Song X, Fueyo J, Fuller GN, Wang H (2008) Constitutive activation of c-Jun N-terminal kinase correlates with histologic grade and EGFR expression in diffuse gliomas. *J Neurooncol* 88:11–17.
37. Magee PN (1969) *In vivo* reactions of nitroso compounds. *Ann NY Acad Sci* 163:717-729.
38. Matsuda K, Sato A, Okada M, Shibuya K, Seino S, Suzuki K, Watanabe E, Narita Y, Shibui S, Kayama T, Kitanaka C (2012) Targeting JNK for therapeutic depletion of stem-like glioblastoma cells. *Sci Rep* 2:516.
39. N'Guessan PD, Schmeck B, Ayim A, Hocke AC, Brell B, Hammerschmidt S, Rosseau S, Suttorp N, Hippenstiel S (2005) Streptococcus pneumoniae R6x induced p38 MAPK and

JNK-mediated caspase-dependent apoptosis in human endothelial cells. *Thromb Haemost* 94:295–303.

40. Nieder C, Schlegel J, Andratschke N, Thamm R, Grosu AL, Molls M (2003) The role of growth factors in central nervous system tumors. *Anticancer Res* 23:1681-1686.
41. Nishio S, Ohta M, Abe M, Kitamura K (1983) Microvascular abnormalities in Ethylnitrosourea (ENU)-induced rat brain tumors: Structural basis for altered blood-brain barrier function. *Acta Neuropathol* 59:1-10.
42. O'Neill JP (2000) DNA damage, DNA repair, cell proliferation, and DNA replication: How do gene mutations result? *Proc Natl Acad Sci U S A* 97:11137–11139
43. Ohgaki H, Kleihues P (2007) Genetic pathways to primary and secondary glioblastoma. *Am J Pathol* 170:1445-1453.
44. Pimienta G, Pascual J (2007) Canonical and alternative MAPK signalling. *Cell Cycle* 6:2628–2632.
45. Potapova O, Gorospe M, Bost F, Dean NM, Gaarde WA, Mercola D, Holbrook NJ (2000) c-Jun N-terminal kinase is essential for growth of human T98G glioblastoma cells. *J Biol Chem* 275:24767-24775.
46. Rahaus M, Desloges N, Wolff MH (2004) Replication of varicellazoster virus is influenced by the levels of JNK/SAPK and p38/MAPK activation. *J Gen Virol* 85:3529–3540.
47. Raman M, Chen W, Cobb MH (2007) Differential regulation and properties of MAPKs. *Oncogene* 26:3100–3112.
48. Reddy KB, Nabha SN, Atanaskova N (2003) Role of MAP kinase in tumor progression and invasion. *Cancer Metastasis Rev* 22:395-403.
49. Rennefahrt UE, Illert B, Kerkhoff E, Troppmair J, Rapp UR (2002) Constitutive JNK activation in NIH 3T3 fibroblasts induces a partially transformed phenotype. *J Biol Chem* 277:29510-29518.
50. Rong Y, Belozerov VE, Tucker-Burden C, Chen G, Durden DL, Oslon JJ, Van Meir EG, Mackman N, Brat DJ (2009) Epidermal growth factor receptor and PTEN modulate tissue factor expression in glioblastoma through JunD/activator protein-1 transcriptional activity, *Cancer Res* 69:2540–2549.
51. Sareddy GR, Challa S, Panigrahi M, Babu PP (2009) Wnt/beta-catenin/Tcf signaling pathway activation in malignant progression of rat gliomas induced by transplacental N-ethyl-N-nitrosourea exposure. *Neurochem Res* 34:1278-88.

52. Schiffer D, Giordana MT, Mauro A, Racagni G, Bruno F, Pezzotta S, Paoletti P (1980) Experimental brain tumors by transplacental ENU. Multifactorial study of the latency period. *Acta Neuropathol* 49:117-122.
53. Schiffer D, Giordana MT, Pezzotta S, Lechner C, Paoletti P (1978) Cerebral tumors induced by transplacental ENU: study of the different tumoral stages, particularly of early proliferations. *Acta Neuropathol*. 41:27-31.
54. Shaul YD, Seger R (2007) The MEK/ERK cascade: from signaling specificity to diverse functions. *Biochim Biophys Acta* 1773:1213–1226.
55. Shibuya T, Morimoto K (1993) A review of the genotoxicity of 1-ethyl-1- nitrosourea. *Mutat Res* 297:3–38.
56. Simmons ML, Lamborn KR, Takahashi M, Chen P, Israel MA, Berger MS, Godfrey T, Nigro J, Prados M, Chang S, 2nd Barker FG, Adalpe K (2001) Analysis of complex relationships between age, p53, epidermal growth factor receptor, and survival in glioblastoma Patients. *Cancer Res* 61:1122-1128.
57. Swenberg JA, Koestner A, Wechsler W, Denlinger RH (1972) Quantitative aspects of transplacental tumor induction with ethylnitrosourea in rats. *Cancer Res* 32:2656-2660.
58. Tabatabai G, Weller M (2011) Glioblastoma stem cells. *Cell Tissue Res* 343:459–465.
59. Tamanini A, Rolfini R, Nicolis E, Melotti P, Cabrini G (2003) MAP kinases and NF-kappaB collaborate to induce ICAM-1 gene expression in the early phase of adenovirus infection. *Virology* 307:228–242.
60. Trosko JE (2001) Commnetary: is the concept of "tumor promotion" a useful paradigm? *Mol Carcinog* 30:131-137.
61. Tsuiki H, Tnani M, Okamoto I (2003) Constitutively Active Forms of c-Jun NH2-terminal Kinase Are Expressed in Primary Glial Tumors. *Cancer Res.* 63:250-255.
62. Wang X, Destrument A, Tournier C (2007) Physiological roles of MKK4 and MKK7: insights from animal models. *Biochim. Biophys. Acta* 1773:1349–1357.
63. Wechsler W, Kleihues P, Matsumoto D (1969) Pathology of experimental neurogenic tumors chemically induced during prenatal and postnatal life. *Ann NY Acad Scie* 159:360-408.
64. Whitmarsh AJ (2006) The JIP family of MAPK scaffold proteins. *Biochem Soc Trans* 34:828–832.
65. Wrensch M, Minn Y, Chew T, Bondy M, Berger MS (2002) Epidemiology of primary brain tumors: current concepts and review of the literature. *Neuro Oncol* 4:278–299.

66. Xie J, Pan H, Yoo S, Gao SJ (2005) Kaposi's sarcoma-associated herpesvirus induction of AP-1 and interleukin 6 during primary infection mediated by multiple mitogen-activated protein kinase pathways. *J Virol* 79:15027–15037.
67. Yoshimura F, Kaidoh T, Inokuchi T, Shigemori M (1998) Changes in VEGF expression and in the vasculature during the growth of earlystage ethylnitrosourea-induced malignant astrocytomas in rats. *Virchows Archive* 433:457–463.
68. Zachos G, Clements B, Conner J (1999) Herpes simplex virus type 1 infection stimulates p38/c-Jun N-terminal mitogen-activated protein kinase pathways and activates transcription factor AP-1. *J. Biol. Chem.* 274:5097– 5103.
69. Zimmerman HM (1969) Brain tumors: their incidence and classification in man and their experimental production. *Ann NY Acad Scie* 159:337-359.
70. Zook BC, Simmens SJ, Jones RV (2000) Evaluation of ENU-induced gliomas in rats: nomenclature, immunohistochemistry, and malignancy. *Toxicol Pathol* 28:193–201.

Chapter - 5

Molecular mechanism involved in antitumor activity of pantoprazole

5.1. Introduction

Glioblastoma (GBM) is the most aggressive and heterogeneous form of malignant glioma. Current treatment modalities for glioma include surgery, radiotherapy and chemotherapy. Despite advanced treatment modalities, survival rate of patients diagnosed with glioma is less than 12 months and only 5% of patients survive up to 5 years (CBTRUS, 2011). The minimal survival period of these patients is due to recurrent nature of GBM (Nupponen and Joensuu, 2006; Ohgaki and Kleihues, 2009). The current chemotherapeutic options for glioma are associated with numerous limitations. Furthermore, most of the chemotherapeutic agents have a limited activity against glioma as a result of partial penetration through the blood brain barrier (Ostermann et al, 2004; Portnow et al, 2009). Factors recently described to play vital role in chemo resistance and hindering the access of drugs to central nervous system (CNS) tumors are: the presence of efflux pumps, low pH and hypoxic environment present around the tumor (Neuwelt et al, 2011; Haar et al, 2012). Hence, there is a need for novel potential drugs which can overcome these impeding factors and penetrate into the tumor core and induce cytotoxicity in the cancer cells without affecting the healthy functioning of non-cancerous cells.

Recent studies have shown that tumor microenvironment promotes maturation of tumor into malignant form. It is proposed that hypoxia and acidity encourage the conversion of benign tumor to its malignant form by promoting the invasion of tumor cells. The acidic environment around the tumor has been shown to play a significant role in chemo resistance, proliferation and metastatic behaviour (Sennoune et al, 2004). Previously, it was hypothesized that tumors are acidic due to their marked rate of lactic acid production (Warburg, 1956). Nevertheless, tumors are able to create the acidic environment also in conditions of reduced production of lactate via glycolysis, signifying that the aerobic metabolism is not the major mechanism responsible for the development of an acidic environment within solid tumors (Newell et al, 1993; Yamagata et al, 1998). Particularly, the causes for the acidic pH in tumors may include (a) deficiencies in tumor perfusion, due to the abnormal vascularization of the tumor mass; (b) hypoxia and metabolic abnormalities associated with transformation and uncontrolled cell growth; and (c) increased capacity for transmembrane pH regulation. These conditions may create a sort of malicious environment that may favour the selection of highly malignant tumor cells which can persist in hypoxic and acidic environment (Fais et al, 2007). Numerous ion exchangers expressed on membranes of cancer cells helps in creating acidic tumor environment. These ion exchangers or protein pumps either pump ions from inside to outside

of the cells or exchange the ions between external and internal space of the cell. This mechanism helps the cancer cells to transport H^+ ions from inside to outside space thereby avoiding the accumulation of these ions within the cell and rescuing cell from fatal activity of lytic enzymes. Vacuolar-type (V-type) H^+-ATPases are the responsible factors for both the establishment and the maintenance of the acidic pH of tumors. These V-H^+-ATPases pump protons across plasma membrane, maintaining a relatively neutral intracellular pH, an acidic luminal pH, and an acidic extracellular pH (Nishi and Forgac, 2002). V-ATPases play a major role in metastatic tumor development because many tumor cells secrete lysosomal enzymes that participate in the extracellular matrix (ECM) degradation necessary for metastatic invasion. These enzymes are most active at low optimal pH and moreover, V-ATPases are responsible for microenvironment acidification (Nishi and Forgac, 2002; Martinez-Zaguilan et al, 1993). Cancer metastasis is an ultimate cause leading to the failure of clinical treatment for patients with malignant tumor (Steeg, 2006). Throughout the entire process of cancer metastasis, degradation and remodelling of ECM almost exist at each step (Gupta and Massague, 2006). Thus, blocking the ECM degradation has become a potential approach in the development of treatment for cancer metastasis. One way to inhibit protease activation in cancer metastasis is to increase the pH of extracellular microenvironment of metastatic cancer cells, in turn entirely suppressing the activation of proteases and blocking the process of degradation and remodelling of ECM (Lu et al, 2005; Rofstad et al, 2006). These evidences suggest that V-ATPases may represent a target of cancer therapy by directly regulating the pH gradient within tumor microenvironment, indirectly avoiding activation of ECM proteases. Molecular silencing and pharmacologic inhibitors of the V-ATPases can delay cancer growth, but such approaches may result in severe toxicity and be unfeasible and problematic. Drugs which inhibit the function of V-H^+ -ATPases are regarded as proton pump inhibitors (PPIs). PPIs, which include omeprazole, esomeprazole, lansoprazole, pantoprazole, and rabeprazole, are substituted 2-pyridyl-methylsulfinyl benzimidazoles. These drugs are in the pro or inactive form, therefore in acidic environment these drugs gets protonated and result in formation of a tetracyclic sulfenamide, which is the active form of the drug (Larsson et al, 1985). These drugs have been used for short and long term treatment of gastritis in very high doses (150 mg/d) without major side effects (Martin de Argila, 2005). Proton pump inhibitors (PPI) have been largely and successfully used for the treatment of peptic diseases, due to their antiacidic properties. After protonation in the acidic spaces of the stomach, PPI irreversibly bind the proton pump, dramatically inhibiting proton translocation and acidification of the extracellular environment. The specific targets of PPIs are H^+-ATPases normally contained within the lumen

of gastric parietal cells. However, PPI also inhibit the activity of V-ATPases, thus blocking proton transport across membranes. The extracellular pH of tumor being low compared to cell cytoplasm impedes the uptake of weakly basic chemotherapeutic drugs thereby reducing their cytotoxic effect on cancer cells. It has been proved in animal models that bicarbonate-induced extracellular alkalinisation was found to increase the chemotherapeutic effect of anti-tumor drugs in significant manner (Raghunand et al, 2003). Besides, many observations in cancer studies have pointed out anti-proliferative activity of PPI's by affecting lysosome mediated autophagy (Andrej et al, 2011) and MAPKinase pathways (Yeo et al, 2008). De Milito et al, have shown that PPI induced cytotoxicity in B-cell tumors through massive reactive oxygen species (ROS) activation and lysosomal membrane perturbation, leading to a caspase-independent cell death (De Milito et al, 2007). The antineoplastic activity of PPI was also observed in pre-B acute lymphoblastic leukemia cells obtained from patients with acute lymphoblastic leukemia, as well as in severe combined immunodeficient mice engrafted with B-cell lymphomas, whose growth was significantly reduced after PPI administration and PPI treatment clocks up the pH gradient by stopping the V-ATPase–mediated H+ efflux, in turn allowing anticancer drugs to enter and exert their action within tumor cells and triggering apoptotic pathways in tumor cells that lead to tumor growth inhibition (De Milito et al, 2007). Moreover, PPI pre-treatment enhanced the cytotoxic effects of anti-tumor drugs on SGC7901 (Chen et al, 2012). Altogether, these results provided the proof of concept that PPIs may be considered not only as chemosensitizer agents, but also as a new class of antineoplastic drugs.

Anomalous activation of NF-κB signaling is found in most of the tumors and regulates all vital properties of cancer like cell proliferation, suppression of apoptosis, angiogenesis and metastasis (Basseres and Baldwin, 2006). In mammals, NF-κB family is composed of five members, RelA (p65), RelB, cRel (Rel), NF-κB1 (p50 and its precursor p105) and NF-κB2 (p52 and its precursor p100) (Ghosh et al, 1998). These proteins exist in homo or hetero dimeric forms. In unstimulated conditions, NF-κB/Rel dimers are bound to inhibitory protein IκB and are retained in the cytoplasm. Wide range of stimuli like TNF-α or IL-1, viruses, genotoxic agents and ionizing radiations activate IKK complex, which phosphorylate at specific serine residues of IκB leading to its ubiquitination and degradation by the proteasome pathway and releasing free NF-κB dimers. These free dimers translocate into nucleus and bind to their specific gene promoters and drive their transcription (Nishikori, 2005). The transcription factor nuclear factor κB (NF-κB) is constitutively expressed in GBM and is associated with enhanced growth, cell cycle progression, and inducible chemo resistance (Wang et al, 1999; Ansari et al,

2001; Nagai et al, 2002). Since, NF-κB signaling is over expressed or activated in glioma tumors compared to healthy brain tissue, inhibition of NF-κB activation appears as a promising strategy to improve the efficacy of conventional anti-glioma therapy.

However, there is no report on the efficacy of PPI's against glioblastoma cell lines, and the underlying mechanism involved in the growth inhibition of glioblastoma cell lines has not been elucidated. So, the present study was undertaken to examine the growth inhibitory effect of proton pump inhibitor pantoprazole on GBM cells and also target NF-κB signaling pathway in C6 glioma cell line.

5.2. Materials and methods

5.2.1. Chemicals and reagents

C6, U87, U373 cell lines were obtained from National Centre for Cell Science (Pune, India) and T98G was provided by Dr. Ellora Sen (National Brain Research Center, India) Pantoprazole sodium hydrate and propidium iodide (PI) were purchased from Sigma-Aldrich Corp. (St. Louis, MO, USA). RPMI-1640 medium, fetal bovine serum (FBS), penicillin, and streptomycin were purchased from Gibco BRL (CA, USA). TNF-α, trypsin– EDTA, and protease inhibitor cocktail were purchased from Sigma Chemicals (St Louis, MO, USA). Primary antibodies BAX, BCL-2, cytochrome *C*, t-Bid, caspase-3, and -8, PARP, p53, Cox-2, iNos, Cyclin D1, p65, IkBα, phospho IkBα, IKKα, GAPDH, Lamin B and β- Actin were obtained from Cell Signaling Technology (Beverly, MA, USA) and the secondary antibodies, horseradish peroxidase (HRP)- linked goat anti-mouse IgG and goat anti-rabbit IgG were purchased from Santa Cruz Biotechnology (Santa Cruz, CA, USA). Ready-To-Glow NF-κB secreted luciferase reporter system assay kit was purchased from Clontech (USA) and pRL-TK vector was purchased from Promega (Madison, WI, USA). The in-situ apoptosis detection kit was obtained from Takara Bio (Japan). The protein assay kit was purchased from Bio-Rad (Hercules, CA, USA).

5.2.2. Cell culture

C6, U87, U373 and T98G cell lines were cultured in RPMI media, supplemented with 10% FBS, 100 IU/ml penicillin, and 100 µg/ml streptomycin in a humidified atmosphere with 5% CO_2 at 37^0C.

5.2.3. Pantoprazole dose

In all experiments, 40 mg of pantoprazole was dissolved in 0.9% saline followed by dilution of 1ml above solution in 9 ml of complete medium. The sub-cultured cells from experiments were treated with varying concentrations of pantoprazole and 0.9% saline in media alone served as control or vehicle.

5.2.4. Assessment of cell viability and morphology

Inhibition of cell proliferation was measured by reduction of 3-(4,5-dimethylthiazol-2-yl)-2,5 diphenyltetrazolium bromide (MTT) to formazan. C6 cells were seeded ($1x10^4$ cells/well) in 96-well plates. After overnight incubation, cells were treated with the following concentrations of pantoprazole (100, 200, 300, 400, 600, 800, 900 µM) or vehicle (0.9% saline) alone for 12 h and 24 h. Then MTT reagent was added to each well and incubated for 4 h at 37^0C. Reduced formazan crystals were then dissolved in acidic iso-propanol and absorbance was measured at 540 nm on a microtiter ELISA plate reader. All treatment was performed in triplicate and results were expressed as mean ± SD.

Clonogenic assay was performed by plating C6 cells (100) in a 6 well plate and treated with different concentrations of pantoprazole or vehicle (0.9% saline) for 12 h. Then cells were allowed to grow for seven days and stained with 0.5% methylene blue in 50% methanol. Colonies that contained more than 50 cells were counted (Du et al, 2004). All treatment was performed in triplicate and results were expressed as mean ± SD.

Approximately $2x10^5$ cells/well of C6 cells were cultured onto 12-well plates in RPMI culture medium and each well was then treated individually with 0.9% saline, 100, 200, 400 and 600 µM of pantoprazole for 24 h. For cell morphological changes examination, cells onto the plate were directly examined and were photographed under a phase-contrast microscope (Yu et al, 2011).

5.2.5. DAPI and TUNEL staining for Apoptosis

Approximately $2x10^5$ cells/well of C6 cells were placed in 12-well plates with RPMI medium as described above for 24 h. Cells were treated individually with 0.9% saline and 400 µM of pantoprazole for 24 h. Cells were stained with 4',6'-diamino-2-phenylendole dihydrochloride (DAPI, Invitrogen Life Technologies) as described previously (Ji et al, 2012). The cells were examined under a fluorescence microscope.

An in-situ apoptosis detection kit was used to detect DNA fragmentation in accordance with the manufacturer's (TAKARA) procedure. Briefly, C6 cells grown on chamber slides were

treated with 400 µM pantoprazole for 24 h. The cells were then fixed with 4% paraformaldehyde for 10 min, and then incubated for 60 min with a reaction mixture containing biotin–dUTP and terminal deoxynucleotidyl transferase. Fluorescein-conjugated avidin was applied to the samples, which were then incubated for 30 min. Positively stained fluorescein labelled cells were photographed using fluorescence microscope.

5.2.6. Flow cytometry analysis

C6 cells were seeded in 6 well plates ($1x10^5$ cells/well) and after overnight incubation cells were treated with pantoprazole (200 µM, 400 µM, 600 µM and 800 µM) or vehicle (0.9% saline) for 24 h. Cells from each plate were then harvested with trypsin, fixed in 70% ethanol, stained with propidium iodide (PI) mixture (50 µg/ml PI, 1% triton x 100, 50 µg/ml Rnase A) and incubated for 20 min in the dark at room temperature. Then, PI stained cells were subjected to flow cytometry using a FACS Calibur (BD Biosciences). Cell cycle parameters were analyzed using Modfit software.

5.2.7. Measurement of Intracellular ROS Generation

Intracellular ROS generation was measured using the DCFHDA (Sigma-Aldrich Corp., St. Louis, MO, USA) assay as previously described (Qiao et al, 2004). C6 glioma cells were plated in 6-well culture plates ($1x10^5$ cells/well), and starved for 16 h. Cells were, then, washed with HEPES-buffered saline (HBS: 135 mM NaCl, 5 mM KCl, 0.62 mM $MgSO_4$, 1.8 mM CaCl2, 10 mM HEPES, 6.0 mM glucose, pH 7.4), and treated with different concentrations of pantoprazole (200 µM, 400 µM, 600 µM and 800 µM) or vehicle (0.9% saline) for 24 h. After removal of pantoprazole, the cells were washed and incubated in HBS with 100 µM DCFHDA for additional 30 min. The fluorescence was monitored with excitation (485 nm) and emission (530 nm) wavelengths using a FACS Calibur (BD Biosciences).

5.2.8. Antioxidant enzyme assay

C6 cells were treated with different concentrations of pantoprazole for 24 h. Later cells were pelleted down, suspended in PBS and lysed by sonication. Cell lysate was used for different anti-oxidant enzymatic assays including Catalase assay (Aebi, 1984), GPX assay (Pagila and
Valentine, 1967), GST assay and Lipid peroxidation assay (Bernheim et al., 1948).

i. Estimation of Catalase activity

The activity of catalase present in the samples was determined by the decomposition of H_2O_2, which can be monitored at 240 nm.

Reagents

50 mM mixed phosphate buffer, pH 7.0: Prepared by mixing 50 mM potassium dihydrogen phosphate, and 50 mM disodium hydrogen phosphate, in the ratio of 1: 1.5.

0.5 M KH_2PO_4 – 5 ml make up to 50 ml (50 mM)

0.5 M Na_2HPO_4 – 5 ml make up to 50 ml (50 mM)

27.5 ml of 50 mM KH_2PO_4 and 22.5 ml of 50 mM Na_2HPO_4 were mixed to get mixed phosphate buffer, pH 7.0.

30 mM H_2O_2 in mixed phosphate buffer.

Assay procedure

The assay mixture contained 10 µl of sample and 1 ml of 30 mM H_2O_2.

The change in the O.D was monitored for three minutes at 30 second intervals. The activity of catalase in the diluted sample is calculated using the first order reaction:

$$K_{30} = (2.303/ 30) * \log (A_1 / A_2)$$

The activity in the sample is expressed as K_{30} / mg protein.

ii. Estimation of GPX (glutathione peroxidase) activity

The extent of oxidation of $NADPH+H^+$ is taken as the measure of the activity of GPX.

Reagents

50 mM phosphate buffer, pH 7.0 containing 2.5 mM EDTA and 2.5 mM Sodium azide.

10 mM reduced glutathione in distilled water.

2.5mM NADPH in 0.1 % $NaHCO_3$ solution.

1U/assay Glutathione Reductase (GR) in Phosphate buffer.

5 mM H_2O_2 in Phosphate buffer.

Preparation of reagents

Phosphate buffer, pH 7.0:

1 M K_2HPO_4 (Mol.wt-174.18) – 4.35 gms in 25 ml of distilled water

1 M KH_2PO_4 (Mol.wt-136.08) – 3.4 gms in 25 ml of distilled water

50 ml of phosphate buffer: 3.075 ml of 1M K_2HPO_4 + 1.925 ml of 1M KH_2PO_4 were mixed and 250 µl of 0.5M EDTA was added the final volume was made up to 50 ml.

10 mM Reduced Glutathione (Brown bottle) - keep on ice

1 reaction requires 100 µl of GSH Solution [3 mg in 1ml of water].

2.5 mM NADPH in 0.1% $NaHCO_3$ solution (Brown bottle) - keep on ice

NADPH mol wt.—833

1 reaction requires 100 µl of NADPH [2 mg in 1 ml of 0.1% $NaHCO_3$ solution].

1U/assay Glutathione Reductase in Phosphate buffer (Brown bottle) - keep on ice

For one reaction, 1U of GR in 20 µl of phosphate buffer.

5 mM H_2O_2 in Phosphate buffer: 5 µl of 30% H_2O_2 in 10 ml of Phosphate buffer.

Procedure:

OD – 340 nm.

Blank- phosphate buffer alone

The reaction mixture contained 660 µl of phosphate buffer, 1U of GR i.e. 20 µl, 100 µl of GSH solution, 100 µl of NADPH solution and the mixture was incubated for 5 min to allow H_2O_2 free oxidation of NADPH and to obtain a base line at 340 nm. The reaction was started by adding 10 µl of the sample and 100 µl of H_2O_2 and change in the absorbance at 340 nm was monitored for 5 min at one min intervals.

iii. Estimation of Glutathione-S-transferase activity

GST catalyses the formation of a conjugate between GSH and a variety of substrates. In this method, 1-chloro-2, 4-dinitrobenzene was used as the substrate. The formation of GSH-CDNB substrate catalysed by GST is monitored at 340nm and the amount of the conjugate formed is a measure of the enzyme activity.

Reagents

0.1 M phosphate buffer, pH 6.5.

1 M K_2HPO_4-4.35 gm/25 ml-------1.79 ml

1 M KH_2PO_4-3.4 gm/25 ml---------3.21 ml

→ Make up to 50 ml with DDW to make 0.1 M K PO4 Buffer

10 mM CDNB in 30% ethanol.

20.2 mg in 1ml of absolute ethanol (100 mM) - 300 µl diluted to 3 ml with 30% ethanol to make 10 mM CDNB.

10 mM reduced glutathione in distilled water- 9.22 mg in 3 ml of DDW.

Assay procedure

The reaction mixture contained 924 µl of phosphate buffer, 33.3 µl of CDNB solution and 10 µl of the sample. The reaction was initiated by adding 33.3 µl of GSH solution to the reaction mixture and the change in the OD was monitored at 340 nm for 5 min. The activity of the enzyme in the sample is calculated using the following formula:

$$\text{GST activity} = \frac{\text{Abs difference } (\Delta \text{ D/ min}) \times 1 \times 100(\text{dilution factor})}{7.6 \times 5 \times \text{protein in mg}}$$

Activity of GST was expressed as µmoles CDNB-GSH conjugate formed / min / mg protein.

iv. Estimation of Lipid Peroxidation products

MDA formed in the samples is taken as the index for the extent of lipid Peroxidation. MDA is a highly reactive 3C dialdehyde produced from lipid hydroperoxides. It is measured by the TBA test.

Reagents

0.33% TBA- 200 mg of TBA is dissolved in 30 ml of distilled water and 30 ml of glacial acetic acid. The solution is mixed well to completely dissolve the TBA. The solution is prepared freshly in an amber colored bottle to protect from light.

-- 250 µl per reaction

10% Trichloro acetic acid in distilled water (10 gm in 100 ml)

Procedure

Preparation of TCA precipitates:

To 0.5 ml of sample 0.5 ml of normal saline and 1 ml of 10% TCA were added, and the solution mixed well and centrifuged at 5000 rpm for 10 minutes. The supernatant was used for the estimation of lipid peroxides.

Assay

1 ml supernatant + 0.25 ml of TBA

↓

Mixed well in a tight capped tube and boiled for at 95^{o}C.

↓

The tubes were then cooled immediately under running water.

↓

Color developed was measured at 532 nm in a UV-visible spectrophotometer.

Standard: 1, 1, 3, 3-tetraethoxy propane (TEP) was used as standard.

Results were expressed as nanomoles of MDA/ mg protein.

5.2.9. Measurement of mitochondrial membrane potential

The cationic fluorochrome rhodamine 123 (R123) (Sigma-Aldrich Corp., St. Louis, MO, USA), which binds specifically to mitochondria of living cells (Darzynkiewicz et al, 1982) was used to measure mitochondrial membrane potential ($\Delta\Psi m$) after pantoprazole

treatment. Briefly, C6 glioma cells were cultured in 6-well plates ($1x10^5$ cells/well), and treated with different concentrations of pantoprazole (200 µM, 400 µM, 600 µM and 800 µM) or vehicle (0.9% saline) for 24 h. After treatment, the cells were washed and incubated with 10µg/ml rhodamine 123 for additional 30 min. The fluorescence was monitored by flow cytometry using a FACS Calibur (BD Biosciences).

5.2.10. Western blotting

Cytosolic and nuclear fractions were performed as reported elsewhere (Sareddy et al, 2012). Briefly, C6 cells were pre-treated with different concentrations of pantoprazole and stimulated with TNF-α (10 ng/ml) for 30 min. Cells were then harvested and washed in ice-cold PBS, lysed in 400 µl cold buffer A (HEPES 10 mmol/l (pH 7.9), KCl 10 mmol/ l, EDTA 1 mmol/l, phenylmethanesulfonyl fluoride (PMSF) 1 mmol/l, EGTA 1 mmol/l, dithiothreitol (DTT) 1 mmol/l, aprotinin 1 mg/l, leupeptin 1 mg/l, and pepstatin A 1 mg/l). After 15 min incubation on ice, 0.1% NP-40 was added to the lysates and the tubes were vigorously rocked for 1 min and centrifuged (20,800xg for 5 min) at 4^0C. The supernatant was collected as cytosolic fraction. Nuclear pellets were then washed with cold buffer A, then resuspended in 50 µl cold buffer B (HEPES 20 mmol/l (pH 7.9), NaCl 420 mmol/l, edetic acid 0.1 mmol/l, egtazic acid 0.1 mmol/l, PMSF 1 mmol/l, DTT 1 mmol/l, aprotinin 1 mg/l, leupeptin 1 mg/l and pepstatin A 1 mg/l) and vigorously rocked for 30 min at 4^0C followed by centrifugation at 20,800g for 5 min and the supernatant was collected as the nuclear fraction.

50 µg proteins were electrophoretically separated through 10% and 12% polyacrylamide gels containing 0.1% SDS in running buffer (25 mM Tris base, 190 mM L-glycine, 1% SDS). Proteins were electrotransferred to polyvinylidene difluoride membranes in transfer buffer (20 mM Tris base, 150 mM L-glycine, 10% methanol, 0.01% SDS) for 2 h at 200 mA. Membranes were blocked for 1 h at room temperature in PBST containing 1% bovine serum albumin and were incubated overnight at 4^0C with primary antibodies in the same buffer. Membranes were then washed with PBST three times for 5 min, incubated for 30–60 min at room temperature with respective horseradish peroxidase-conjugated secondary antibody and then washed again with PBST twice for 30 min. Signal detection was accomplished by using chemiluminescence (ECL) kit (Amersham, les Ulis, France).

5.2.11. Immunofluorescence staining

Cells were grown on glass coverslips (approximately $2x10^5$ cells per coverslip) and were treated with 400 µM, 600 µM pantoprazole or vehicle (0.9% saline) for 24 h, the cells

were then stimulated with TNF-α (10 ng/ml) for 30 min and washed with Hank's balanced salt solution followed by fixation in 4% paraformaldehyde for 15 min at room temperature. Fixed cells were washed with PBS and permeabilised with cold (-20^{0}C) acetone for 1 min. After washing with PBS, cells were incubated with p65 primary antibody for 1h at room temperature. After three washes with PBS, cells were incubated with anti-FITC-conjugated rabbit secondary antibody for 1 h at room temperature. Cells were washed thrice in PBS and cover slips were mounted with Vecta Shield mounting medium and fluorescence was captured under a Leica confocal microscope.

5.2.12. Transient transfection and luciferase assays

To examine the effect of pantoprazole on TNF-α-induced NF-κB reporter activity, C6 cells were seeded in 24 well plates and transiently transfected with 1µg of pNF-κB-MetLuc2-reporter, 1µg of pMetLuc2-Control, and 0.5 µg pRL-TK (for normalization of transfection efficiency) vectors by use of lipofectamine2000. After 6h, cells were treated with pantoprazole (200 µM, 400 µM, 600 µM, 800 µM and 1000 µM) or vehicle (0.9% saline) for 24h followed by TNF-α (10 ng/ml) treatment. The cell-culture medium was harvested after 24h and subjected to metridia luciferase activity in accordance with the manufacturer's procedure (Clontech, USA). For renilla luciferase activity cells were lysed in passive lysis buffer and the luciferase activity was measured with a luminometer (Promega, Madison, WI, USA). NF-κB metridia luciferase activity was normalized to renilla luciferase values. Each transfection was conducted in triplicate and each experiment was repeated 3 times.

5.2.13. Statistical analysis

All experiments were repeated at least thrice and the representative data are shown in here. All data are presented as mean ± standard deviation (SD). The difference between two groups was evaluated using Student's t test. Significant difference among three or more groups was determined by one-way ANOVA with a post hoc analysis (Turkey test). $P < 0.05$ was considered statistically significant.

5.3. Results

5.3.1. Pantoprazole inhibits GBM cell proliferation in dose and time dependent manner

Effect of pantoprazole on C6, U87, U373 and T98G cell viability was examined quantitatively using MTT assay. Pantoprazole significantly reduced the proliferation of GBM cells in dose and time dependent manner (Fig. 5.1a). Approximately 50% of cells died at a

concentration of 400 µM pantoprazole after 24 h. C6 cells treated with different concentrations of pantoprazole were examined under bright field microscope. As shown in fig. 5.1b saline treated or control C6 cells were intact and normal with smooth surface membranes. In contrast C6 cells treated with pantoprazole exhibited shrunken morphological feature. To further characterize the effect of pantoprazole on cell proliferation, clonogenic assay was performed. Vehicle treated cells attained 100% cloning efficiency, whereas pantoprazole inhibited the colony forming ability of C6 cells effectively at 400 µM (~ 45%), 600 µM (~ 15%) and 800 µM (~ 5%) (Fig. 5.2). Altogether, these experiments demonstrate that pantoprazole inhibited C6 glioma cell proliferation.

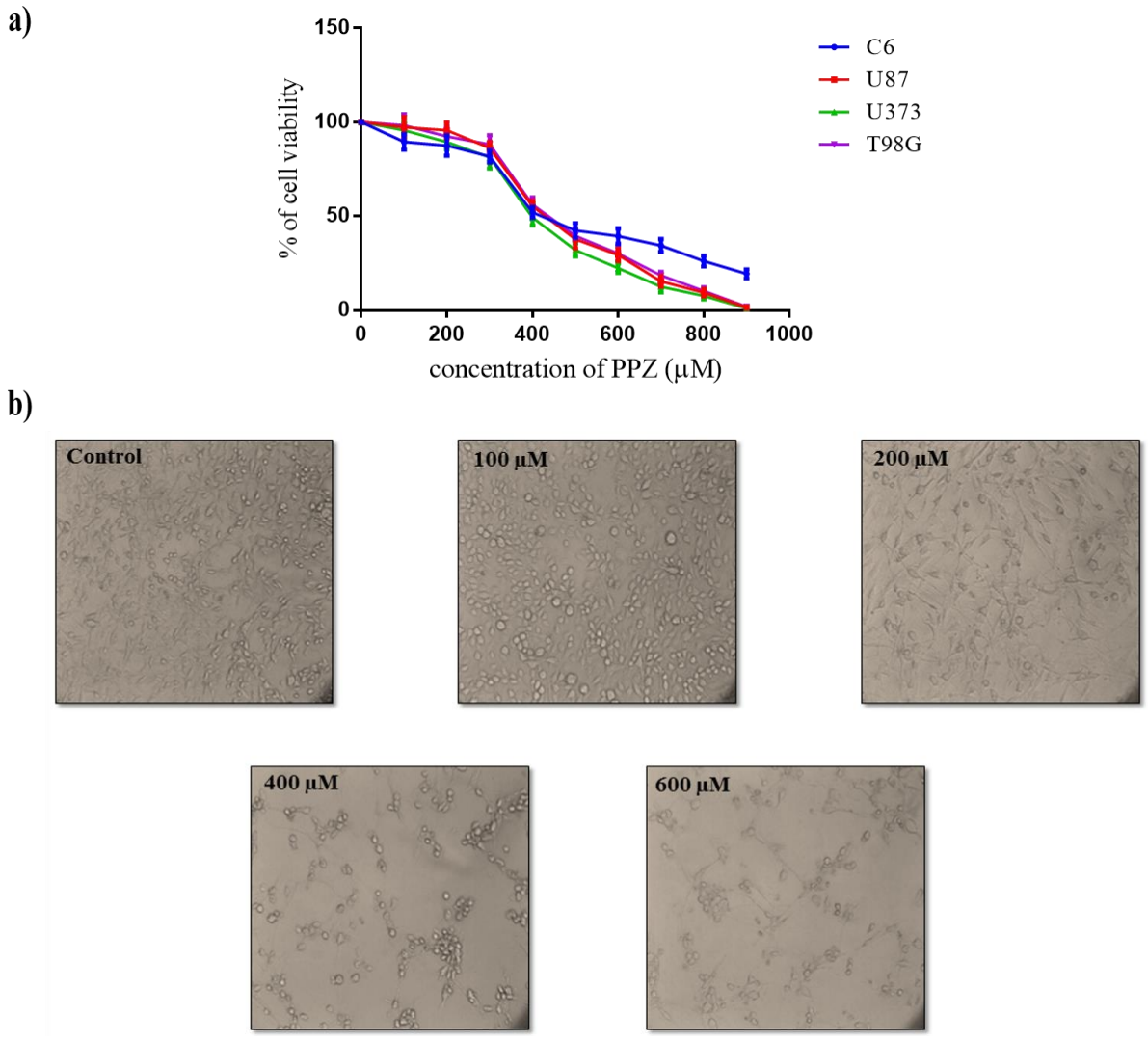

Fig. 5.1. Effect of pantoprazole (PPZ) on growth of C6 cells. (a) C6, U87, U373 and T98G cells were treated with vehicle (0.9% saline) or the specified concentrations of pantoprazole for 12 h & 24 h and subjected to MTT assay. This data is representative of three independent

experiments. **(b)** C6 cells were treated with vehicle (0.9% saline) or the indicated concentrations of pantoprazole for 24 h. The bright field images were taken at 40X. This data is representative of three independent experiments.

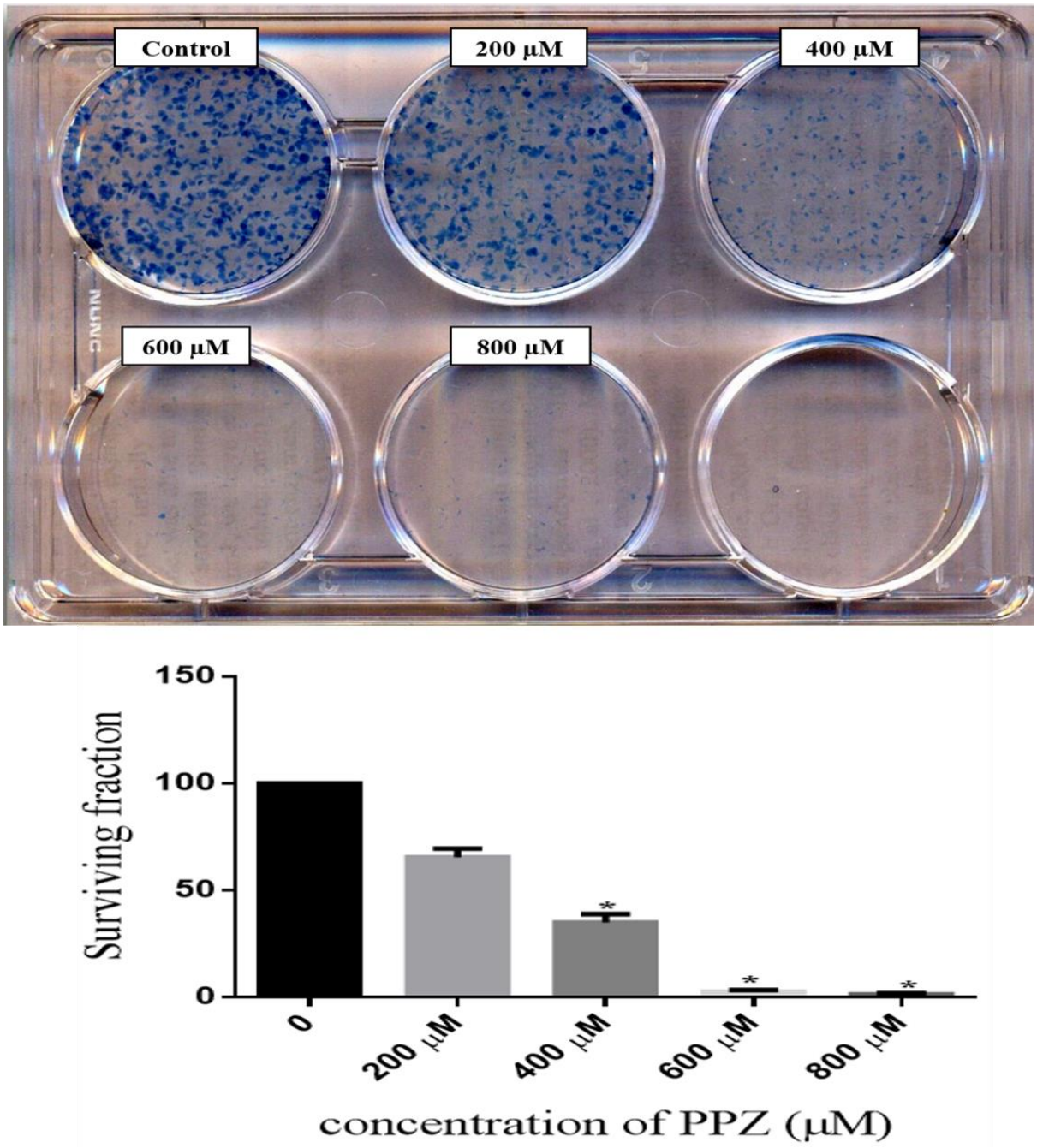

Fig. 5.2. Effect of pantoprazole on cloning efficiency. C6 cells (100) were plated in each well of 6 well plate and after 12 h cells were treated with vehicle (0.9% saline) or indicated concentrations of pantoprazole for 12 h. After four days colonies were stained with methylene blue and colonies that contained >50 cells were counted. The results are expressed as

percentage of control. Each bar represented is the mean ± SD of three independent experiments. *Statistically significant at $p < 0.05$ in comparison to control.

5.3.2. Pantoprazole alters cell cycle and induces apoptosis in C6 glioma cells

Uncontrolled cell cycle is one of the prominent characteristics of GBM cells. To ascertain the effect of pantoprazole on cell cycle distribution, C6 cells were treated with pantoprazole for 24 h followed by staining with PI and subjected to FACS analysis. PI stained cells show DNA profile representing cells in G1 phase, S phase and G2M phase with apoptotic cells being represented by sub GO/G1 phase. Pantoprazole increased the sub G0/G1 cell population at the expense of other cell cycle phases, suggesting that pantoprazole arrested cell cycle at sub G0/G1 phase (Fig. 5.3).To determine whether pantoprazole induces apoptotic cell death, extent of nuclear and DNA fragmentation was determined by DAPI and TdT-mediated dUTP biotin nick end labelling (TUNEL) staining respectively. DNA and nuclear fragmentation represent the characteristic hallmark of apoptosis. Vehicle (0.9% saline) treated cells had round and smooth nuclei, while pantoprazole treated cells showed uneven and severed nuclei (Fig. 5.4a). To further confirm the PPZ induced DNA fragmentation TUNEL assay was performed. C6 cells treated with 400 µM (~ 65%) PPZ were TUNEL positive marked with higher FITC fluorescent intensity with a green coloured nuclei under fluorescence microscope compared with vehicle (0.9 % saline) treated cells (< 5%) (Fig. 5.4b).

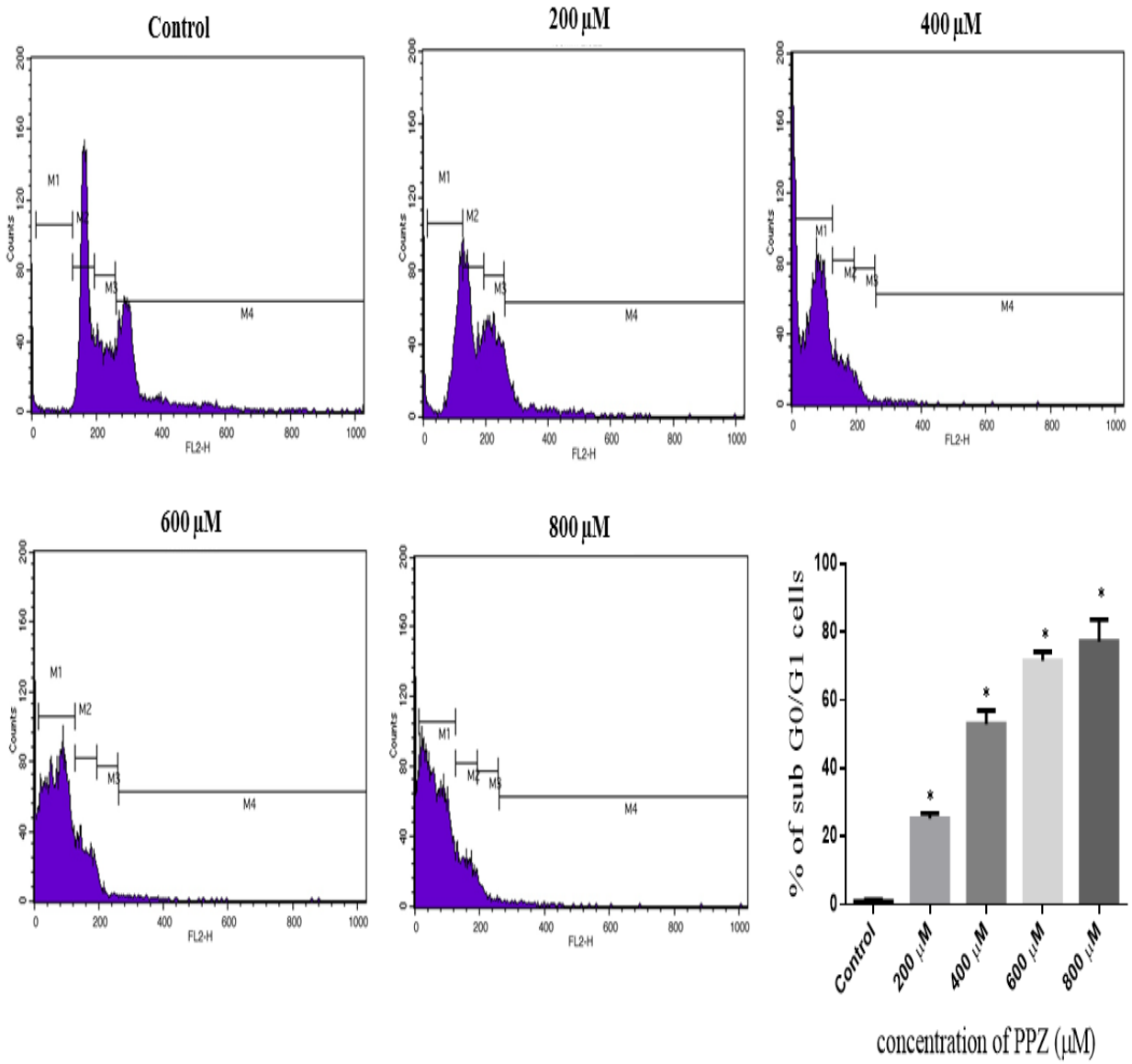

Fig. 5.3. Effect of pantoprazole (PPZ) on cell cycle distribution. C6 cells were treated with indicated concentrations of pantoprazole for 24 h, fixed in 70% cold ethanol followed by PI staining to analyze DNA content by flow cytometry. Treatment with Pantoprazole induced accumulation of C6 cells in sub G0/G1 phase indicative of apoptosis.

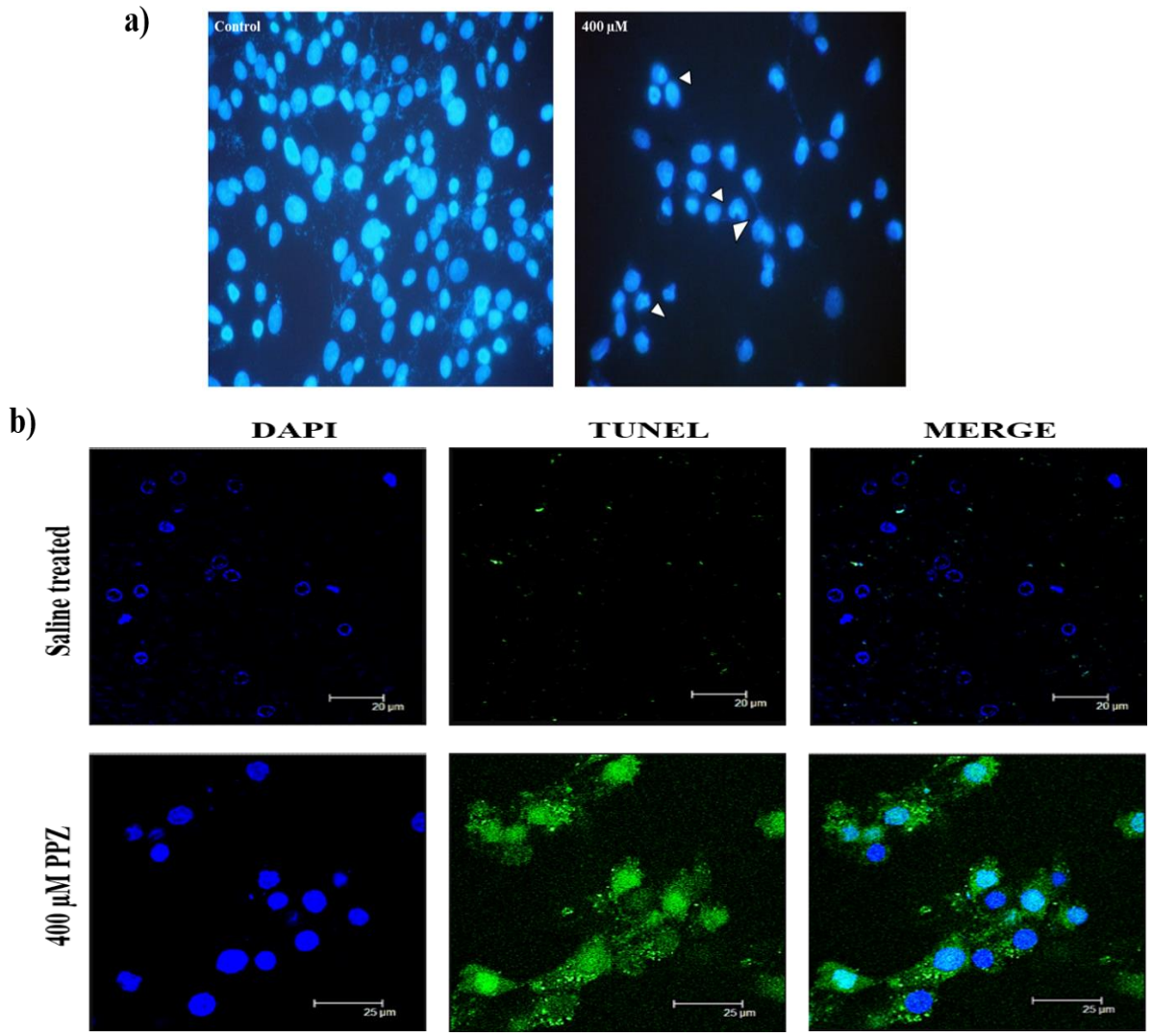

Fig. 5.4. Pantoprazole induces nuclear fragmentation and TUNEL positivity. **(a)** C6 cells were treated with vehicle (0.9% saline) and 400 µM pantoprazole for 24 h, thereafter apoptotic nuclear morphology was assessed using DAPI. Morphological features were visualised using fluorescence microscopy. Original magnification 40X. **(b)** C6 cells were seeded in chamber slides and treated with vehicle (0.9% saline) or the indicated concentrations of pantoprazole for 24 h. TUNEL positive cells were visualised using fluorescence microscope.

5.3.3. Pantoprazole treatment leads to loss of mitochondrial membrane potential (Δψ*m*) with increased caspase-3, caspase-8 and PARP cleavage

To better understand whether mitochondrial mediated apoptosis is involved, we studied the effect of pantoprazole on Δψ*m* in C6 glioma cells using rhodamine- 123. The retention of fluorescent probe rhodamine- 123 is proportional to mitochondrial membrane potential. In our

study, it was observed that 24 h treatment of C6 cells with different pantoprazole concentrations caused significant decrease in membrane potential compared with incubation in control medium having 0.9% saline (Fig. 5.5). Quantitative analysis of the fluorescence intensity in C6 glioma cells showed pantoprazole induced dose dependent increase in loss of mitochondrial membrane potential ($\Delta\psi m$) (n = 3, P <0.05). To further confirm whether the cell death was apoptotic, whole cell lysate was subjected to western blotting to identify anti-apoptotic proteins like Bcl-2, Bcl-XL and pro-apoptotic proteins BAX, t-Bid, cytochrome-C, caspase-8, cleaved caspase-3, PARP and p53. As shown in fig. 5.6, pantoprazole treatment significantly decreased the anti-apoptotic protein level with simultaneous increase in the pro-apoptotic protein levels in dose dependent manner. These results suggest that pantoprazole induced caspase dependent apoptotic cell death in C6 glioma cells.

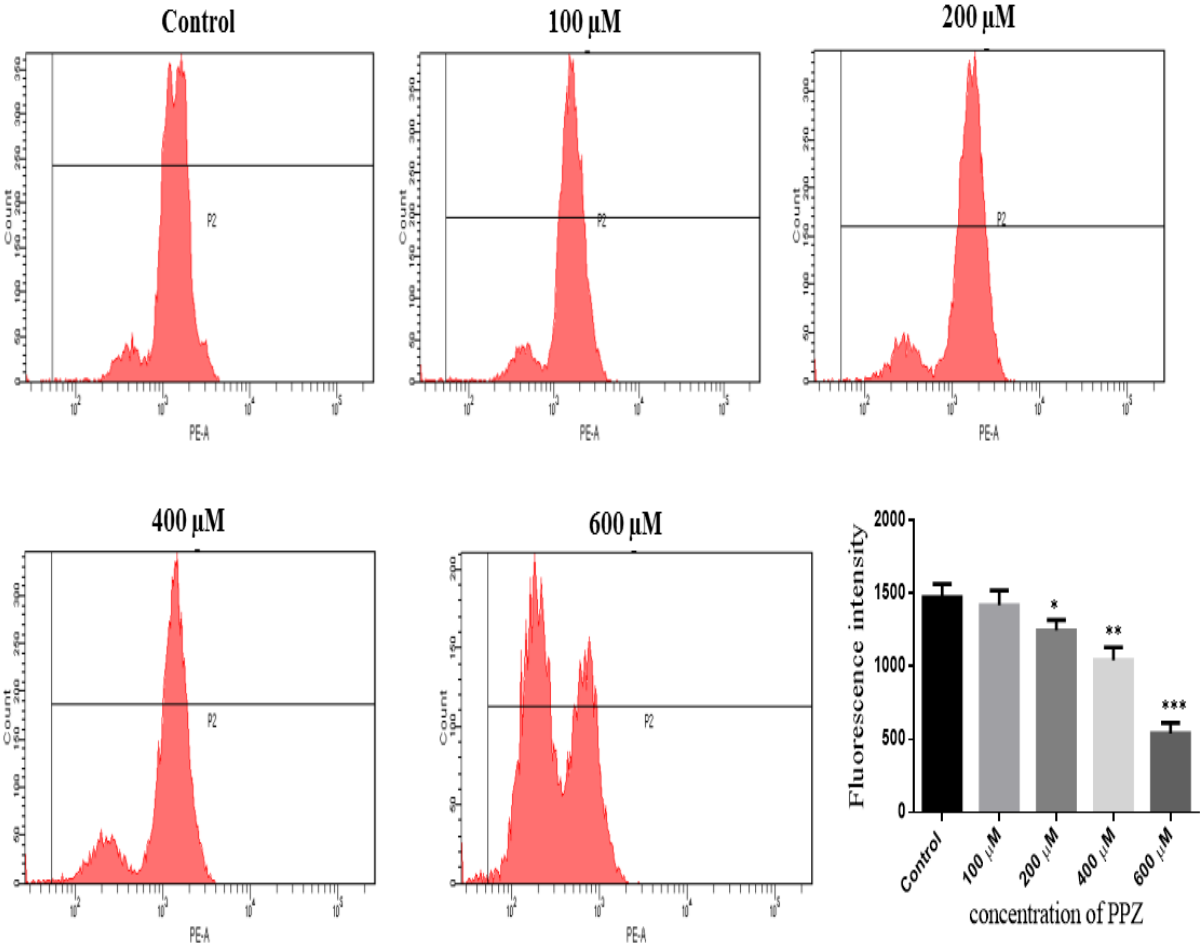

Fig. 5.5. Loss of mitochondrial membrane potential *(Δψm)* in pantoprazole (PPZ) treated C6 cells. Briefly, C6 cells were treated with specified concentration of pantoprazole for 24 h at 37^0C and stained with rhodamine123 to mark intact mitochondria. 10,000 cells were analysed by flow cytometry. Data are the average of three independent experiments and expressed as mean ± SD. *, significant difference (p <0.05) compared to control.

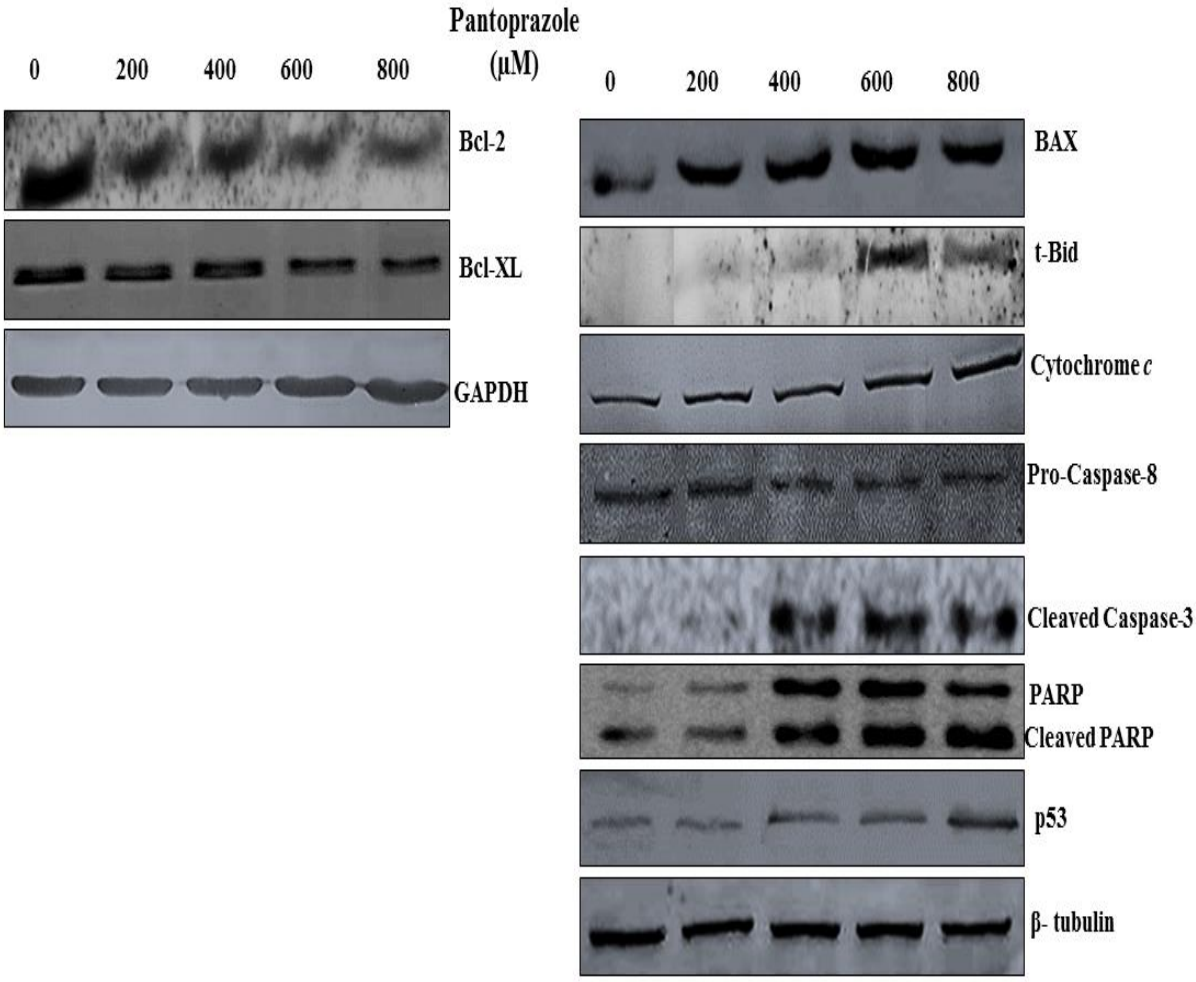

Fig. 5.6. Alteration of apoptotic components in pantoprazole (PPZ) treated C6 cells. Immunoblots of apoptosis related proteins in pantoprazole treated C6 cells. C6 cells were treated with increasing concentrations of pantoprazole for 24 h at 37^0C. Whole cell lysates were prepared, separated by SDS PAGE and transferred onto nitro cellulose membrane followed by immunoblotting with Bcl-2, Bcl-XL, BAX, t-Bid, cytochrome-*c*, pro-caspase-8, cleaved caspase-3, PARP and p53. GAPDH and β-tubulin served as loading control.

5.3.4. Higher concentrations of pantoprazole treatment lead to increased production of reactive oxygen species (ROS)

DCFHDA is a nonpolar compound that readily diffuses into cells, where it is hydrolysed to the nonfluorescent polar derivative DCFH and thereby is trapped within the cells (Bass et al, 1983). In the presence of a proper oxidant, DCFH is oxidized to the highly fluorescent 2', 7'-dichlorofluorescein (DCF). We detected significant increase in the ROS production upon pantoprazole treatment in C6 glioma cells within 24 h incubation compared

with control cells treated with 0.9% saline (Fig. 5.7). Quantitative analysis of the fluorescence intensity in C6 glioma cells showed that pantoprazole induced significant increase in ROS at 600 µM and 800 µM compared to control (n = 3, P <0.05).

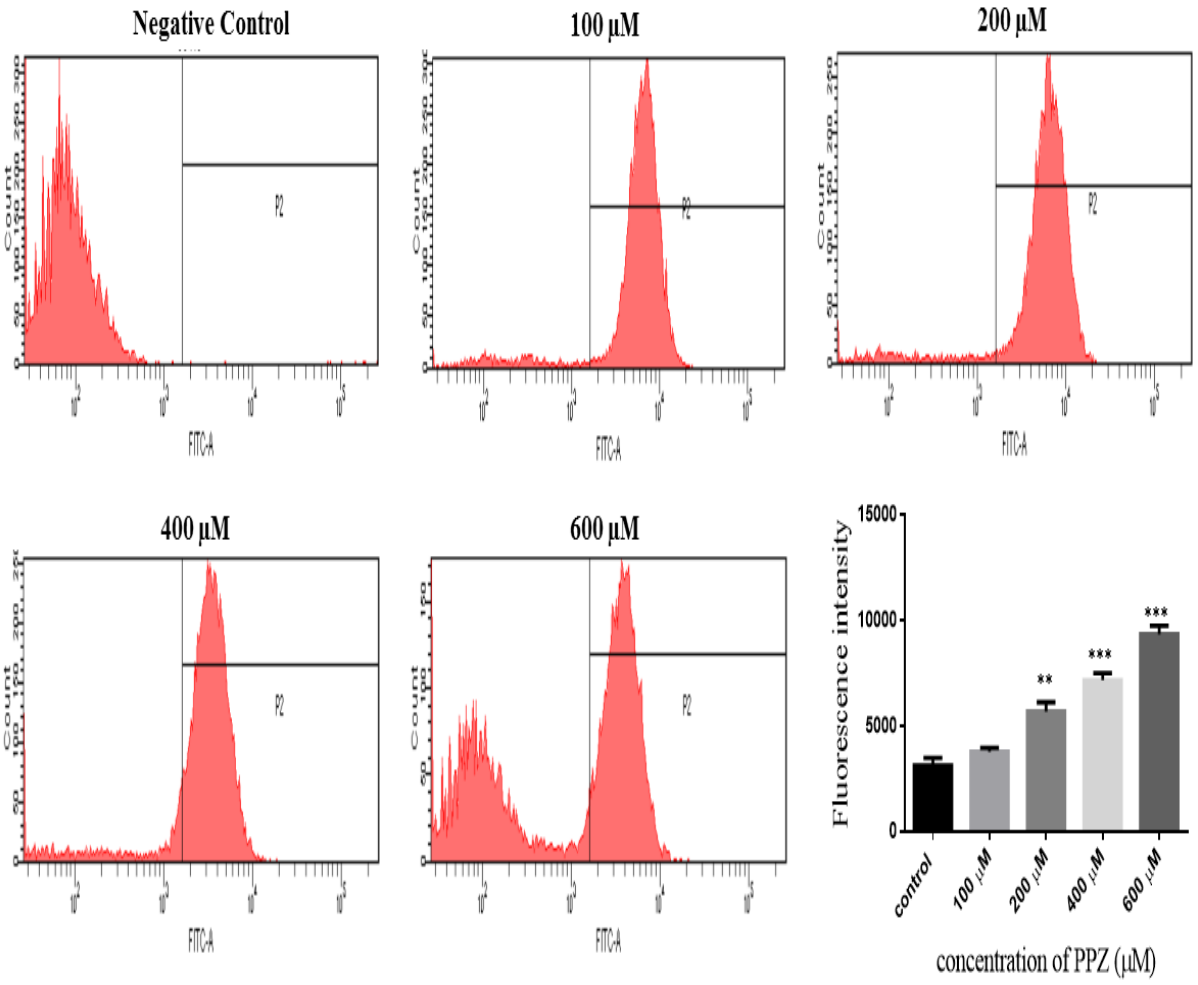

Fig. 5.7. Effect of pantoprazole (PPZ) on reactive oxygen species (ROS). C6 cells were treated with increasing concentrations of pantoprazole for 24 h at 37^0C. Later cells were stained with H2DCFDA for 30 min in growth conditions and cells were analysed by flow cytometry. Values are given as the means ± SD of three independent experiments. The significance was determined by Student's t test. *P < 0.05 compared with control.

5.3.5. Pantoprazole modulates anti-oxidant enzyme activity

Pantoprazole was able to act as ROS scavenger by modulating the expression level of antioxidant enzyme levels. Pantoprazole treatment lead to the increased activity of antioxidant defence mechanism of Catalase, GPX and GST. Simultaneously, amount of lipid peroxidation decreased with increase in concentration of pantoprazole treatment (Fig. 5.8).

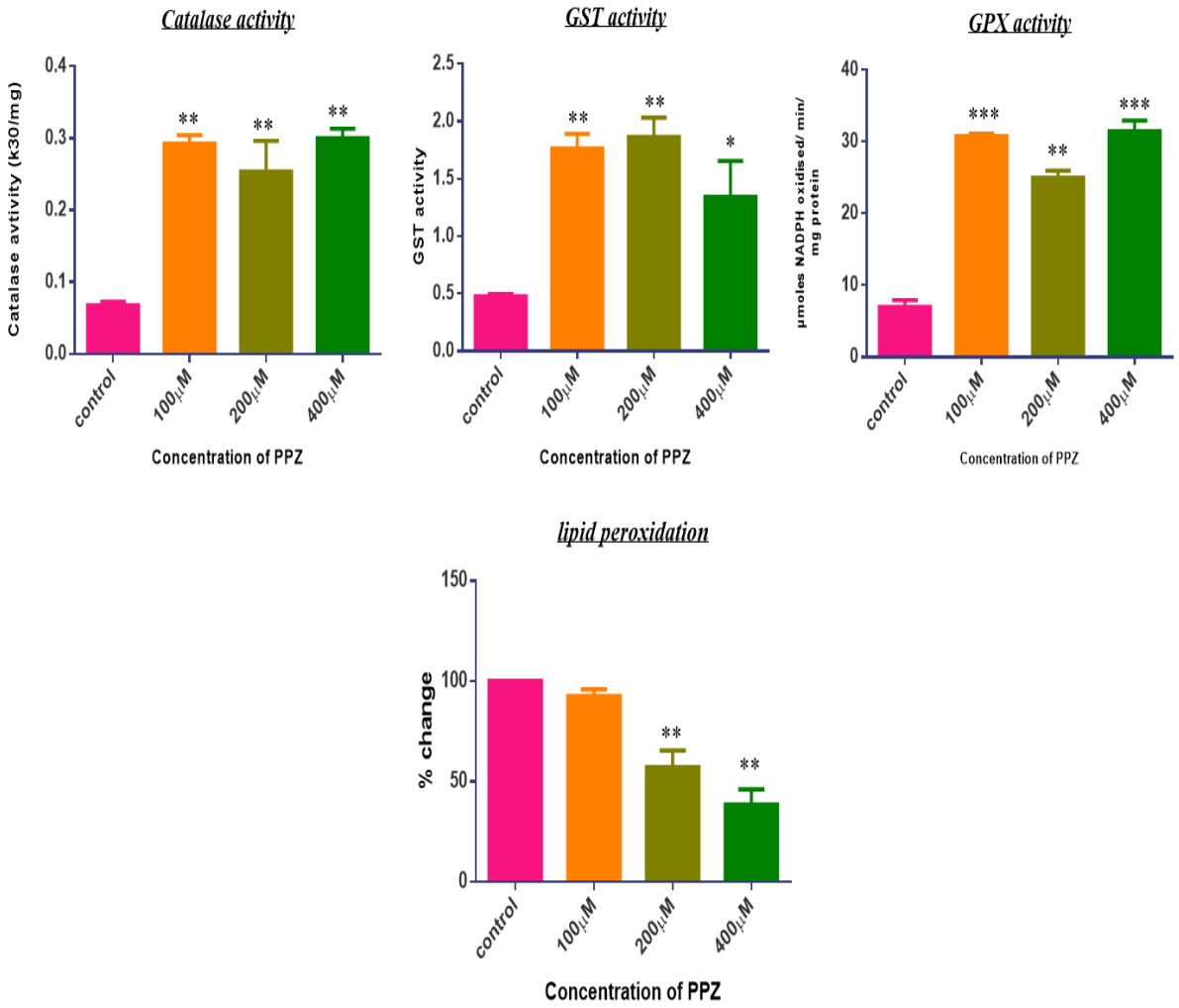

Fig. 5.8. Effect of pantoprazole on anti-oxidant enzyme activity. C6 cells were treated with vehicle (0.9% saline) or indicated concentrations of pantoprazole for 24 h and cells were processed to check activity of anti-oxidants like catalase, GST, GPX and amount of lipid peroxidation. All data presented are the mean ± SD and are representative of three independent experiments. The significance was determined by a Student's t test. *P < 0.05 compared with control.

5.3.6. Pantoprazole inhibits TNF-α induced NF-κB translocation by suppressing phosphorylation and degradation of IκBα

To characterize the effect of pantoprazole on the TNF-α induced nuclear translocation of NF-κB, C6 cells were treated with pantoprazole followed by analysis of cytosolic and nuclear levels of p65. The cytosolic p65 levels (Fig. 5.9) were significantly increased with decreased nuclear translocation (Fig. 5.9) following pantoprazole treatment and TNFα

stimulation compared to vehicle treated cells in a dose dependent manner. The translocation of NF-κB is tightly regulated by the phosphorylation, ubiquitination, and proteolytic degradation of IκBα. To determine the effect of pantoprazole on phosphorylation and degradation of IκBα, we checked total cytoplasmic IκBα and phosphorylated IκBα levels. In TNF-α stimulated cells pantoprazole treatment significantly reduced IKKα levels, increased the total IκBα levels. In contrast phosphorylated IκBα levels decreased in dose dependent manner (Fig. 5.9). To confirm inhibition of nuclear translocation of p65, C6 cells were treated with 400 µM pantoprazole, stimulated with TNFα and subjected to immunofluorescence analysis. In vehicle (0.9% saline) treated C6 cells, we observed nuclear localization of p65 following TNFα stimulation in C6 cells, where as in pantoprazole treated cells p65 was localized mainly in the cytosol (Fig. 5.10). Similarly, 350 µM pantoprazole was able to inhibit the nuclear translocation of p65 in TNFα stimulated U373 cell line compared to vehicle treatment (Fig. 5.11).

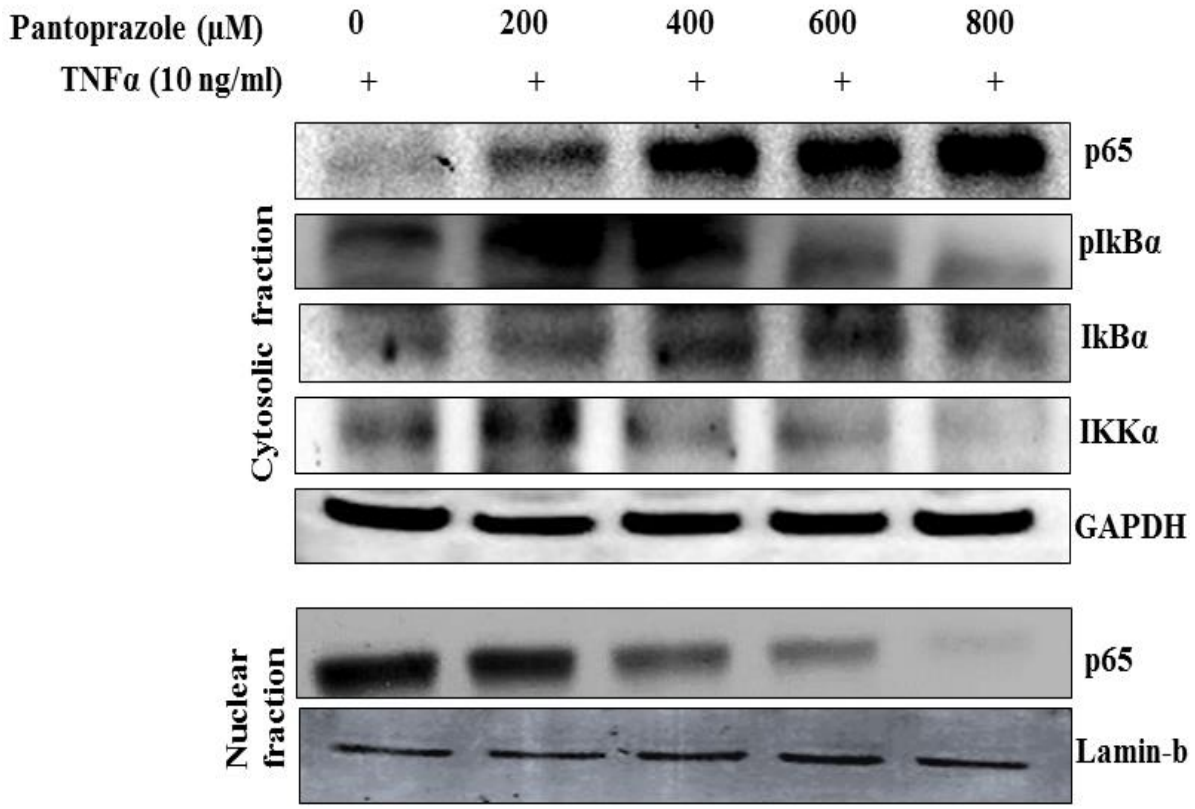

Fig. 5.9. Effect of pantoprazole (PPZ) on TNF-α induced nuclear translocation of p65. C6 cells were plated in 100-mm dishes and treated with vehicle (0.9% saline) or indicated concentrations of pantoprazole for 24 h followed by TNF-α (10 ng/ml) stimulation for 30 min. Cytoplasmic and nuclear extracts were prepared from treated C6 cells and subjected to

immunoblotting with p65, pIkBα, IkBα and IKKα. GAPDH and Lamin-b were used as loading controls for cytoplasmic and nuclear fractions, respectively. The blots are representative of three independent experiments.

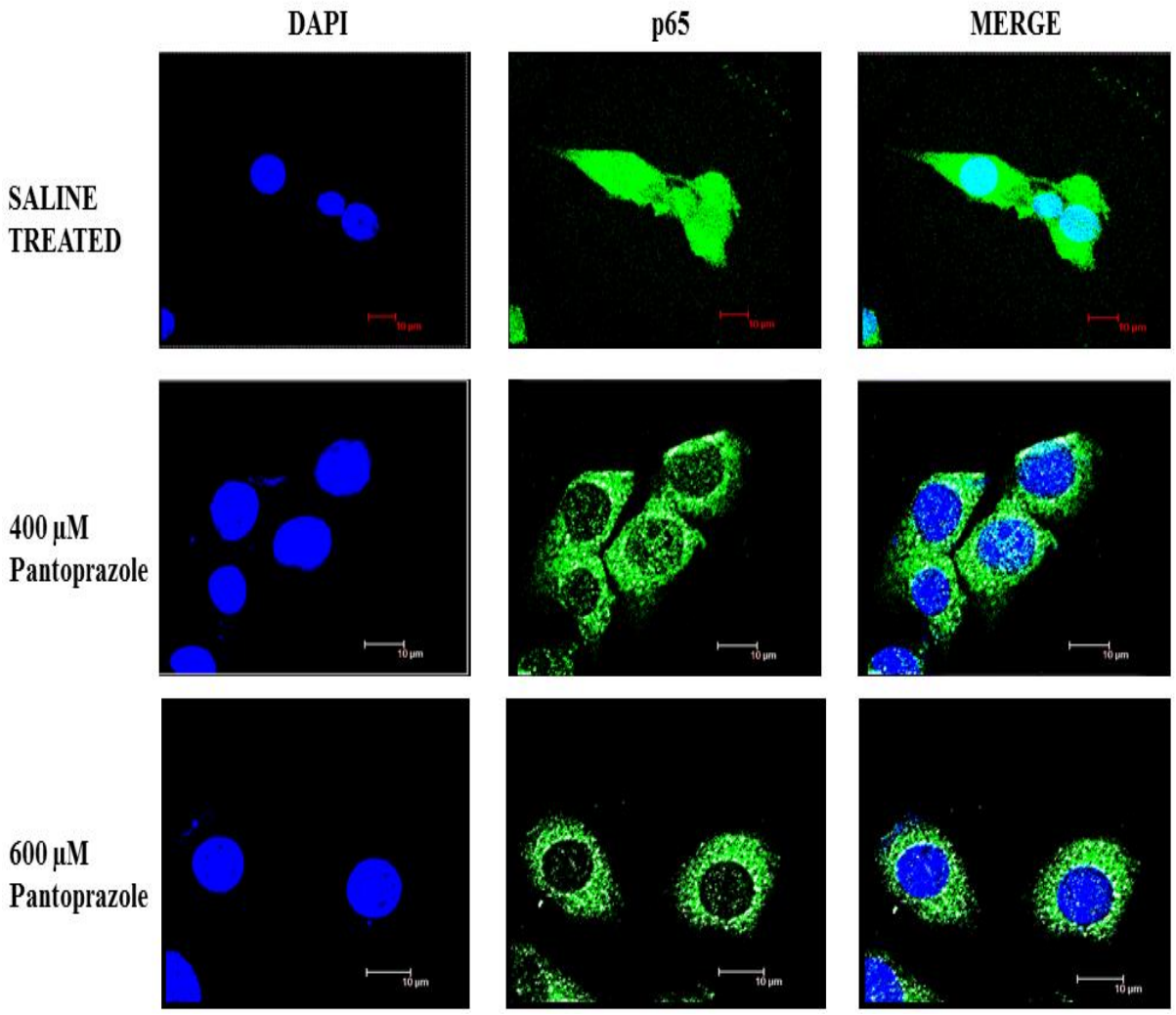

Fig. 5.10. Effect of pantoprazole on p65 localisation in C6 cells. C6 cells were plated onto coverslips in 24 well plates and treated with vehicle (0.9% saline) or indicated concentrations of pantoprazole for 24 h followed by TNF-α (10 ng/ml) stimulation for 30 min. Cells were then fixed with 4% paraformaldehyde and incubated with p65 primary antibody and anti-FITC secondary antibodies for 1 h at room temperature. Fluorescence was captured under a Leica confocal microscope. DAPI was used to visualize the nuclei.

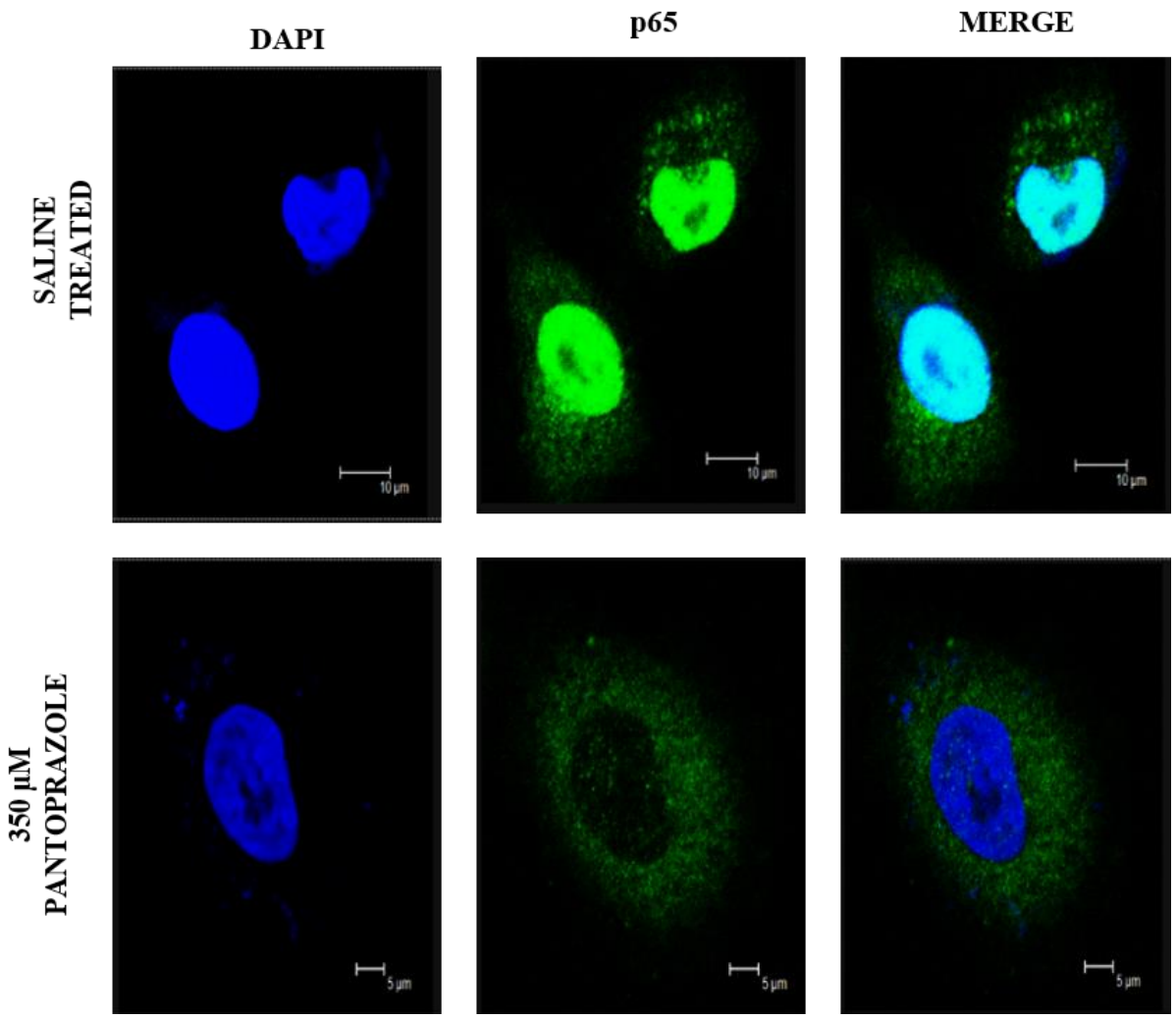

Fig. 5.11. Effect of pantoprazole on p65 localisation in U373 cells. U373 cells were plated onto coverslips in 24 well plates and treated with vehicle (0.9% saline) or indicated concentrations of pantoprazole for 24 h followed by TNF-α (10 ng/ml) stimulation for 30 min. Cells were then fixed with 4% paraformaldehyde and incubated with p65 primary antibody and anti-FITC secondary antibodies for 1 h at room temperature. Fluorescence was captured under a Leica confocal microscope. DAPI was used to visualize the nuclei.

5.3.7. Pantoprazole down-regulates NF-κB reporter gene expression with decreased expression of NF-κB target genes

After the release of p50/p65 complex from IκBα, NF-κB gets translocated into nucleus and binds to gene specific promoter to transcribe the genes. In order to study the effect of pantoprazole on NF-κB activation, C6 cells were briefly transfected with pNF-κB-MetLuc2-Reporter, and pRL-TK (for normalization of transfection efficiency) plasmids, and treated with

pantoprazole followed by TNFα stimulation. Pantoprazole was able to hamper NF-κB reporter gene activity in dose dependent manner (Fig. 5.12a). These results evidently demonstrate that pantoprazole repressed NF-κB dependent reporter gene expression by hindering the degradation and phosphorylation of IκBα. Since, COX-2, iNOS and cyclin-D1 are NF-κB regulated genes, we further investigated the expression levels of these genes. Pantoprazole significantly reduced the expression of these NF-κB target genes in dose dependent manner (Fig. 5.12b).

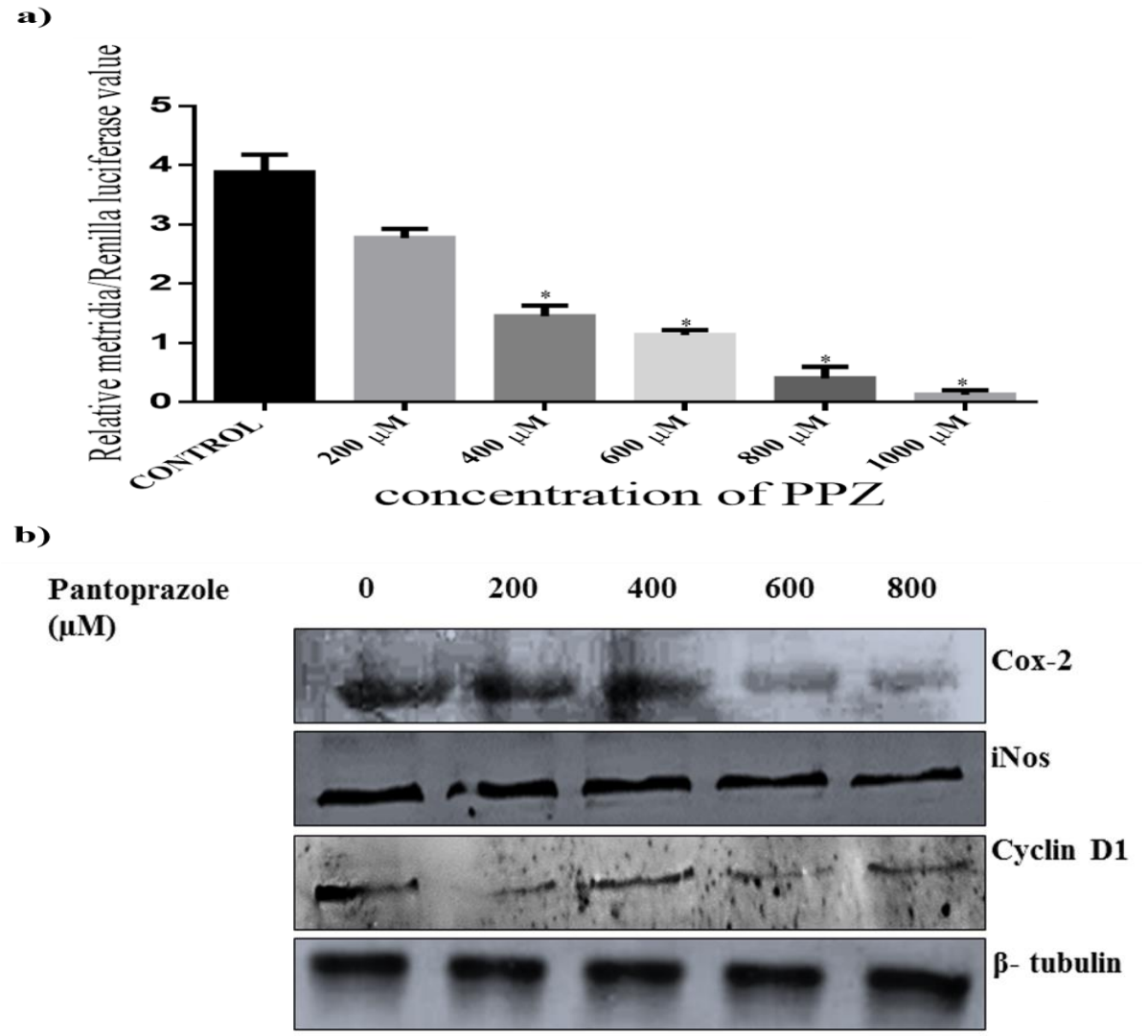

Fig. 5.12. Effect of pantoprazole (PPZ) on NF-κB dependent reporter gene expression and its target genes. (a) NF-κB reporter activity is enhanced substantially after TNF-α stimulation and this enhanced reporter activity is potentially inhibited by pantoprazole in a concentration-dependent manner. The metridia luciferase activity was normalized against renilla luciferase activities. Data expressed as mean ± SD and are representative of three independent experiments. *P<0.05, compared with control. **(b)** Decreased expression of NF-κB target genes

Cox-2, iNOS, Cyclin D1 observed with increase in the concentration of PPZ. β- tubulin served as internal control.

5.4. Discussion

Regulation of intra and extra cellular pH is of utmost important for healthy functioning of the cells, in particular for the survival of cancer cells as these cells live in most ischemic conditions with low extra cellular pH (Stubbs et al, 1999). The cause of tumor acidification is aerobic glycolysis. The acidic metabolites formed during aerobic glycolysis are expelled out into the tumor environment lowering the extracellular pH compared to intracellular pH levels (Helmlinger et al, 1997). The main player of tumor acidification in cancer cells is H+-ATPase (v-ATPase) of plasma membrane, the bicarbonate transporter, and the proton-lactate symporter (Finbow and Harrison, 1997). One of the major hypotheses for resistance of cancer cells to cytotoxic drugs is acidification of tumor environment (Izumi et al, 2003). This mechanism is explained in two ways (a) neutralization of weak base anti-tumor drugs in acidified tumor environment (b) sequestering the anti-tumor drugs in acidic vesicles and eliminating them from cells through exocytosis pathway. Recent observations in different studies have pointed out that chemo resistant cancer cells can be sensitized to anti-tumor drugs by modulating the activity of H^+-ATPase (v-ATPase). Luciani F *et al*, reported that pre-treatment of chemo-resistant melanoma and adenocarcinoma cells with PPI made susceptible to various anti-tumor drugs like cisplatin, 5-FU and vinblastine (Luciani et al, 2004). Cheng M *et al*, proved that pantoprazole pre-treatment boosts the cytotoxic effects of chemo-therapeutic drugs on SGC7901 and inverses MDR of SGC7901/ADR by alleviating the V-ATPases/mTOR/HIF-1α/P-gp and MRP1 signaling pathway (Chen et al, 2012).

Recent studies have indicated that PPIs are able to induce cell death by modulating various growth promoting and inhibitor molecules or pathways. Omeprazole, one of the PPIs was able to modulate lysosomal transport pathway and autophagy activity in pancreatic cancer cell line and predispose the cells to apoptosis (Andrej et al, 2011). In similar way pantoprazole was able to induce apoptosis in gastric cancer cells by inhibiting MAP kinases (in particular ERK and JNK molecules) projecting it as possible anti-cancer drug. But non-cancerous gastric mucosal cells were resistant to apoptotic cell death induced by pantoprazole by over expressing anti-apoptotic molecules HSP70 and HSP27 (Yeo et al, 2008). The pro-apoptotic activity of pantoprazole was also confirmed in B-cell lymphoma SCID mouse and B-cell tumor cell lines

by altering the pH gradient, increasing the ROS production and depolarization of mitochondrial membrane potential (De Milito et al, 2007). Since these drugs against V- H+-ATPase were able to induce cell death in cancer cells without affecting the non-cancerous cells, this feature validate them as potential anti-tumor drugs. Besides, these PPIs need acidic environment to get activated and these active forms get accumulated in acidic compartments resulting in induction of significant apoptosis.

These observations made us to investigate whether these PPI's in particular pantoprazole could show a similar pattern of growth inhibition in C6 glioma cell line. In our study we found that pantoprazole has significant anti-proliferative activity. MTT assay and clonogenic assay revealed that pantoprazole was able to inhibit cell viability in dose and time dependent manner. Further, pantoprazole treatment led to arrest of C6 cells in sub G0/G1 phase of cell cycle which is indicative of cell death and altered cellular and nuclear morphology with increase in TUNEL positive cells. Interestingly, we observed tBID (a processed form of full length BID that translocates from cytosol to mitochondria) after pantoprazole treatment with concomitant increase in the expression of pro-apoptotic BAX, which might have caused $\Delta\psi m$ and increase in cytochrome *c* levels observed in the current study. Increased expression of pro-caspase-8 that facilitates the processing of BID into tBID further supports the notion. Processing of caspase-3 and PARP, which is indicative of apoptotic process initiated from mitochondria, is also consistent after treatment in C6 glioma cell line. It has been reported previously that $\Delta\psi m$ may be induced by ROS (Reactive Oxygen Species) generation (Kowaltowski and Vercesi, 1999). In our study we found elevated levels of ROS upon treatment with pantoprazole and it correlated with depolarization of mitochondrial membrane ($\Delta\psi m$) in dose dependent manner. ROS levels were found to be increased significantly at higher concentrations of pantoprazole. At lower concentrations of pantoprazole treatment there was increased activity of anti-oxidant enzymes like catalase, GST, GPX with simultaneous decrease in the lipid peroxidation, thereby protecting C6 cells from ROS induced toxicity.

NF-κB signaling pathway is an important transcription factor for induction of genes responsible for uninterrupted cell proliferation and invasion of cancer cells (Luo et al, 2005). Previous reports suggest that acidic pH favours the expression of VEGF-C in melanoma cells through NF-κB transcription factor and a proton pump inhibitor omeprazole was able to prevent the expression of VEGF-C interfering with NF-κB signaling pathway (Peppicelli et al, 2013). However, no reports demonstrated the effects of pantoprazole on NF-κB pathway in

glioblastoma. Many of the anti-tumor drugs show anti-carcinogenic property via inhibition of NF-κB pathway. Here we hypothesize that pantoprazole inhibit C6 glioma cell proliferation by inhibiting NF-κB activation. We evaluated the inhibitory effect of pantoprazole on IκBα phosphorylation and degradation, NF-κB nuclear translocation, NF-κB reporter activity and expression of its target gene. Our results showed that pantoprazole was able to repress TNF-α induced NF-κB activation, nuclear translocation and reporter gene expression via inhibiting IKKα expression, IκBα phosphorylation and degradation. Tanigawa *et al*, showed that lansoprazole, a proton pump inhibitor suppressed the production of pro-inflammatory cytokines by human monocytic cells stimulated by bacterial components like LPS and HpWE (Tanigawa et al, 2009), indicating anti-inflammatory role of proton pump inhibitor. Our results indicated that pantoprazole repressed the expression of NF-κB regulated inflammatory mediators COX-2, iNOS and cell cycle promoter cyclin-D1 in dose dependent manner which are over-expressed in glioma**.**

5.5. Conclusion

In conclusion, our results suggest that pantoprazole inhibits C6 glioma cell proliferation and induces apoptosis relatively by subduing the NF-κB signaling. Pantoprazole is widely used in clinical practice for treatment of peptic ulcers and reflux esophagitis. Our observations indicate that pantoprazole might play a vital role in controlling glioma progression via regulating the apoptotic pathways. Consistent with its cost effective, lower toxicity and higher efficacy it is possible to extend its clinical application to glioma also.

5.6. References

1. Aebi H (1984) Catalase *in vitro*. *Methods Enzymol* 105:121-6.
2. Andrej U, Andreas K, Stefan E, Landfester K, Walther P, Klapperstueck T, Wohlrab J, Henne-Bruns D, Knippschild U, Würl P (2011) Omeprazole Inhibits Proliferation and Modulates Autophagy in Pancreatic Cancer Cells. *Plos One* 6:20143.
3. Ansari SA, Safak M, Del Valle L, Enam S, Amini S, Khalili K (2001) Cell cycle regulation of NF-kappa b-binding activity in cells from human glioblastomas. *Exp Cell Res* 265:221–233.
4. Bass DA, Parce JW, Dechatelet LR, Szejda P, Seeds MC, Thomas M (1983) Flow cytometric studies of oxidative product formation by neutrophils: a graded response to membrane stimulation. *J Immunol* 130:1910–1917.

5. Basseres DS, Baldwin AS (2006) Nuclear factor-kappaB and inhibitor of kappaB kinase pathways in oncogenic initiation and progression. *Oncogene* 25:6817–30.
6. Bernheim F, Bernheim ML, Wilbur KM (1948) The reaction between thiobarbituric acid and the oxidation products of certain lipides. *J Biol Chem* 174:257-64.
7. CBTRUS (Central Brain Tumor Registry of the United States): CBTRUS Statistical Reoprt: Primary Brain and Central Nervous System Tumors Diagnosed in the United States in 2004-2007. Central Brain Tumor Registry of the United States, Hinsdale, Illinois, USA. 2011.
8. Chen M, Huang SL, Zhang XQ, Zhang B, Zhu H, Yang VW, Zou XP (2012) Reversal effects of pantoprazole on multidrug resistance in human gastric adenocarcinoma cells by down-regulating the V-ATPases/mTOR/HIF-1a/P-gp and MRP1 signaling pathway *in vitro* and *in vivo*. *J Cell Biochem* 113:2474-87.
9. Darzynkiewicz Z, Traganos F, Staiano-Coico L, Kapuscinski J, Melamed MR (1982) Interaction of rhodamine 123 with living cells studied by flow cytometry. *Cancer Res* 42:799-806.
10. De Milito A, Iessi E, Logozzi MA, Lozupone F, Spada M, Marino ML, Federici C, Perdicchio M, Matarrese P, Lugini L, Nilsson A, Fais S (2007) Proton pump inhibitors induce apoptosis of human B cell tumors through a caspase-independent mechanism involving reactive oxygen species. *Cancer Res* 67:5408–17.
11. Du L, Lyle CS, Obey TB, Gaarde WA, Muir JA, Bennett BL, Chambers TC (2004) Inhibition of cell proliferation and cell cycle progression by specific inhibition of basal JNK activity. *J Biol Chem* 279:11957–11966.
12. Fais S, De Milito A, You HY and Qin WX (2007) Targeting vacuolar H+-ATPases as a new strategy against cancer. *Cancer Res* 67:10627-30.
13. Finbow ME, Harrison MA (1997) The vacuolar H+-ATPase: a universal proton pump of eukaryotes. *Biochem J* 324: 697–712.
14. Ghosh S, May MJ, Kopp EB (1998) NF-kappa B and Rel proteins: evolutionarily conserved mediators of immune responses. *Annu Rev Immunol* 16:225–60.
15. Gupta GP, Massague J (2006) Cancer metastasis: building a framework. *Cell* 127:679–95.
16. Haar CP, Hebbar P, Wallace GC 4th, Das A, Vandergrift WA 3rd, Smith JA, Giglio P, Patel SJ, Ray SK, Banik NL (2012) Drug resistance in glioblastoma: a mini review. *Neurochem Res* 37(6):1192-1200.

17. Helmlinger G, Yuan F, Dellian M, Jain RK (1997) Interstitial pH and pO2 gradients in solid tumor *in vivo*: high resolution measurements reveal a lack of correlation. *Nat Med* 3: 177–82.
18. Izumi H, Torigoe T, Ishiguchu H, Uramoto H, Yoshida Y, Tanabe M, Ise T, Murakami T, Yoshida T, Nomoto M, Kohno K (2003) Cellular pH regulators: potentially promising molecular targets for cancer chemotherapy. *Cancer Treat Rev* 29:541–9.
19. Ji BC, Yu CC, Yang ST, Hsia TC, Yang JS, Lai KC, Ko YC, Lin JJ, Lai TY, Chung JG (2012) Induction of DNA damage by deguelin is mediated through reducing DNA repair genes in human non-small cell lung cancer NCI-H460 cells. *Oncol Rep* 27:959–964.
20. Kowaltowski AJ, Vercesi AE (1999) Mitochondrial damage induced by conditions of oxidative stress. *Free Radic Biol Med* 26:463-47.
21. Larsson H, Mattson H, Sundell G, Carlsson E (1985) Animal pharmacodynamics of omeprazole. A survey of its pharmacological properties *in vivo*. *Scand J Gastroenterol* Suppl 108:23-35.
22. Lu X, Qin W, Li J, Tan N, Pan D, Zhang H, Xie L, Yao G, Shu H, Yao M, Wan D, Gu J, Yang S (2005) The growth and metastasis of human hepatocellular carcinoma xenografts are inhibited by small interfering RNA targeting to the subunit ATP6L of proton pump. *Cancer Res* 65:6843–9.
23. Luciani F, Spada M, De Milito A, Molinari A, Rivoltini L, Montinaro A, Marra M, Lugini L, Logozzi M, Lozupone F, Federici C, Iessi E, Parmiani G, Arancia G,Belardelli F, Fais S (2004) Effect of proton pump inhibitor pretreatment on resistance of solid tumors to cytotoxic drugs. *J Natl Cancer Inst* 96:1702-13.
24. Luo JL, Kamata H, Karin M (2005) IKK/NF-kappaB signaling: balancing life and death--a new approach to cancer therapy. *J Clin Invest* 115:2625-32.
25. Martin de Argila C (2005) Safety of potent gastric acid inhibition. *Drugs* 65 Suppl 1:97–104.
26. Martinez-Zaguilan R, Lynch RM, Martinez GM, Gillies RJ (1993) "Vacuolar-type H(+)-ATPases are functionally expressed in plasma membranes of human tumor cells", *AJP - Cell Physiology* 265:1015-1029.
27. Nagai S, Washiyama K, Kurimoto M, Takaku A, Endo S, Kumanishi T (2002) Aberrant nuclear factor-kappaB activity and its participation in the growth of human malignant astrocytoma. *J Neurosurg* 96:909–917.

28. Neuwelt EA, Bauer B, Fahlke C, Fricker G, Iadecola C, Janigro D, Leybaert L, Molnár Z, O'Donnell ME, Povlishock JT, Saunders NR, Sharp F, Stanimirovic D,Watts RJ, Drewes LR (2011) Engaging neuroscience to advance translational research in brain barrier biology. *Nat Rev Neurosci* 12:169-182.
29. Newell K, Franchi A, Pouyssegur J, Tannock I (1993) Studies with glycolysis-deficient cells suggest that production of lactic acid is not the only cause of tumor acidity. *Proc Natl Acad Sci U S A* 90:1127–31.
30. Nishi T, Forgac M (2002) The vacuolar (H+)-ATPases—nature's most versatile proton pumps. *Nat Rev Mol Cell Biol* 3:94 –103.
31. Nishikori M (2005) Classical and alternative NF-κB activation pathways and their roles in lymphoid malignancies. *J Clin Exp Hematopathol* 45:15–24.
32. Nupponen NN, Joensuu H (2006) Molecular pathology of gliomas. *Curr Diagn Pathol* 12:394–402.
33. Ohgaki H, Kleihues P (2009) Genetic alterations and signaling pathways in the evolution of gliomas. *Cancer Sci* 100:2235–2241.
34. Ostermann S, Csajka C, Buclin T, Leyvraz S, Lejeune F, Decosterd LA, Stupp R (2004) Plasma and cerebrospinal fluid population pharmacokinetics of temozolomide in malignant glioma patients. *Clin Cancer Res* 10:3728-3736.
35. Paglia DE, Valentine WN (1967) Studies on the quantitative and qualitative characterization of erythrocyte glutathione peroxidase. *J Lab Clin Med* 70:158-69.
36. Peppicelli S, Bianchini F, Contena C, Tombaccini D, Calorini L (2013) Acidic pH via NF-κB favours VEGF-C expression in human melanoma cells. *Clin Exp Metastasis* 30:957-67.
37. Portnow J, Badie B, Chen M, Liu A, Blanchard S, Synold TW (2009) The neuropharmacokinetics of temozolomide in patients with resectable brain tumors: potential implications for the current approach to chemoradiation. *Clin Cancer Res* 15:7092-7098.
38. Qiao S, Li W, Tsubouchi R, Murakami K, Yoshino M (2004) Role of vanilloid receptors in the capsaicin-mediated induction of iNOS in PC12 cells. *Neurochem Res* 29:687–693.
39. Raghunand N, Mahoney BP, Gillies RJ (2003) Tumor acidity, ion trapping and chemotherapeutics II. pH- dependent partition coefficients predict importance of ion trapping on pharmacokinetics of weakly basic therapeutic agents. *Biochem Pharmacol* 66:1219 –29.

40. Rofstad EK, Mathiesen B, Kindem K, Galappathi K (2006) Acidic extracellular pH promotes experimental metastasis of human melanoma cells in athymic nude mice. *Cancer Res* 66:6699–707.
41. Sareddy GR, Geeviman K, Ramulu C, Babu PP (2012) The nonsteroidal anti-inflammatory drug celecoxib suppresses the growth and induces apoptosis of human glioblastoma cells via the NF-κB pathway. *J Neurooncol* 106:99-109.
42. Sennoune SR, Bakunts K, Martinez GM, Chua-Tuan JL, Kebir Y, Attaya MN (2004) Vacuolar H+-ATPase in human breast cancer cells with distinct metastatic potential: distribution and functional activity. *Am J Physiol Cell Physiol* 286:1443-52.
43. Steeg PS (2006) Tumor metastasis: mechanistic insights and clinical challenges. *Nat Med* 12:895–904.
44. Stubbs M, McSheeh PM, Griffiths JR (1999) Causes and consequences of acidic pH in tumors: a magnetic resonance study. *Adv Enzyme Regul* 39:13–30.
45. Tanigawa T, Watanabe T, Higuchi K, Machida H, Okazaki H, Yamagami H, Watanabe K, Tominaga K, Fujiwara Y, Oshitani N, Arakawa T (2009) Lansoprazole, a Proton Pump Inhibitor, Suppresses Production of Tumor Necrosis Factor-α and Interleukin-1β Induced by Lipopolysaccharide and *Helicobacter Pylori*Bacterial Components in Human Monocytic Cells via Inhibition of Activation of Nuclear Factor-κB and Extracellular Signal-Regulated Kinase. *J. Clin Biochem Nutr* 45: 86–92.
46. Wang CY, Cusack JC Jr, Liu R, Baldwin AS Jr (1999) Control of inducible chemoresistance: enhanced anti-tumor therapy through increased apoptosis by inhibition of NF-kappaB. *Nat Med* 5:412–417.
47. Warburg O (1956) On the origin of cancer cells. *Science* 123:309–14.
48. Yamagata M, Hasuda K, Stamato T, Tannock IF (1998) The contribution of lactic acid to acidification of tumours: studies of variant cells lacking lactate dehydrogenase. *Br J Cancer* 77:1726–31.
49. Yeo M, Kim DK, Park HJ, Cho SW, Cheong JY, Lee KJ (2008) Blockage of intracellular proton extrusion with proton extrusions with proton pump inhibitor induces apoptosis in gastric cancer. *Cancer Sci* 99:185.
50. Yu FS, Yang JS, Yu CS, Lu CC, Chiang JH, Lin CW, Chung JG (2011) Safrole induces apoptosis in human oral cancer HSC-3 cells. *J Dent Res* 90:168–174.

Summary

Glioma is the most destructive and intractable brain tumor developed by abnormal and uncontrolled cell division/proliferation of glial cells of the brain. They are more common in adults compared to children and incidence rate is high in males than females. After diagnosis patients are subjected to standard care therapy which consists of surgery followed by radiation and chemotherapy. Further, advancement in understanding molecular pathogenesis of these tumors has led to development of novel drugs targeting molecules and signaling pathways involved in gliomagenesis and progression. To certain extent this has helped in effective treatment and improved outcome of patient compared with current standard therapies. In spite of aggressive therapy, overall survival period of glioma patients has not much improved much over the past few decades.

Current treatment approach for glioma patients is hindered by major limitations at various levels like histopathological differentiation of low grade tumors, extent of therapy to which the patient should be subjected and resistance to chemotherapy and radiotherapy. These confinements can be overcome partially by identifying proper diagnostic and prognostic markers and finding drugs which can overcome resistance posed by the tumor. Following are the major limitations of existing glioma therapy.

1. Though pilocytic and diffuse astrocytomas are low grade tumors, distinguishing between them is a major problem confronted by pathologists since both the tumors exhibit common features like increased cellular and nuclear pleomorphism. Besides there is no efficient immuno-histochemical marker to differentiate them and thus differential diagnosis between them is subjective.
2. Management of glioma employs aggressive treatment approaches like postoperative radiation therapy and chemotherapy. But these approaches do not benefit all the patients similarly. Hostile side effects associated with this kind of treatment further declines quality of life. Therefore personalised treatment has become very important and plays a vital role in brain tumor management. Prognosis plays a vital role in patient management and trail design. Prognostic biomarker identifies important risk factors and their effects and help neuro-oncologists to identify patient and tumor specific factors that can be used to select maximum effective therapy and minimize treatment related adverse side effects. Even though current treatment for glioma is highly customised, but variations in the treatment plans between patients with same histology are based mainly on tumor location or patient specific factors, instead of biological differences

between tumors. Therefore, finding molecular events responsible for the biological differences in tumors may enhance the benefits of therapy along with personalised therapeutic involvement for glioma patients.

3. Controlling the glioma cell survival and proliferation is the key for long term survival of the glioma patients. Thus it is very much in need to target glioma cell growth promoting pathways and overcome chemo-resistance to provide a survival benefit.

Considering these lacunae in glioma treatment we undertook this study to address serious clinical problems faced in treatment, with the clear intention to find possible diagnostic marker to distinguish between low grade tumors, identifying a prognostic factor for glioma patient management and trail design and drugs targeting the survival pathways and chemo-resistance posed by glioma**.**

Salient findings:

- ✓ We demonstrate that there is a differential expression of Wnt pathway components β-catenin, Lef1, Tcf4 and c-Myc in pilocytic and diffuse astrocytoma. Therefore differential expression of these molecules might help in distinguishing pilocytic astrocytoma from diffuse astrocytoma.
- ✓ Our data provides convincing evidence that deregulated expression of cell polarity genes is associated with astrocytoma progression. Besides reduced expression of hSCRIB at gene and protein levels is associated with poor outcome in astrocytoma patients. hSCRIB might play an inhibitive role during the development of astrocytoma and may be a potential prognosis predictor of astrocytoma.
- ✓ Using ENU induced rat glioma model we found that JNK pathway is involved in ENU induced glioma progression and JNK might be an attractive target for therapeutic depletion of glioma.
- ✓ We found that pantoprazole a proton pump inhibitor was able to inhibit the survival of glioma cell line via induction of mitochondrial pathway mediated apoptosis and inhibition of p65 translocation from cytosol to nucleus.

Publications

1) Sareddy GR, **Geeviman K**, Ramulu C, Babu PP. **(2012)** The nonsteroidal anti-inflammatory drug celecoxib suppresses the growth and induces apoptosis of human glioblastoma cells via the NF-κB pathway. ***J Neurooncol.***

2) Sareddy GR, **Geeviman K**, Panigrahi M, Challa S, Mahadevan A, Babu PP. **(2012)** Increased β-catenin/Tcf signaling in pilocytic astrocytomas: a comparative study to distinguish pilocytic astrocytomas from low-grade diffuse astrocytomas. ***Neurochem Res.***

3) **Khamushavalli Geevimaan** and Phanithi Prakash Babu. **(2013)** Deregulation of Cell Polarity Proteins in Gliomagenesis. ***InTech, Chapters published under CC BY 3.0 license*.**

4) Anwita Mudiraj, **Khamushavalli Geeviman**, Phanithi Prakash Babu, A. Ram Reddy. **(2014)** Triazolo aspirins inhibit proliferation of C6 glioma cell line *in vitro*. **Journal of Pharmacy Research.**

5) Phanithi Prakash Babu, **Khamushavalli Geeviman**. **(2014)** Targeting V-H^+-ATPases to inhibit the growth of glioma *in vitro* using proton pump inhibitor and LASS2 gene expression. **Journal of Neurochemistry** (supplementary material).

6) **Khamushavalli Geeviman** and Phanithi Prakash Babu. Role of SAPK/JNK signaling pathway in tumorigenesis and tumor progression in N-ethyl-N-nitrosourea induced transplacental glioma rat model. (***Manuscript under preparation***)

7) **Khamushavalli Geeviman** and Phanithi Prakash Babu. Pantoprazole induces alterations in Mitochondrial Membrane Potential and attenuates NF-κB signaling in rat C6 glioma cell line. (***Under communication***)